Response: We thank both reviewers for thoughtful suggestions and constructive criticism that have helped us improve our manuscript. Below we provide responses to each reviewer's concerns and suggestions in blue font. The largest concern by the reviewers had to do with our original use of 1-second data and we have addressed this by using longer time scales (e.g., e-folding time scale) and show that the key results and conclusions are preserved.

Interactive comment on "Precipitation Susceptibility in Marine Stratocumulus and Shallow Cumulus from Airborne Measurements" by E. Jung et al.

Anonymous Referee #1
Received and published: 18 April 2016
Review of Jung et al. "Precipitation Susceptibility in Marine Stratocumulus and Shallow Cumulus from Airborne Measurements"

General comments
This study examines the precipitation susceptibility metric using consistent measurements from a variety of field campaigns to ask whether the qualitative behavior of the susceptibility varies with cloud type. Whereas previous studies appear to disagree on whether susceptibility should increase and then decrease with cloud thickness or whether they should decrease monotonically, different retrieval methods were used in these previous studies, so it has not been clear whether the differences are due to cloud types, retrieval methods, or analysis methods.
This study does not suffer from many of the same issues, because the measurements are made from the same aircraft, using the same instruments and sampling strategy.

The authors show that the precipitation susceptibility increases, and then decreases, regardless of whether cumulus or stratocumulus clouds are examined. After presenting their susceptibility estimates, they provide possible explanations for the why the results of Terai et al. (2012) do not capture the increase in susceptibility at lower cloud thicknesses.

The study addresses an existing disagreement in the qualitative behavior amongst precipitation susceptibility estimates and provides valuable observations to add to the existing observed estimates and to try to reconcile the disagreements. However, there some issues that need to be addressed before I recommend publication. In particular, issues of N_d and H covariability and the statistical independence of the 1-second data should be addressed.

Response: As we will elaborate upon below, we have addressed both of these issues. We show that in our datasets, N_d and H do not co-vary and have showed that our results and conclusions are robust using 1-second data in favor of other methods proposed by the reviewers.

Major comments 1) In the study, it appears that a good amount of consecutive data are included in the log(Nd) vs. log(R) regression slopes. Given that N and R estimates from every second are used, there is the possibility that covariability between N and H at those smaller spatial scales might affect S_0 estimates. For example, even within the same cloud thickness bin, the N and H can covary in a flight leg due to updraft/downdraft organization. In other words, where there are stronger updrafts, Nd will likely be higher, as well as H. This can impact S0, because H also controls R. Therefore, I would like the authors to examine the extent to which the covariability between N and H exist and how they might affect S0. Do data need to be averaged over longer timesteps to reduce the covariability?

Response: The scatter diagram of N_d and H is shown in Fig. 1 for E-PEACE as an example. There is a weak correlation (or co-variability) between N_d and H. The correlation (r) between two is about ~0.03, and the covariance is about 0.18. We also show results below for a couple representative individual flights and show that N_d and H do not co-vary all the time.

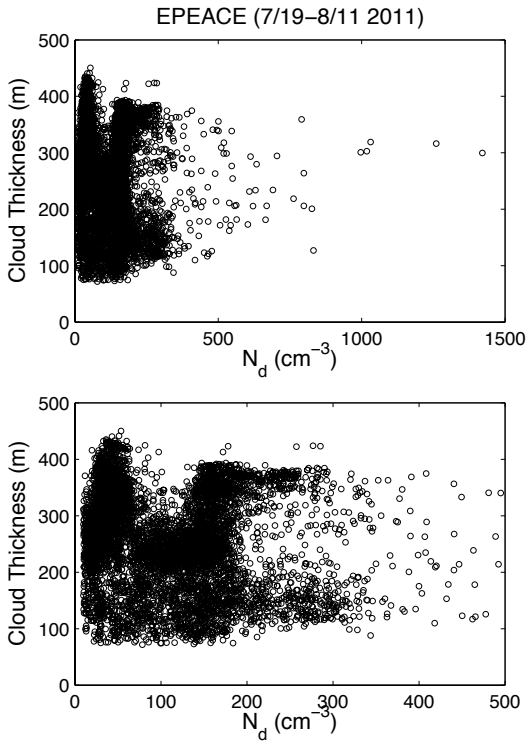

Figure 1A. Scatter diagrams of N_d and H for the ten flights of E-PEACE.

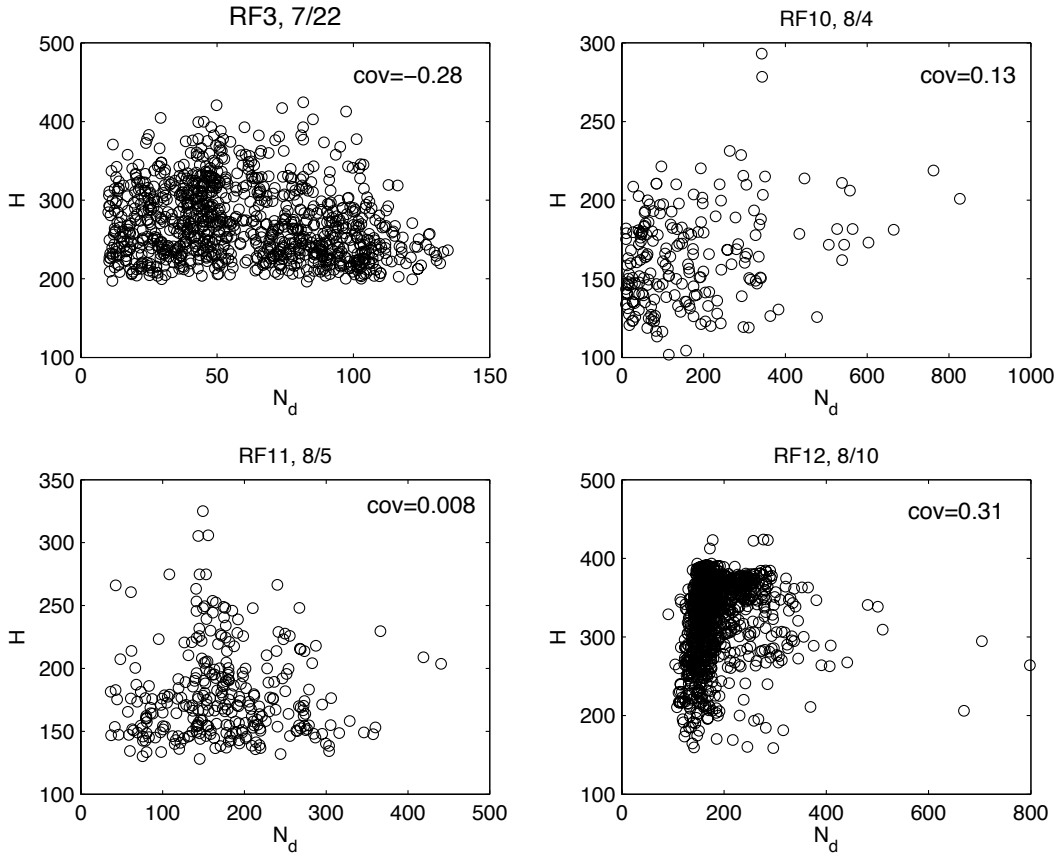

Figure 1B. Scatter diagrams of N_d and H for the random individual flights during E-PEACE. Numbers on the upper right corner indicates a covariability between N_d and H for a given flight.

As a result, the data do not need to be averaged over longer time-steps to reduce the co-variability as the co-variability is small. However, we also calculated S_o with data that are averaged over longer time-steps by considering the independence of the 1-second data (shown later).

2) Similarly, I would like to see the authors demonstrate whether 1-second of data (N, R) is statistically independent from one another. For example, Leith et al. (1973) provide a method to determine the e-folding time scale, which will help determine whether using the 1-second data is indeed appropriate.
Leith, C. E. (1973), The Standard Error of Time-Average Estimates of Climatic Means, J. Appl. Meteorl., 12, 1066–1069.

Response: We find that the e-folding time of N_d during E-PEACE varies from about 4-6 minutes to 10 minutes, and an e-folding time of R varies from a few seconds to 1-2 minutes. The e-folding time of N_d within the VOCALS-TO flights varied between 2-6 minutes, and for the cloud-base precipitation was less than (or approximately)

1 minute (less than 3 km, consistent with Terai et al., 2012). In the case of BACEX (Cu), the overall e-folding times were much shorter, varying from 1-2 minutes for N_d and less than 1 minute for R. The e-folding times of N_d and R are summarized in Table 1 for VOCALS, E-PEACE and BACEX. KWACEX was not included since there were only four flights.

We calculated S_o with data averaged over the upper bounds of the e-folding time (i.e., e-folding time of N_d) for E-PEACE, BACEX and VOCALS flights, and the qualitative behavior of S_o reported with 1-second data is unchanged: S_o increases with H then peaks before it decreases again (Fig. 5 for BACEX and E-PEACE and Fig. 6 for VOCALS. Fig. 6 is shown later). However, it should be noted that the H that S_o peak is shifted toward the lower H, *which is* consistent with the results of Duong et al. (2011). The shift of H to the lower H is substantial in Sc where the overall H is smaller than H of Cu.

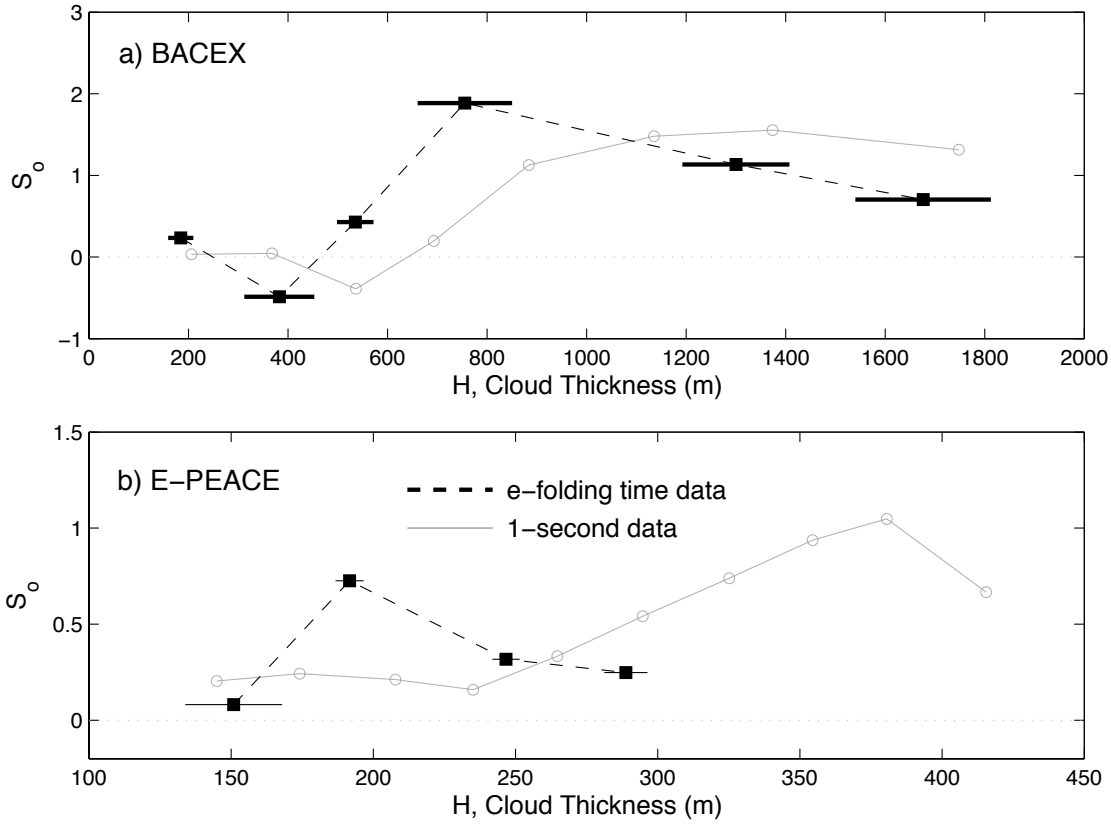

Figure 5. S_o estimated with aircraft measurements for (a) BACEX (Cu) and (b) E-PEACE (Sc). The 1-second data of individual flights are reduced by averaging over the e-folding time of N_d for each day prior to the calculation.

3) Whenever a slope is calculated, the statistical uncertainties should also be reported, since the relationship does not appear to be linear in many of the cases (Fig. 2).

Response: The slope is calculated from ln(N_d) and -ln(R) that are shown in Fig. 3, whereas Fig. 2 shows N_d and log(R). The linear correlations (r) is added in the ln(N_d) and –ln(R) diagrams and r and P-values indicating the statistically significant level of confidence for the fitted lines are summarized in Table A2 for given H intervals.

4) Possible explanations are presented as to why the results in this study disagree from what is presented in Terai et al. (2012) but are not tested. I believe some of the issues can be tested using the data analyzed this study. For example, the authors can test whether the method used in Terai et al. (2012) gives a different behavior than when a linear regression is used.

Response: Please refer to the replies to "P14 L6-7" later (tercile log-differencing versus linear regression). We also believe that one of the most fundamental reasons causing the difference comes from the differences in cloud fields between that were sampled during the flights. For example, VOCALS TO sampled cloud fields close to the continent that had high aerosol concentration with weak precipitation. In contrast, VOCAL C-130 flight sampled the cloud fields in the open ocean where the cloud fields consisted of Pockets of Open Cells (in many cases), and more intense and frequent precipitation was observed. The effect of precipitation on the S_o estimates (and the effect of high R threshold on the S_o estimates) are shown later (Please refer to the replies to #7 for the second reviewer or Figure B2 and section 3.2).

5) Many times, in comparing with the results of Terai et al. (2012), their SR is compared with the S_0 in this study. Is this the right comparison to make? Or should SI be compared with S_0 in this study, since S_I captures the effect of aerosols on measureable precipitation rates.

Response:
Terai et al. define the $S_o=S_I+S_f$, which corresponds to S_o in current study.

Terai et al. used 10-km segment-averaged cloud data and determined the fraction and intensity of the drizzle in each segment. The segment-mean precipitation rates R is partitioned into the fraction of the cloud columns that are drizzling f, and the mean drizzle rate in that column (drizzle intensity I). Their SI is calculated exclusively for the clouds that produce measurable precipitation, which is set by the R threshold, and their S_f is considered for all clouds.

On the other hand, in the current study, cloud data are included in the analysis if the given precipitation rate is greater than a threshold of 0.001 mm day^{-1}. The low R threshold is intended to include both non-precipitating and precipitating clouds.

Minor and specific comments
P1 L23: "R" and other variables (e.g. Nd) should be italicized throughout the manuscript

Response: Revised as the reviewer suggested.

P2 L26-27: "S0 is insensitive to aerosol perturbations where clouds do not precipitate": S0 should be undefined where clouds do not precipitate, not zero.

Response: The manuscript is revised to clarify the point as follows: At low LWP, not enough water is available with which to initiate rain, and S_o is insensitive to aerosol perturbations

P2 L30: Please write out what VOCALS stands for.

Response: Revised as VAMOS Ocean-Cloud-Atmosphere-Land Study-Regional Experiment (VOCALS-REx).

P3 L6: (and subsequent uses) Replace "GCCM" with "GCM"? If it is supposed to be GCCM, please state what it is an acronym for.

Response: Corrected.

P3 L12: Please define the acronym ARM.

Response: Revised as Atmospheric Radiation Measurement (ARM)

P3 L16: For completeness, at some point in the paragraph the study of Hill et al. 2015 should be mentioned. There are a number of other instances throughout the study where comparison with results of Hill et al. (2015) would also be good to make.

Hill, A. A., B. J. Shipway, and I. A. Boutle (2015), How sensitive are aerosol-precipitation interactions to the warm rain representation?, J. Adv. Model. Earth Syst., 7, 987–1004, doi:10.1002/2014MS000422.

Response: The reference is added in the revised manuscript.

P4 L12: "LCL varied little for Cu" Can the authors attach some numbers to this statement?

Response: Revised as follows: "The LCL varied little for Cu, for example, during the Barbados Aerosol Cloud Experiment (Sect. 2.3), the LCLs were 653.9±146 m on average from the aircraft measurements, which agreed with the two-year LCL climatology in this region (700±150 m) documented in Nuijens et al. (2014)"

P4 L18-26: How long were these cloud base level flights? In other words, over what length scales are cloud thicknesses assumed to be constant, and is this a good approximation?

Response: Cloud-base level flights last about 10-20 minutes. H=CT-CB where H indicates cloud thickness, CT and CB indicate cloud tops and cloud base heights, respectively. In this study (both Sc and Cu but except for the VOCALS TO flight), a single LCL is used for the cloud-base height for a given cloud-base level flight. However, the cloud tops have a 1-second resolution (from cloud radar). Thus, the cloud thickness has a 1-second resolution for the cloud-base level leg flights.

However, note that in case that the cloud radar is not operational such as VOCALS TO flights, both cloud tops and bases are estimated from the vertical structure of LWC, which has one value per cloud-base level-leg flight for a given day (daily resolution). Consequently, the cloud thickness is assumed to be constant during the cloud-base level flights, which are not as good as high resolution, and why we need either the cloud radar or G-band radiometer to measure cloud thickness and LWP directly at high resolution.

We examined the S_o that calculated with the 1-second resolution of H, N_d, and R by using cloud radar (both tops and bases where cloud bases have used the heights of cloud-base level leg flights). Although it is not shown in the paper, the results were robust. An example of S_o that is calculated with a 1second resolution of cloud data for BACEX is shown here.

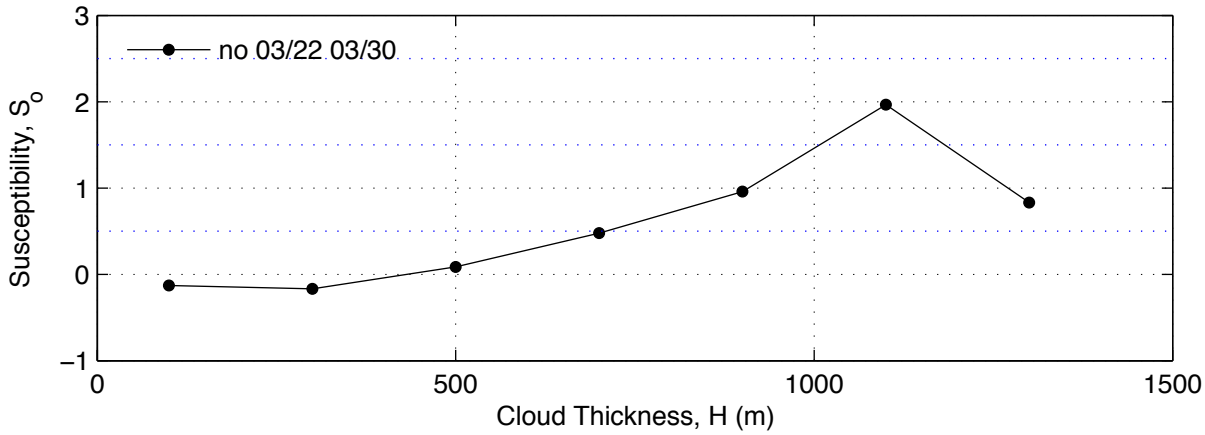

Figure. Precipitation susceptibility as calculated from BACEX aircraft data.

Note that the cloud thickness in the above figure is not the same as H in the manuscript (e.g., Fig. 4) because the cloud bases in this figure have used the heights of cloud-base level leg flights, which are relatively constant during the flight is slightly higher than the actual cloud bases, resulting in overall lower H values.

P4 L28-29: Is using 1 second data appropriate? Given the sampling volume rate and scarcity of drizzle drops I wonder how statistically robust the R retrievals are. Just based on counting statistics, what are the measurement uncertainties in R? What is the theoretical minimum threshold on R given the sampling rate of 1 second?

Response: The CAS probe collects drops at 10 Hz then the DSDs are averaged to 1 Hz at each channel, whereas CIP collects drops at 1 Hz.

In the CIP and CAS (all the optical particle counters and size spectrometers), the counting statistics would be estimated for each channel by Poisons statistics, i,e. the square root of the total count. Thus for hundred particles in a channel, counting statistics would set the error at ± 10 counts, or 10 %. For 10 counts in the channel, the Poisson error is ±3.1 or 31%. If 1-second data is giving 10 particles in a channel, then the counting error is 31%, but by counting for ten seconds, you have reduced the error to 10%. In a channel where the count is 1 particle over the counting period, the error is 100%.

In a CN counter we don't try to determine size but count everything. There we have no issue because there are so many small particles that counting statistics is always satisfied. When we start analyzing the signals each particle generates, and trying to tell its size from the value of the signal we receive; then we run into counting statistics problems. We indicate that a particle that generates signals within a certain range belong to a size range and the narrower you make that range, the fewer particles you will sample in a given period of time. So if in any channel you have 100 particles, there would be 10% uncertainty in that number on account of Poisson statistics alone, then there will be an additional uncertainty due to viewing volume and electronic issues.

The manuscript is revised as "CIP acquire data every 1 second, but CAS probes acquire data every 10 Hz then the DSDs at each channel are averaged to 1 Hz. The cloud radar receives data every 3 Hz then is averaged to 1 Hz to pair with probe data."

P5 L3-6: Same question can be applied to z.

Response: Please see the above. In the revised manuscript we removed the Z-associated figure and text.

P6 L6: What are the 95 or 99% confidence intervals on this estimate? The scatter in Fig. 2 appears rather large.

Response: The confidence level is calculated from log (N_d) and –log(R) diagram such as Fig. 3.

P7 L2: A measure of the uncertainty will be helpful here as well.

Response: We added *r* for the S_o in the last paragraph on Page 6.

P7 L8: How were the H intervals chosen? Do the results vary with larger or smaller H bins?

Response: We chose the H intervals that include a similar number of data points in the H interval, and (at the same time) the H that gives the robust results even though we choose slightly different H. The effect of H interval on the S_o estimates and it is discussed in Appendix C of the current manuscript

Appendix C. The effect of H intervals on S_o estimates.

S_o calculated with different H intervals can be seen by comparing Fig. 4 and Fig. A1 as an example. H intervals in Fig. 4(b) are about 30 m, while H intervals in Fig. A1 are about 50 m. The qualitative H-dependent behavior of S_o is robust regardless of the chosen H intervals in case 1-second data are used. However, the chosen H interval may have effect on the estimate of S_o that is calculated with a fewer data points, such as S_o that is calculated with data averaged over the e-folding time.

The effect of H-intervals on S_o estimates, which is estimated with data averaged over the e-folding time, is shown in Fig. B1. In summary, the results are robust regardless of H interval in general. However, if the H interval is chosen across the cloud thickness where the S_o changes substantially (such as in which the cloud properties change substantially), the pattern of S_o can be changed, indicating that the finer H interval would provide more accurate S_o. This is shown in Figs. 7 and 8. In Fig. 7, an H interval of 50 m hides the variation of S_o between H 150 m and 200 m. The ln (N_d) and –ln(R) diagrams for H widths of 40 and 50 m are shown in Fig. 7. However, in case that the S_o does not change substantially across the H intervals, the S_o does not change even if the larger H interval is used (e.g., Fig. 8d). For example, S_o calculated with subsets of data (e.g., 220 ≤H<250m, 250≤H<280m, 280≤H<310m) are about ~ 0.24 to 0.25. If the S_o is estimated with all the data that fall into the three intervals (e.g., H > 200 m), the value is about 0.28, which is similar to three individual S_o values. The results may indicate that the cloud properties such as cloud thickness where the cloud begins to precipitate could be of importance for accurate estimates of S_o by affecting the optimal H interval and/or ranges.

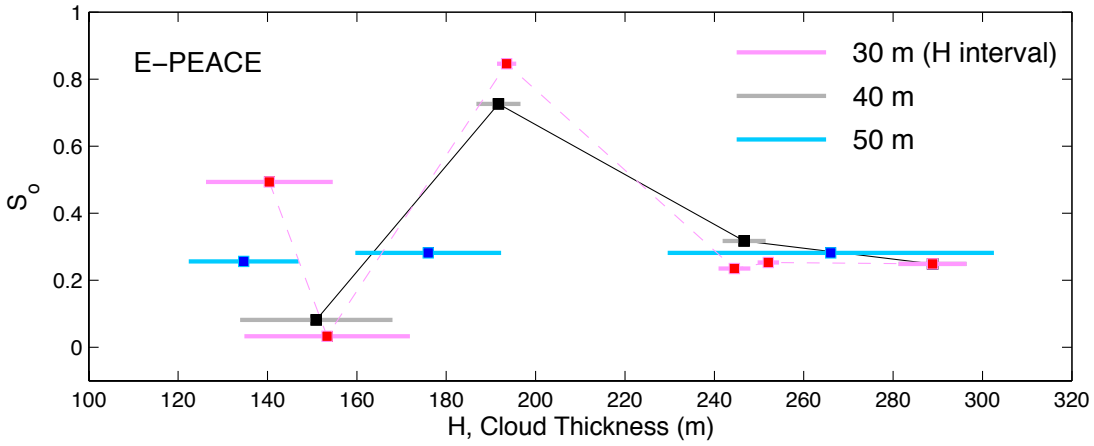

Figure C1. S_o is calculated with cloud data that are averaged over an e-folding time for E-PEACE. S_o calculated with three H intervals (Δ30 m, Δ40 m, and Δ50 m) are shown. Horizontal bar indicates ±1σ cloud thickness for a given H interval.

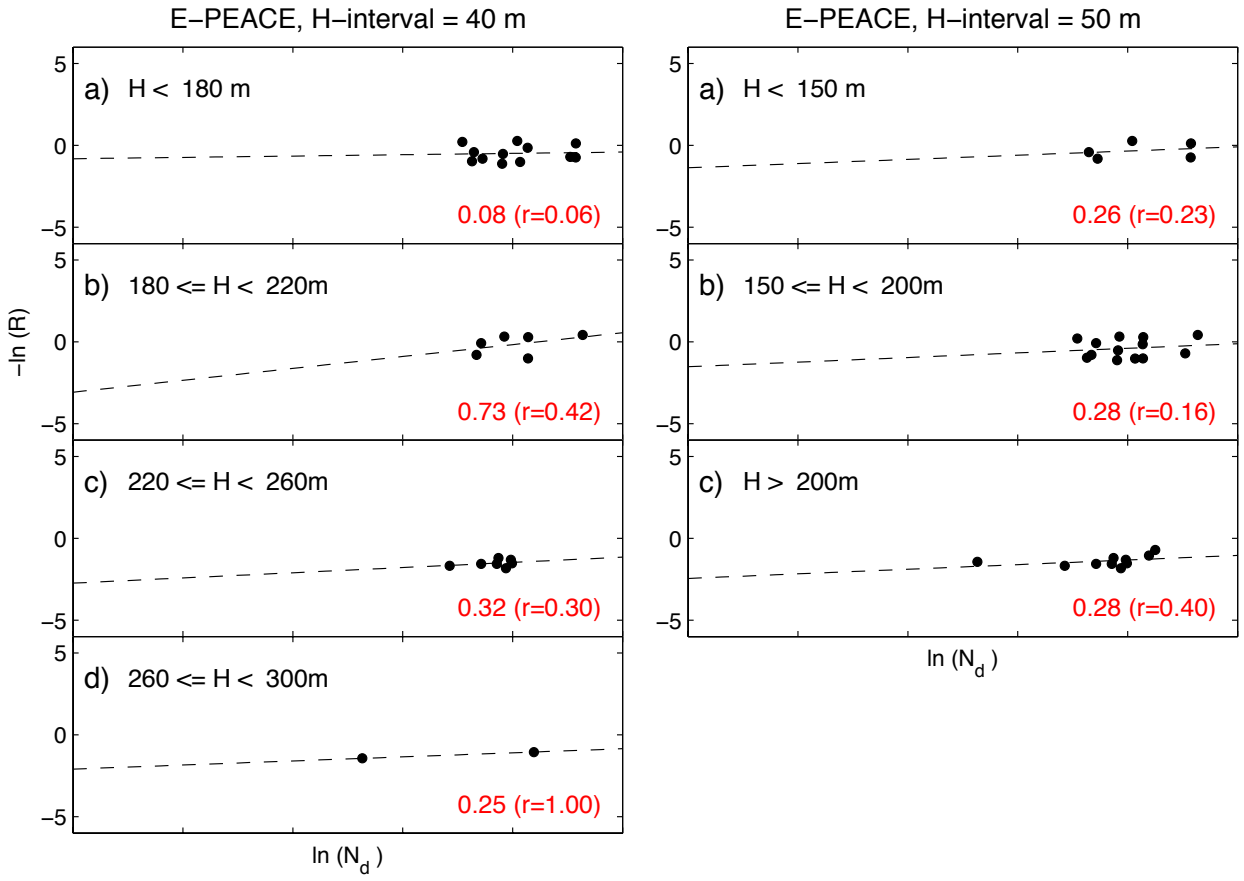

Figure C2. The ln (N_d) and −ln (R) diagrams with fixed H intervals: (left) ΔH=40 m, (right) ΔH=50 m.

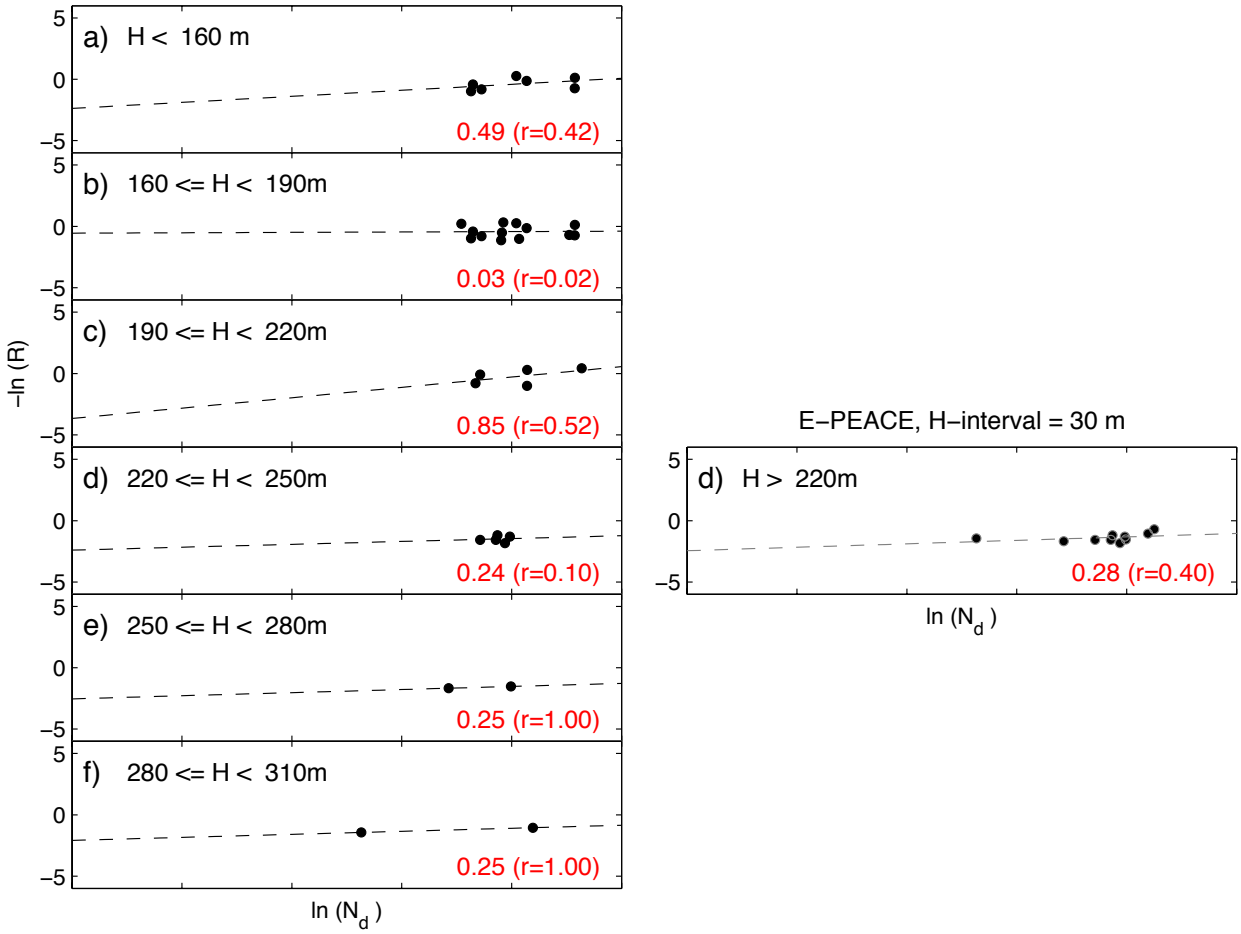

Figure C3. The ln (N_d) and –ln (R) diagrams with fixed H intervals (ΔH=30 m).

P7 L14-15: "We noted that S0 tended : : :. (not shown)." Why do the authors think that when the N_d variations are small, S0 is high? Are N and h covariations leading to unrealistically high S0? Do uncertainties in the slopes increase in this case?

Response: We revised the sentence as follows: " We tested and applied a few criteria in the S_o calculations, such as minimum R thresholds, and the total number of cloud data points and spans of N_d for a given H interval. Based on these sensitivity tests, we calculated S_o exclusively if N_d varied a sufficient amount (e.g., dln(N_d) spans at least 2.2) for a given H interval since little variation of N_d does not provide the proper perturbation of aerosols".

P7 L16: "if dlog(Nd) spans at least 2.2" Is the natural log used here? If so, what is the threshold of max(Nd)/min(Nd) used here? Perhaps around 10?

Response: It is natural log and yes it is around 9. We wanted to consider dataset only if N_d varies large enough because S_o metrics measure changes in R with

changes in N_d. Thus, when N_d changes little, it is not reasonable to calculate S_o. We removed the particular number in the revised manuscript. Further, we changed log to ln in the revised manuscript to avoid confusion.

P7 L16-17: "exceeds six for a given H" – this seems like a very small sample size for calculating slopes. Uncertainties in the slopes should be shown.

Response: There was hardly a case that had only 6 points. The criteria were used when we calculate S_o in every 10 seconds, which corresponded to grey squares in the original Fig. 4. However, in a revised Fig. 4, we did not include gray squares because we additionally calculated S_o over longer time-steps by considering the independence of the 1-second dataset. The smallest data points used for S_o estimates (for Fig. 4) was 23 for BACEX in the lowest H interval and 10 for E-PEACE for the highest H interval. The sentence was removed from the revised manuscript as we no longer include the grey square symbols in Fig. 4.

P7 L20: "statistically significant at the 99% confidence level" - I suspect this means statistically significant with a comparison with a slope of 0. This is only the case if the each 1-second of data is independent of another. The authors need to demonstrate that this is the case, perhaps using the method of Leith (1973) or Bretherton (1999).

Response: We have addressed this by using longer time scales (e.g., e-folding time scale) and by resampling random flights and proved results are still robust.

Leith, C. E. (1973), The Standard Error of Time-Average Estimates of Climatic Means, J. Appl. Meteorl., 12, 1066–1069.
Bretherton, C. S. et al. (1999), The Effective Number of Spatial Degrees of Freedom of a Time-Varying Field, J. Clim., 12,7, 1990-2009.

P 7 L29-30: "S_0 tends to be overestimated: : :" Based on what has been shown so far, it doesn't appear that S_0 in necessarily overestimated when a larger 'averaging length scale' is used. It can be that S_0 is underestimated when every second of data are included.

Response: In Fig. 4, in fact, we did not average the length-scale. S_o with the data of n=4 just indicates that we sub-sample the data every 4 seconds intervals (the data that chosen was still 1-second data but sub-sampled). Since the grey square symbols do not add any further insights to the Fig. 4, we removed the figure and associated text in the revised manuscript.

P7 L32: "H is estimated from the vertical structure of LWC for each day" - If daily mean H is used, then the sub-scale covariance between N and H should be examined, based on the other measurements. To what extent are H and N covarying and how can that potentially affect susceptibility estimates?

Response: We recalculated S_o with data averaged over an e-folding time. By averaging over the cloud data, a cloud-mean H is used that is averaging over both H and N variations, so that their covariability is not consequential in this case (blue below). Further, the dependence of 1-second data is examined by comparing S_o that calculated with 1-second dataset (grey in Fig. 6) with S_o that calculated with data averaged over an e-folding time (blue in Fig. 6).

The overall pattern of the S_o is robust (an increase and then a decrease) (Fig. 6). The main difference between two S_o (by using 1-second data and by using data that averaged over the e-folding time) may be the leftward shift of H that peaks S_o. The e-folding time for VOCALS TO flights is summarized in Table 1.

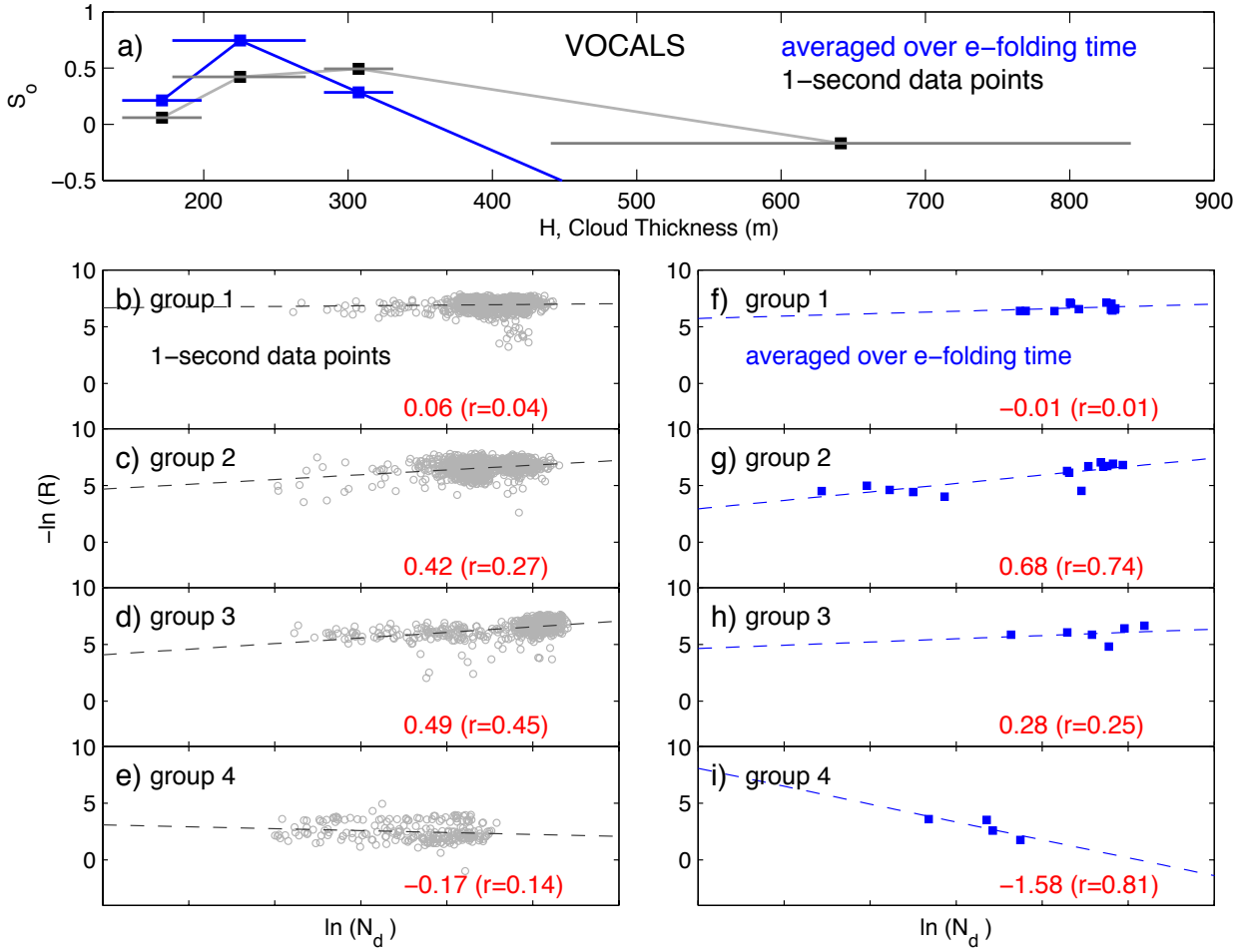

Figure 6. S_o for VOCALS TO flight is calculated with 1-second data (grey) and cloud data that are averaged over an e-folding time for each day (blue). The ln(N_d) and –ln(R) diagram is shown for each H interval. The horizontal bar in (a) indicates ±1σ. S_o is calculated for the cloud data in groups with similar H (shown in Table 1).

P8 L1: "H of 9 Nov. (164+/- 18m)" To what extent is using daily mean H to group data appropriate? What is the true range of H from each day of flight? Are there cases where data from one day could potentially lie in a different bin?

Response: When the H is classified, we carefully chose the bins that are not overlapped withits neighboring bins; consequently, we only ended up with four groups. The cloud thickness for a given day is added in Table 1.

The daily mean H for VOCALS is included in Table 1.

Table 1. Dates used for this analysis during each experiment. Cloud thickness is shown (mean±1σ) for VOCALS with numbers of group category.

No.	VOCALS (Sc)
Period	Oct.-Nov., 2008
Location	Southeast Pacific Sc decks
RF1	10/16 (2), 232
RF2	10/18 (3), 292±22
RF3	10/19 (3)323±16
RF4	10/21 (1) 172
RF5	10/22 (2) 224
RF6	10/26 (2) 208
RF7	10/27 (1) 142±38
RF8	10/30 (2) 213
RF9	11/1 (4) 641
RF10	11/9 (1) 164±18
RF11	11/10 (1) 194±21
RF12	11/12 (2) 249
RF13	11/13 (1) 183

P8 L3: "as the each" – remove "the"

Response: Removed "the" in the manuscript.

P9 L9: "no data were available between 800 m and 1500 m that satisfied the data analysis" – were there not enough data points that existed in this range to calculate the regressions or was the range of N too small? Could bins have been combined to get an estimate? In Fig. 5, it is difficult to make out much of a trend based on three susceptibility estimates.

Response: There was no data point (Please see Fig. 2d)

P9 L17-19: "The negative values of S0 in the largest: : : in that category" – based on the open circle designation (Fig. 4b), it appears that the susceptibility is statistically indistinguishable from zero, so there is no need to explain why it has a negative value.

Response: We reduced text by removing the details.

P9 L20-22: ": : : if the H varied substantially during the cloud-base level-leg flight on the day which S0 was calculated with a daily mean H." I wonder how the susceptibility estimates from the thinner clouds are similarly affected from the VOCALS flights. Can the authors point to any other data or references, which show that the cloud thickness variability in a flight day are smaller than the variability from flight to flight?

Response: This can be referred by Table 1 where the mean H (and 1σ) is shown. H variability within a day for the thinner cloud is larger than daily H variability, if S_o is calculated with a daily mean H. For example, H variability on 10 Nov (RF11) is 21 m (and thus, H ranges 173-215m on 10 Nov.). H variability on 9 Nov (RF 10) is 18 m (and thus H ranges 146-182), indicating that the cloud thickness for these two days overlaps. However, it should be noted that the S_o for VOCALS was calculated with a grouping method where we classified these two days into the same group (i.e., group1). Furthermore, cloud thickness in group1 and group2 for VOCALS does not overlap, and that's why we only had four H intervals for VOCALS dataset.
We agree with the reviewer that the thinner cloud may experience larger uncertainty of H than that in the thicker cloud. It may be possible that if one has a negative S_o in thinner clouds, that could have resulted from the H uncertainty among many possible other sources of the error.

P10 L5-7: "probably show the impacts of meteorology on S0 within the fixed H, because the cloud data points close to each other with similar H are more likely to experience the same meteorology": Although the authors appear to argue that using larger averaging lengths lead to an overestimation of S0, can you not argue that S0 can be underestimated with a shorter averaging length due to covariance between N and H and smaller spatial scales?

Response: We removed S_o calculated with n=1 to n=10 as it does not add more insight and is confusing.

P10 L7: The authors have addressed the similarity in the qualitative behavior of susceptibility between Cu and Sc clouds. Can they comment on how they agree in terms of absolute values? And at which thicknesses the peaks occur? Based on previous studies, is there a prior expectation of whether the peak should occur at the same location (H-value)?

Response: We cannot say anything about the absolute value of H where the S_o peaks across the clouds. However, we suspect that the thickness at which the peaks occur could be related with the cloud thickness where the cloud precipitates. That being said we guess that S_o peaks at a H value slightly higher than H where the cloud begins to precipitate. In fact, we are interested in examining this by using more observational datasets, by considering the normalized cloud depth since the cloud thickness varies spatiotemporally.

P11 L3-5: ": : : indicating a longer tc for the clouds sampled at mid-cloud level compared with those sampled at cloud-base." - In the developing stages of precipitation, this may be true, but if the drops start to fall out, they will eventually fall through bottom of the cloud, which means they will have a longer tc at the bottom of the cloud. One would expect the cloud base measurements to be a combination of parcels with short tc and with long tc.

Response: It is true that the t_c (at cloud base and/or mid-cloud) is related to the cycle of clouds (cloud lifetime cycle) that were sampled. We removed t_c and Z related text from section 3.2 and revised the manuscript accordingly.

P11 L19-20: Include comparison and references to Mann et al., 2014 and Hill et al., 2015.

Response: The references are included.

P11 L27: "Note that not all of the data shown in Fig. 1 in Terai et al. (2012) are used for the S0 calculations in their study." Because their SR included a component coming from Sf, which took into account non-precipitating clouds, all of the data was used to calculate SR. Not all of the data was used for SI.

Response: We removed the sentence in the revised manuscript.

P12 L1-3: "As an example, this R threshold rejects all the data in Fig. 2a.." How about the H in the two datasets? Are there overlaps? Do the H and R values agree between the two studies?

Response: H overlaps between two of the datasets. However, the dataset from VOCALS (C-130) sampled cloud fields mainly in the open ocean (east to west direction) where POC dominates the clouds, and the clouds are thicker and precipitating (more intense and frequent precipitation). In contrast, VOCALS TO flights sampled the cloud fields near the continent where the environment was more polluted, less precipitating and consisted of smaller droplets compared with

clouds sampled from VOCALS C-130 flights. Therefore, even though the cloud overlaps in H and R somehow, clouds in TO flights are mainly thinner with less precipitation.

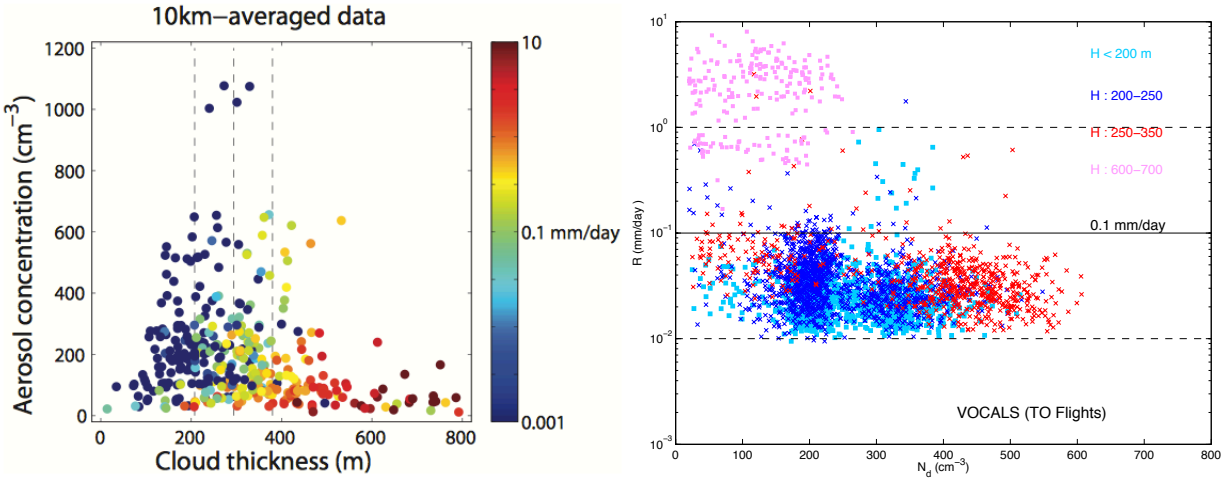

Figure. Cloud data for VOCALS C-130 flights (left) and VOCALS TO flights (right).

P12 L15-16: This is not the case. Their reflectivities were mainly taken from cloudbase retrievals and their N was the accumulation aerosol concentration, not the cloud droplet number.

Response: The arguments on the cloud-base and mid-cloud were removed in the revised manuscript as *R* measurements (converted from *Z*) were taken from the cloud base.

P12 L25: Would the authors summarize the main conclusion of the paragraph? Is it that Terai et al. (2012) examined relationships in mid-cloud level, where accretion rates are high, and therefore, examine only the downward tail of susceptibility?

Response: We simply pointed out that the dataset from VOCALS C-130 flights sampled cloud field where accretion rates are high, and therefore, captures the downward tail of susceptibility predominantly. The argument of mid-cloud level versus cloud-base level associated with t_c was removed and the manuscript is revised.

P13 L4-5: "This procedure can overestimate precipitation for a given Nd" – please elaborate on why this is the case. In many heavily precipitating clouds, the reflectivity is highest at cloud base.

Response: It is true that the reflectivity is highest at cloud base on many occasions in the heavily precipitating clouds, but not all the time. The actual *Z* can be equal to

or less than the column maximum Z because the column maximum Z is the maximum Z along the column.

P13 L28-29: Although the use of sub-cloud aerosol concentration to calculate the susceptibility in Terai et al. (2012) might explain some of the differences between the susceptibility in this study and the susceptibility in their study, they did not make the assumption that the sub-cloud aerosol concentrations and cloud-base Nd were linearly related (see their Fig. 2 and the corresponding discussion).

Response: The manuscript is revised by focusing on some of the discrepancies between S_o in current and Terai et al. could be contributed by the use of sub-cloud aerosols.

P14 L4: replace "Terei" with "Terai"

Response: Corrected.

P14 L6-7: "This method possibly could affect/change the slope: : :" One way to test this is to apply their method to the data in this study to determine whether susceptibility values using the data in this study are indeed overestimated when using their method.

Response: We removed the sentence as Terai et al. (2015) stated that the S_o calculated from the linear regression of the bin mean N_d and R shows nearly identical S_o to that calculated from the tercile log difference method of Terai et al. (2012).

P14 L24-25: "We also note that Z increases with height that is consistent with the H dependent: : :" The Z will also increase with height just from an increase in condensed water that you would get from an adiabatic increase with height.

Response: We removed arguments on Z with heights in the revised manuscript.

P15 L26: "the lower R minimum threshold is desirable to use" – what threshold should the minimum be? Should sedimentation of cloud droplets be included? The appendix in Hill et al. 2015 suggests that the asymptotic limit of S0 for small LWP, where 'precipitation' is dominated by cloud sedimentation, is 2/3.

Response: We think the cloud droplets should include since susceptibility metrics explains of the second indirect effect.

Table 1: In the captions please specify what the numbers in parentheses mean.

Response: Revised as suggested.

Figure 2: What does the dashed line indicate?

Response: The dashed line indicates the Rainfall rate of 0.14 mm day^{-1} and the changes are made in the manuscript.

Figure 3: Please provide the uncertainties in the slopes.

Response: The figure is revised.

Figure 4: What do the lighter pink colors indicate? As in my previous comment, the uncertainties in the slopes should be shown.

Response: Light pink indicates the S_o for the KWACEX. The figure is modified in the revised manuscript.

Figure 5a: What do the horizontal bars indicate?

Response: One standard deviation of D_e. The figure caption is modified.

Figure 6: What do the horizontal bars indicate?

Response: One standard deviation of D_e. The figure caption is modified.

Figure 7a: What do A and B indicate?

Response: The figure caption is modified.

Interactive comment on "Precipitation Susceptibility in Marine Stratocumulus and Shallow Cumulus from Airborne Measurements" by E. Jung et al.

Anonymous Referee #2

Received and published: 10 May 2016

The authors prepare an analysis of precipitation susceptibility based on in situ measurements from four field campaigns with nearly identical aircraft payloads, two that sampled cumulus clouds and two that sampled stratocumulus. The authors report robust patterns, and advance hypotheses for the trends that they find, as well as possible explanations for differences between their findings and the results of past studies. The methodology for how to best make such calculations is not clearly settled upon, as evidenced by some of the sensitivity tests presented, but details are sufficient for this work to be reproduced. I rate that revisions to address the following comments can make this into a methodologically sound contribution that is suitable for publication. In particular, I think it needs to be taken into account whether 1-s samples are statistically independent when evaluating sample size. In addition, the authors seem to conflate sample size and horizontal scale dependence, which appears illogical. I also could not follow the arguments about

autoconversion versus accretion using this data set, leaving final statements seeming unsupported by the evidence provided. Comments are enumerated below.

1. There should be some guidance on the spatial scale over which equation 1 applies. A reader must assume implicitly based on this work that it is intended to apply to one second of flight time (100 m in horizontal and full vertical column)? Also a GCM grid cell (100 km in horizontal and full vertical column)? Really both identically? Please offer at least brief guidance for the reader in the introduction.

Response: revised as suggested in the introduction (near Eq. (1) and near the end of the introduction)

2. Can you pls comment on whether treating Nd as a proxy for Na has any relevant consequences? For instance, does that proxy give stronger So than using Na owing to a decreasing fraction of aerosol activated with Na increasing, all else being equal?

Response: We added the follows in the last section of the discussion: "In cases where sub-cloud aerosols are used for the S_o estimates, these estimates give a smaller S_o than those using N_d due to the decreasing fraction of aerosol activated with N_a increasing, all else being equal (e.g., Lu et al., 2009)"

3. I recommend revising the text to reflect the fact that not all current climate models use equation 2, such as those with prognostic precipitation species.

Response: Revised as suggested (near Eq. 2)

4. Should GCCM be GCM throughout?

Response: Corrected in the manuscript.

5. Using 1-second data, there is a big enough sample volume to accurately calculate Z from dZ/dD? For instance, can you show evidence that your 1-s sample volume is large enough to produce a smoothly continuous DSD? If everyone except me knows that this is possible, perhaps you can just point to a reference or provide a figure outside of the manuscript.

Response: In a revised manuscript we removed Fig. 5(b and c).

6. Page 6, line 17: It is stated that figure 2 "essentially shows that as Nd increases, R decreases." I would not jump to that conclusion from that figure. The amount of scatter around the trend in figure 3 demonstrates why. I would recommend leaving this statement out of the introduction to figure 2 and focusing instead on the fact that it shows well the range of R and Nd sampled during each experiment.

Response: Removed as suggested.

7. Page 7, paragraph containing line 25: Can the authors present evidence to indicate that sequential 1-s samples are statistically independent? It seems to me that a methodologically appropriate test of sample size for this study would be to randomly resample the data (if consecutive 1-s points are statistically independent) or else randomly resample the flights used (if they are not).

Response: We calculated S_o by randomly resampling the flights as the reviewer suggested and the behavior of S_o is robust (e.g., Fig. 8). The details are summarized in section 3.2 in the revised manuscript.

In this section, we estimated S_o by randomly resampling the flights of E-PEACE to see whether the sequential 1-second samples are statistically independent. We mainly used 12 flights in this part (Fig. 6 and Fig. 8) to avoid further complication by including RF13 of which e-folding time of N_d is much shorter than other flights (several seconds compared with 4-10 minutes of other flights. See Table 1 for the e-folding time).

S_o calculated with random flights, at first glance, showed two distinctive types of behavior (Fig.7A). One is a similar pattern to that of the current S_o (red and magenta in Fig. 7A) shown in Fig. 4 while the other is an almost constant S_o near zero (blue and cyan in Fig. 7A).

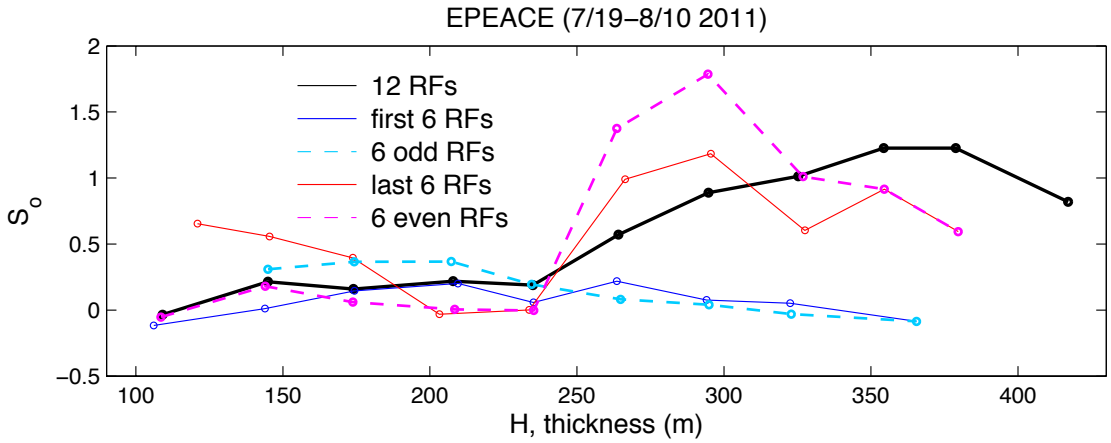

Figure 7A. S_o calculated from the randomly resample the flights.

The cloud data sampled during E-PEACE formed two groups (denoted as A and B in Figure 7). For example, group B lie in the lower- and left- side of the diagram that has lower R for the given N_d, but also includes top two highest R flights (RF 13 and RF3). Group B include RFs 3, 5, 6, 9, 10 and 13, and one whereas group A include flights 2, 4, 6, 7 11, and 12.

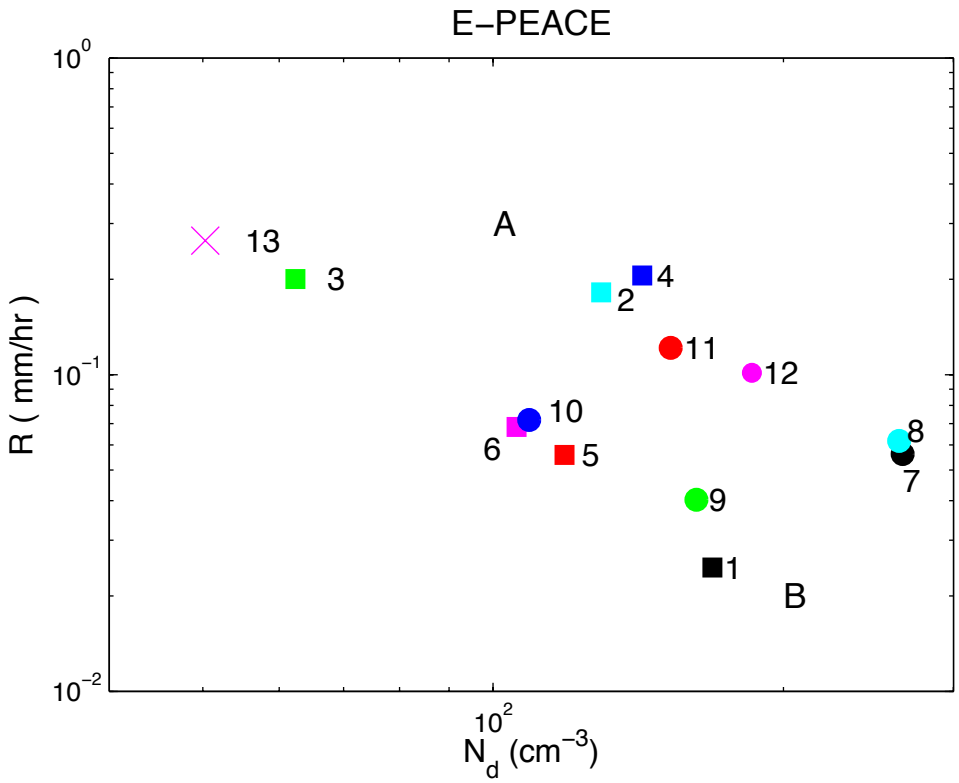

Figure 7. Daily mean values of N_d and R for the 13 E-PEACE flights. Numbers indicate the flight numbers shown in Table 1.

The S_o calculated with cloud data of group A and B is shown in Fig. 8. The S_o pattern calculated with cloud data of group A is similar to S_o shown in Fig. 4: S_o is constant at lower H, followed by an increase then a decrease (Fig. 8a). In contrast, S_o values calculated from group B were relatively constant near zero S_o with the descending branch only (blue in Fig. 8c). It is of interest in Fig. 8 that if the S_o is calculated with cloud data within the same category (upper or lower groups), the So shows the robust pattern (Fig. 8b and 8c). We did not examine here why the cloud properties in group A and B are substantially different, but it would be of interest for future work.

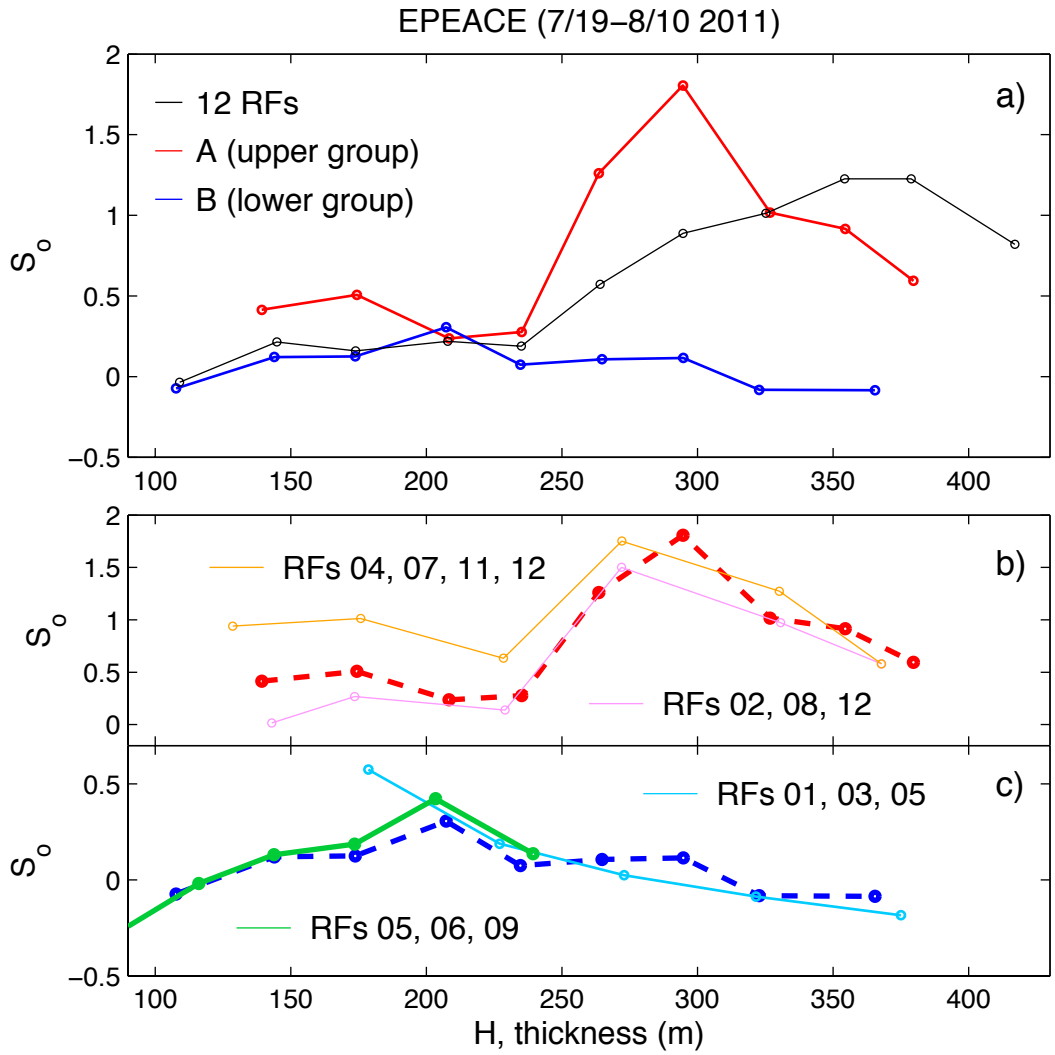

Figure 8. S_o with cloud thickness for (a) 12 E-PEACE flights, for groups A and B shown in Fig. 7. (b) S_o calculated with randomly resampled RFs within the group (b) A and (b) B.

Further analysis shows that the two RFs (RF13 and RF03) that have relatively small N_d with high R makes the differences in the S_o pattern, depending on whether we include the data from those two low-N_d with high R into the dataset or not. For example, 6 odd flights (RFs, 1,3,5,7,9,11) and the first 6 RFs (RFs, 1-6) in Fig. 7A include RF03. Figure 9 also shows that if the S_o is calculated with cloud data that do not include data from clean with heavy precipitating environments (i.e., RF13 and RF03), S_o shows a similar pattern as that in Fig. 4. This also links to #11 (below) that shows how RF03 and RF13 changes the pattern of S_o.

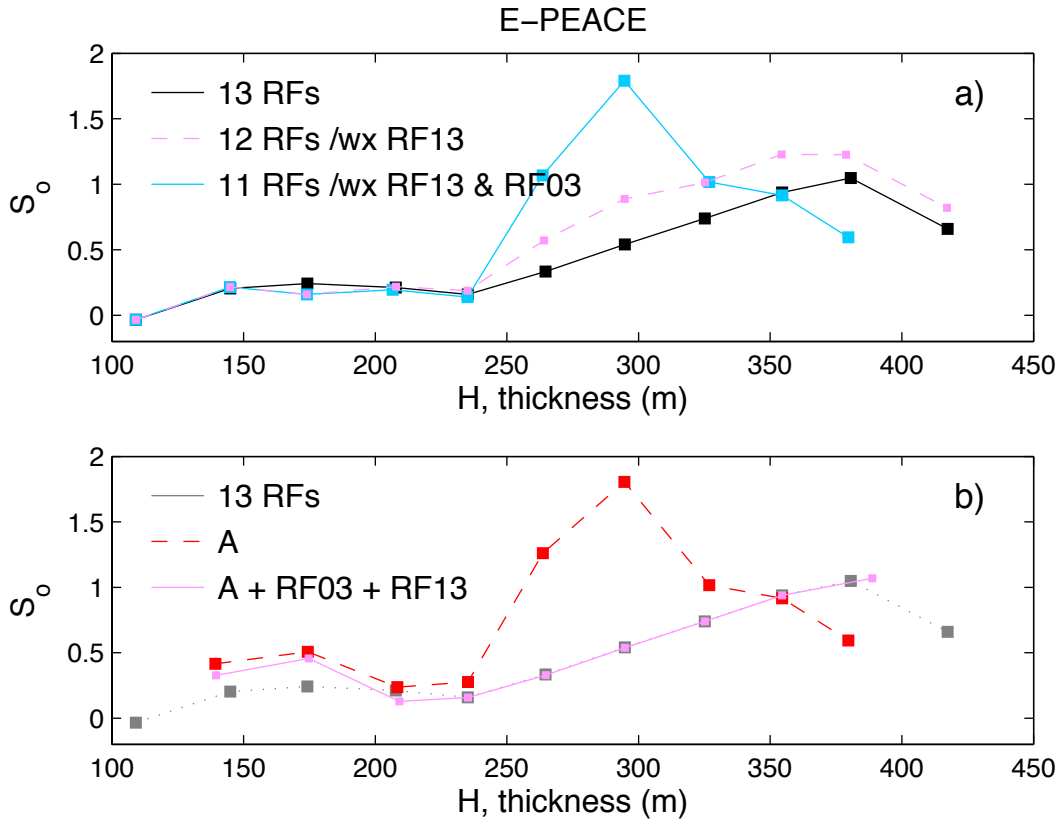

Figure 9. The effects of RF03 and RF13 on S_o estimates. (a) S_o calculated for 13 flights during E-PEACE in addition to when either, or both, RF03 and RF13 are excluded. RF03 and RF 13 are the flights with high precipitation rates. (b) S_o is calculated from group A with and without RF03 and RF13. R and N_d information for each flight is shown in Fig. 7.

8. Page 8, lines 9-11: Are the authors suggesting to use one LWP profile for each date for Sc and Cu? Unclear if this statement is limited to Sc.

Response: The sentence applies to both Sc and Cu. However, no one wants to do this for Cu. The text was revised as follows: Nevertheless, if we calculate LWP by integrating LWC with height (e.g., in Sc), we would obtain one LWP profile that could be used for the entire cloud layer on a given day.

9. Page 10, first paragraph: This logic is not sound as currently written. First the authors state that So decreases with increasing sample size. There must be a limit to that if the system is well-defined and the significance of the results robustly evaluated, right? Then the authors compare such behavior to that found by others when decreasing the averaging length scale, which is a different issue entirely (see comment 1).

Response: The reviewer raises a good point and our original text was distracting. To address this point, we removed the time-averaging argument as it does not add any further insight in this study, but causes confusion.

10. 2nd paragraph of section 3.2: I really couldn't follow this paragraph. I would remove section 3.2 and figures 5 and 6 if the point of this paragraph can't be significantly clarified. Stating "But it is not discussed here." furthered this reader's impression that the Z analysis did not really add anything to this study.

Response: We removed arguments on the mid-cloud level versus cloud-base and the relevant argument as the process is associated with the cycle of cloud lifetime.

11. Page 11, line 23: There is no reason to show a figure such as A2. Simply state that results are insensitive. I would be much more interested to see a clear demonstration of a case where the R threshold is very important. It seems clear to the authors, but is not so clear to me how figure 4 would be affected, for instance.

Response: We replaced Fig. A2 with revised Fig. A2 that includes the S_o calculated with different R thresholds (R > 0.1, 0.5, 1.0, 1.5 and 2.5 mm/day). Figure A2 shows that S_o become closer to zero as the R threshold increases (as So is not sensitive under the heavy precipitation). The Text has revised accordingly.

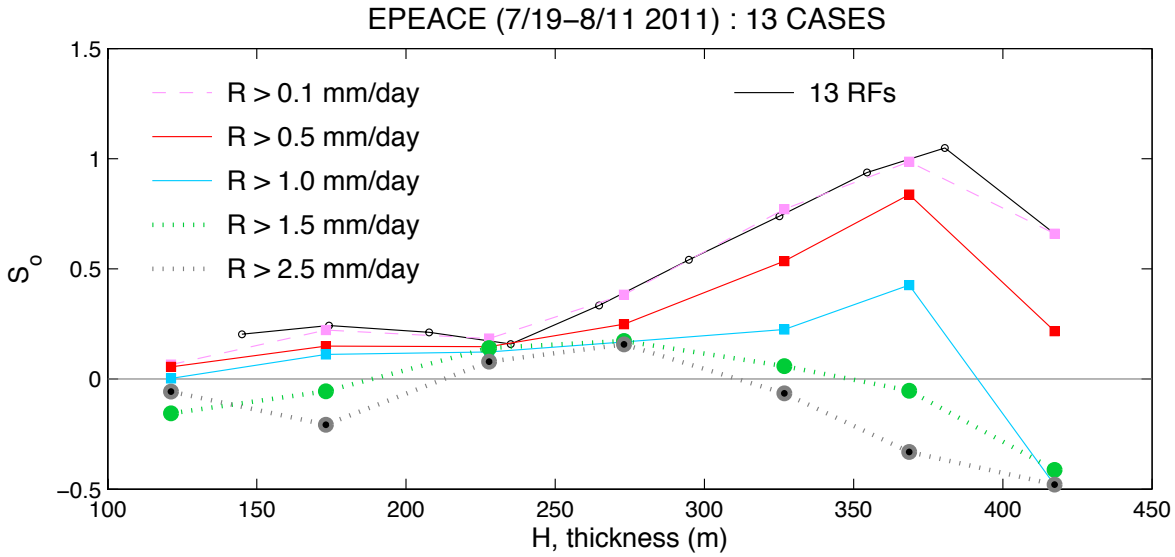

Figure A2. Precipitation susceptibility with the R thresholds.

Further, S_o calculated with cloud data sampled during (1) RF13, (2) RF3, (3) RF13 and RF3, and (4) RFs 2,3,4, and 13 show the same results, which supports the insensitivity of S_o under the high precipitation conditions (due to the dominance of accretion process) (Figure 11A shown below).

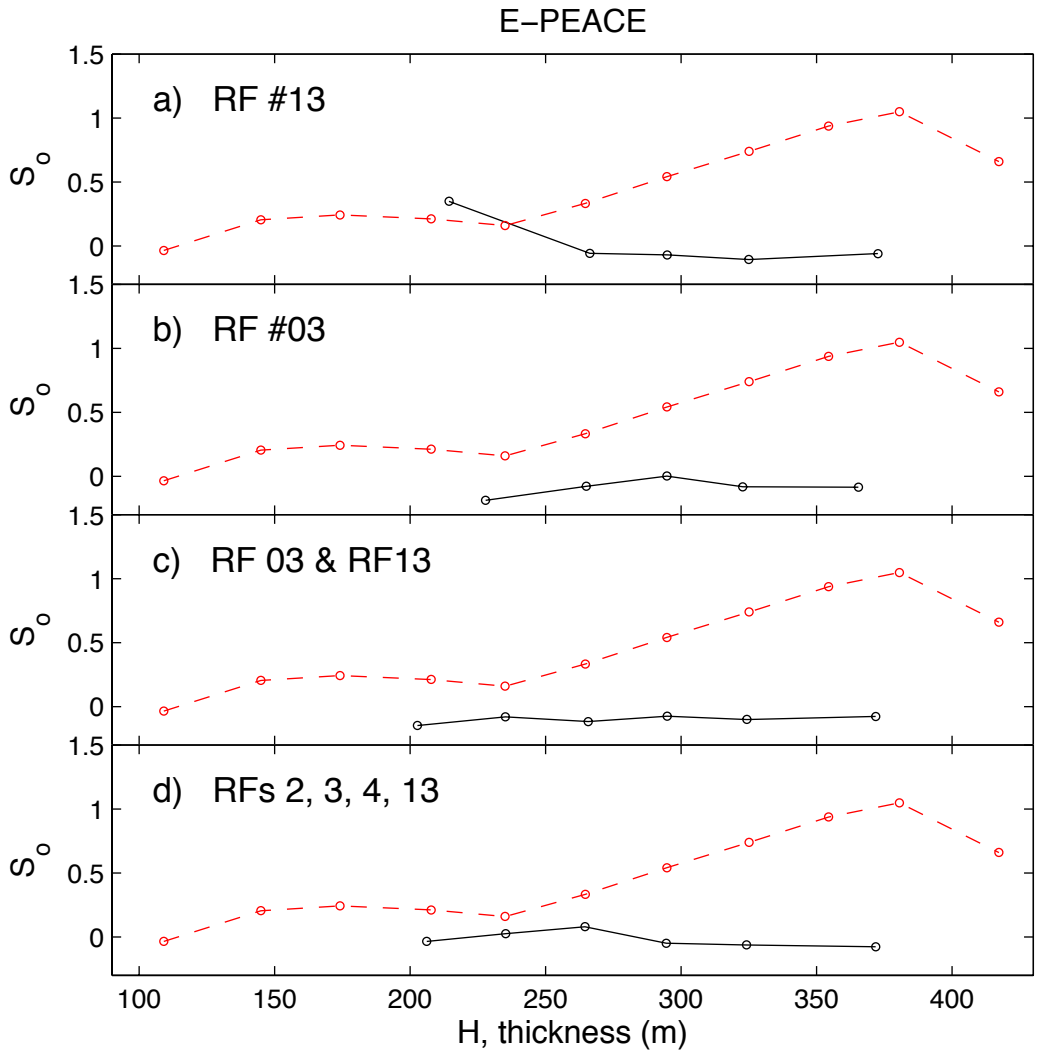

Figure 11A. So calculated with cloud data sampled during (a) RF 13, (b) RF 3, (c) RFs 3 and 13, and (d) RFs 2, 3, 4, and 13. The flights are chosen based on N_d and R diagram where those flights sampled under the high precipitation conditions (The figure is not shown in the revised manuscript).

In addition, the effect of precipitation on the S_o estimates is also shown in Fig. 9 (above #7).

12. Page 14, line 24: I really did not take away the autoconversion versus accretion behavior. There seemed to be a lot of handwaving in section 3.2. I basically feel that this statement is just not supported by the material shown. I think this needs to be much clarified or else removed.

Response: We removed t_c and Z related text from section 3.2 and revised the manuscript accordingly.

13. I don't understand the last sentence of the paper. The authors call for more studies on which range of H is most susceptible to preciptiation rate? This is a study on susceptibility of precipitation rate to Nd. Are the authors suggesting another thing? If the authors meant to further study So as defined here, why are further studies needed? All previous sentences in the last paragraph would indicate that the authors have already shown within which range of H Sc and Cu are most susceptible. Are these results somehow uncertain or incomplete? If that could be clarified and its relevance to the conclusions made here (regarding the general behavior of So in Sc and Cu found; is that uncertain?), I think that would better support this closing argument, if I understand it correctly.

Response: We removed the last sentence.

14. So many grammatical errors appear here in a paper with so many capable coauthors that I will not take my time to enumerate them, but merely note that this sometimes impacted my ability to evaluate the work (as in comment 13 above).

We carefully went through the text and corrected the language.

15. Please label N_d axis units on figures 2 and 3.

Response: Labeled as suggested.

Precipitation Susceptibility in Marine Stratocumulus and Shallow Cumulus from Airborne Measurements

Eunsil Jung[1], Bruce A. Albrecht[1], Armin Sorooshian[2,3], Paquita Zuidema[1], Haflidi H. Jonsson[4]

[1]Department of Atmospheric Sciences, University of Miami, Miami, FL, 33149, United States
[2]Department of Chemical and Environmental Engineering, University of Arizona, Tucson, AZ, 85721, USA
[3]Department of Hydrology and Atmospheric Sciences, University of Arizona, Tucson, AZ, 85721, USA
[4]Naval Postgraduate School, Monterey, CA, 93943, USA

Correspondence to: Eunsil Jung (eunsil.jung@gmail.com)

Abstract. Precipitation tends to decrease as aerosol concentration increases in warm marine boundary layer clouds at fixed liquid water path (LWP). The quantitative nature of this relationship is captured using the precipitation susceptibility (S_o) metric. Previously published works disagree on the qualitative behavior of S_o in marine low clouds: S_o decreases monotonically with increasing LWP or cloud depth (H) in stratocumulus clouds (Sc), while it increases and then decreases in shallow cumulus clouds (Cu). This study uses airborne measurements from four field campaigns on Cu and Sc with similar instrument packages and flight maneuvers to examine if and why S_o behavior varies as a function of cloud type. The findings show that S_o increases with H and then decreases in both Sc and Cu. Possible reasons for why these results differ from those in previous studies of Sc are discussed.

1 Introduction

Cloud-aerosol interactions are considered to be one of the most important forcing mechanisms in the climate system (IPCC, 2013). It is believed that aerosols suppress precipitation in warm boundary layer clouds. However, there is considerable disagreement on the magnitude and even on the sign of how aerosol perturbations affect cloud fraction and lifetime (Stevens and Feingold, 2009). Furthermore, aerosol effects on clouds and precipitation are not readily separable from the effects of meteorology. The precipitation susceptibility metric, S_o, quantifies how aerosol perturbations alter the magnitude of the precipitation rate (R) while minimizing the effects of macrophysical factors (i.e., meteorology) (Feingold and Siebert, 2009). It is defined as

$$S_o = -\frac{d\ln R}{d\ln N_d}, \quad (1)$$

and is evaluated ~~with~~ at fixed cloud macrophysical properties, such as cloud thickness (H) or liquid water path (LWP). In Eq. (1), aerosol effects are embedded in the cloud droplet number concentration (N_d) variable since aerosols serve as cloud condensation nuclei (e.g., as aerosol concentration increases, N_d increases). The minus sign is used in Eq. (1) to achieve a positive value of S_o due to the expectation that increasing aerosols reduce precipitation (all else fixed). Towards improving

the representation of precipitation in larger-scale models, the application of Eq. (1) has also been studied using more highly resolved models and remote sensing (e.g., Feingold and Siebert, 2009; Sorooshian et al., 2009; Terai et al., 2015; Hill et al., 2015). In the original work on~~of~~ S_o (Feingold and Siebert, 2009), cloud-base R and N_d were used. Since then, slightly different definitions of S_o have been ~~adapted to present S_o~~applied~~, depending on the dataset used~~. For example, Sorooshian et al. (2009) used an aerosol proxy (e.g., Aerosol Optical Depth and Aerosol Index) instead of N_d for their satellite data analysis. Terai et al. (2012, 2015) ~~introduced~~ further defined precipitation susceptibility ~~using~~ as the sum of the susceptibilities of drizzle intensity (S_I) and drizzle fraction (S_f), $S_R = S_I + S_f$, where ~~S_f is equivalent to S_{pop} (probability of precipitation) and~~ S_I is analogous to S_o but ~~S_o is~~ calculated exclusively for ~~the~~ clouds that produce measurable precipitation. ~~and thus~~ S_I is equivalent to S_o only~~for the clouds~~ when 100 % of the sampled clouds are ~~fraction is~~ precipitating. Other studies focus on the probability of precipitation (~~precipitation rate of those clouds that are precipitating. The~~ POP), ~~is~~ defined as the ratio of the number of precipitating events over the total number of cloudy events. ~~The~~ S_{pop} is used in some studies of precipitation susceptibility (e.g., Wang et al., 2012; Mann et al., 2014; Terai et al., 2015), and is equivalent to the S_I used within Terai et al. (2012). ~~,~~ In addition to the different definitions of precipitation susceptibility, various forms of R and N_d (e.g., cloud-base, vertically integrated, or ground-based values) with different data thresholds have been used for the calculation of the precipitation susceptibility depending on the data available. In this study, precipitation susceptibility indicates S_o as defined in Eq. (1) unless otherwise stated.

In global climate models (GCMs), these aerosol effects on precipitation are represented by either a prognostic scheme or an empirical diagnostic scheme.~~In an empirical scheme ,~~When GCMs consider aerosols~~ at all, GCMs~~the rainrate R is often ~~parameterized R~~ in terms of LWP and N_d as Eq. (2).~~the collision coalescence process (see Sect. 3.2), which is parameterized by a power-law relationship among R, LWP, and N_d as~~,

$$R = LWP^{\alpha} N_d^{-\beta}. \quad (2)$$

Climate models typically assume a fixed value of the autoconversion parameter (β in Eq. 2), ranging between approximately 0 and 2 (e.g., Rasch and Kristjansson, 1998; Khairoutdinov and Kogan, 2000; Jones et al., 2001; Rotstayn and Liu, 2005; Takemura et al., 2005). S_o in Eq. (1) is equivalent to the exponent β in Eq. (2) at fixed LWP. F~~For f~~ield studies of precipitating stratocumulus (Sc) clouds have reported ~~,~~β values ranging from ~~has been reported in the range of~~ 0.8 to 1.75 at fixed LWP (e.g., Pawlowska and Brenguier, 2003; Comstock et al., 2004; vanZanten and Stevens, 2005; Lu et al., 2009). However, such ~~these~~ single power law fits do not capture~~show~~ the changes in S_o with LWP or H, which is important since previous works have revealed that the response of cloud rainrates to aerosol perturbations vary ~~within specific ranges~~as a function of LWP (or H)~~ are more susceptible to aerosol perturbations in terms of changes in precipitation~~.

The qualitative behavior of S_o has been studied for low clouds using models, remote sensing data, and in situ measurements. For model studies of warm cumulus clouds (e.g., the adiabatic parcel model of Feingold and Siebert, 2009), S_o varies from 0.5 to 1.1 with increasing LWP, and exhibits three regimes. ~~At low LWP, S_o is insensitive to aerosol~~

perturbation where clouds do not precipitate. At low LWP, not enough water is available with which to initiate rain, and S_o is insensitive to aerosol perturbations. At intermediate LWP, suppression of collision-coalescence by the increased aerosols is most effective. We will refer to this regime as the ascending branch of S_o following Feingold et al. (2013). At high LWP, the precipitation rate is more strongly influenced by the LWP, and S_o decreases with increasing LWP (the hereafter the descending branch of S_o). This LWP-dependent pattern of S_o is supported by satellite observations (Sorooshian et al., 2009; 2010) and large-eddy simulations (LES) (Jiang et al., 2010) for warm trade cumulus clouds. In contrast, Terai et al. (2012) showed that S_R monotonically decreased with increasing LWP and H in Sc clouds by usingbased on in- situ measurements acquired during the VOCALSVAMOS Ocean-Cloud-Atmosphere-Land Study-Regional Experiment (VOCALS-REx) field study, while their S_I, value,[which is similar to S_o in aforementioned studies, did not reveal any significant change with H and maintained a value of ~0.6. These inconsistent results have raised questions of how cloud type impacts behavior of S_o as a function of either H or LWP.

To begin to unravel why differences in the various studies exist, Feingold et al. (2013) showed in modeling studies that the time available for collision-coalescence (t_c) is critical for determining the LWP-dependent behavior of S_o, and may be at least partly responsible for some of the differences. Gettelman et al. (2013) also showed how the microphysical process rates impact S_o in a global climate model (the NCAR Community Atmosphere Model version 5 (CAM5) global climate model (GCCM.)). They showed that the behavior of S_o with LWP differs between the GCCM and the steady-state model of (Wood et al., (2009); tThe values of S_o were constant or decreased with LWP in thea steady state model (consistent with Terai et al., 2012; Mann et al., 2014), whereas the GCM LWP-dependent S_o behavior was found in the GCCM (was more consistent with Feingold and Siebert , (2009). ;; Sorooshian et al. , (2009, 2010). ; Jiang et al. , (2010). ; Feingold et al. (2013), and; Hill et al. (2015). In their study, aAltered microphysical process rates were able to significantly changed the values magnitudes of S_o, but the qualitative behavior of S_o with LWP remained unchanged (i.e., S_o increases with LWP, and peaks at an intermediate LWP thenbefore decreasesing with LWP). More recently, Mann et al. (2014) analyzed 28 days of data from the Azores Atmospheric Radiation Measurement (ARM) Mobile Facility where the prevalent type of clouds are cumulus (20 %), cumulus under stratocumulus (10-30 %) and single-layer stratocumulus (10 %). They showed that S_{pop} slightly decreased with LWP. Terai et al. (2015) estimated precipitation susceptibility (S_I+S_{pop}) in low-level marine stratiform clouds, which included stratus and stratocumulus clouds, using satellite data. The values of S_o in their study generally showed similar behavior to that reported by Mann et al. (2014). Hill et al. (2015) examined how the representation of cloud microphysics in climate model contributes to the behavior of S_o. They found it work shows that single-moment precipitation schemes, which are commonly used in GCMs, produce the largest uncertainty in S_o. Only through increasing the number of prognostic moments (i.e., multi-moment schemes capable of prognosing prognosticatingprognosing the rain droplet number as well as mass) couldreduces the scheme dependence of S_o on a particular scheme be reduced.

~~This study is motivated by the~~The inconsistent behavior of S_o in previous studies for warm boundary layer clouds motivates the current study. The focus of this paper is to examine and compare the qualitative behavior of S_o in Cu and Sc using similar airborne measurements encompassing~~across~~ four field campaigns. Two~~ of them~~ were focused on Sc clouds (VOCALS-Rex and the Eastern Pacific Emitted Aerosol Cloud Experiment, Sect. 2.2) and two campaigns~~of them~~ targeted Cu clouds (Barbados and Key West Aerosol Cloud Experiments, Sect. 2.3). The strength of these four field campaigns' ~~s~~ airborne measurements is that the same research aircraft was deployed ~~in the campaigns~~ with a similar flight strategy and instrument packages, ~~which~~ facilitating a~~es~~ comparative analysis. Each of the~~These~~ four field experiments ~~have each~~ ~~been~~ sampled over an area of about 100 × 100 km, and thus, the interrelationships examined are representative of the GCM spatial resolution. Data and methods are discussed in Section 2, followed by results and discussion in Sections 3 and 4, respectively. The findings are summarized in Section 5. Acronyms used in this study are listed in Table A1 of the Appendix.

2 Data and methods

2.1 TO aircraft

The Center for Interdisciplinary Remotely Piloted Aircraft Studies (CIRPAS) Twin Otter (TO) research aircraft served as the principal platform from which observations for these four experiments were made. During these four deployments, the TO supported~~had~~ similar instrument packages, and performed~~made~~ similar cloud sampling ~~flight~~ maneuvers ~~in the vicinity of clouds~~, including vertical soundings and level-leg flights below, inside, and above the clouds. Each research flight ~~had a duration of~~lasted ~3-4 hours. The TO included the following three *in-situ* probes for characterizing aerosol, cloud, and precipitation size distributions: the Passive Cavity Aerosol Spectrometer Probe (PCASP), Cloud Aerosol Spectrometer (CAS) and Cloud Imaging Probe (CIP), with each ~~that~~ resolving~~e~~ particles of~~in~~ diameters ~~ranges from~~ 0.1–2.5 μm, 0.6-60 μm and 25-1550 μm, respectively. A zenith-pointing 95-GHz Doppler radar was mounted on top of the aircraft and detected cloud and precipitation structures above the aircraft. Detailed information of the instruments on the TO and flight strategies is provided elsewhere (Zheng et al., 2011; Jung, 2012). All the instruments were operational during the flights analyzed in this study except for the cloud radar, which was not operational during the VOCALS TO flights.

S_o is ~~consistently~~ calculated from Eq. (1) ~~with~~ within bins of the cloud thickness H ~~as the macrophysical factor~~. H was estimated as the height difference between cloud tops and bases. Cloud tops were determined by the cloud radar with a time ~~the~~ resolution~~s~~ of 3 Hz ~~in time~~ and vertical resolution of 24 m (5 m) in height for Cu (Sc) ~~while the TO was flying near the cloud base (cloud base level leg flight)~~. Cloud bases of Cu were determined by the~~from~~ l~~L~~ifting c~~C~~ondensation l~~L~~evel (LCL) ~~, which were~~ calculated from the average thermodynamic properties of the sub-cloud layer for a given day. ~~cloud base determined .Since the cloud base level leg flight was designed to fly as close as possible to the cloud base,~~ The ~~and further,~~

LCL varied little for Cu, for example, during the Barbados Aerosol Cloud Experiment (Sect. 2.3), t~~.~~ The LCLs were ~~(~~653.9±146 m on average from the aircraft measurements, which agreed with the two-year LCL climatology ~~of LCL~~ in this region (700±150 m) as documented in~~by~~ ~~e.g.,~~ Nuijens et al. (2014)~~.~~ ~~)~~. ~~A~~lthough it is not shown in this study, ~~,~~ S_o was also estimated by using the cloud base heights determined from the Cu cloud-base level-leg flights; these ~~and the~~ results were ~~using these cloud base heights gave results~~ similar to those based on the sub-cloud LCL.

In stratocumulus clouds, cloud tops are well defined due to the strong capping temperature inversion (see Zheng et al., 2011)~~;~~ ~~however~~and~~,~~ cloud bases vary more than tops (e.g., Fig. 2 of Bretherton et al., 2010). As a result, the way that the cloud-base is determined may affect S_o since the changes in cloud base alternatively can change the cloud thickness. Therefore, we estimate S_o using three different definitions for cloud base. The first method is with LCL calculated from the average thermodynamic properties of the sub-cloud layer (shown as cb-lcl in Fig. 4, same as Cu). For the second and third definitions (cb-local~~l~~ and cb-mean), cloud bases are determined from the lowest heights where the vertical gradients of liquid water contents (LWC) are the greatest from the LWC profiles. The ~~, where the~~ LWC profiles are obtained i) when the aircraft enters the cloud decks to conduct level legs (cb-local), and ii) from the nearest one or two soundings to the cloud-base level-leg flights. The average height of these two lowest heights (cb-mean, the average of i and ii) is used in this study, along with cb-lcl and cb-local (Fig. 4 later). In general, the heights approximately corresponded to the lowest heights that the liquid water contents (LWC) exceeded 0.01 g m^{-3}. S_o was also estimated by using the heights from the cloud-base level-leg flights as the cloud bases as did for Cu, and the qualitative behavior of S_o was preserved (not shown).

N_d and R were calculated from the drop size distribution (DSD), which is obtained from CAS (forward scattering) and CIP probes during the cloud-base level-leg flights, respectively. The CAS probe acquires data every 10 Hz and then the DSDs at each channel are averaged to 1 Hz. The CIP acquires data every 1 second. ~~, but CAS and CIP probes acquire data every 10 Hz then the DSDs at each channel are averaged to 1 Hz second.~~ The ~~,~~ ~~and~~ cloud radar samples at ~~receives data every~~ 3 Hz and then is averaged to 1 Hz to ~~pair with~~match the probe data. Therefore, N_d, R and H in Eq. (1) were calculated in 1 s resolution (except for VOCALS-Rex, see Sect. 2.4). The ~~dependence of 1-second data and the effects~~impact of using one-second data on the S_o estimates will be discussed later in Sect. 3.2. R is defined as

$$R = \frac{\pi}{6}\int_{25\mu m}^{1550\mu m} N(D)D^3u(D)dD \text{ ,}$$

~~$$R = \frac{\rho}{6}\int_{25mm}^{1550mm} N(D)D^3u(D)dD \text{ ,}$$~~

~~(3)~~

~~where $u(D)$ (m s^{-1}) is the terminal fall velocity following Gunn and Kinzer (1949) and $N(D)$ (m^{-3} mm^{-1}) is the number of drops in a unit volume and given diameter interval dD centered at D (mm).~~ ~~where~~ where $u(D)$ is the fall speed of a drop with

Field Code Changed

diameter D. Three fall speed formulations are used: (1) $u = k_1 r^2$ with $k_1 \approx 1.19\times10^6$ cm^{-1} s^{-1} was used for cloud droplets up to 30 µm radius; (2) $u = k_3 r$ with $k_3 \approx 8\times10^3$ s^{-1} was used for the size range of 40 µm < r < 0.6 mm; and (3) $u = k_2 r^{1/2}$ with $k_2 \approx 2.01\times10^3$ cm$^{1/2}$ s^{-1} for droplets of 0.6 mm < r < 2 mm.

~~Radar reflectivity Z is calculated from drop size distributions that were obtained from CAS and CIP probes. CAS DSD and CIP DSD were combined to include cloud droplets, rain embryo and drizzle drops, Z=10log(z), where~~

~~$z = \int N(D) D^6 dD$,~~ ~~(4)~~

~~in units of mm^{6}m^{-3}.~~

2.2 Stratocumulus cloud field campaigns: VOCALS-Rex and E-PEACE

From October to November 2008, the VAMOS Ocean-Cloud-Atmosphere-Land Study-Regional Experiment (VOCALS-REx) took place over the Southeast Pacific (69°W-86°W, 12°S-31°S), an area extending from the near coastal region of northern Chile and southern Peru to the remote ocean (Zheng et al., 2011; Wood et al., 2011; also see Fig. 1). Three aircraft were deployed during VOCALS from 14 October to 15 November (NSF/NCAR C-130, DOE G-1, CIRPAS TO). ~~As one of the observational platforms, T~~the TO sampled more coastal marine stratocumulus decks ~~in the~~ near ~~coastal region of the VOCALS domain of~~ 20 °S 72°W (Fig. 1) than the other two planes. Readers should note that the ~~the~~ data in Terai et al. (2012) used for their S_{R_e} calculations, ~~with which we will compare with later,~~ were also obtained from VOCALS. However, their results were based on NSF/NCAR C-130 flights that sampled cloud decks away from the coastal area (Fig. 1). ~~In the Southeast Pacific Sc decks, the intensity and frequency of drizzle tends to increase westward from the coast (Bretherton et al., 2010).~~ Wood et al. (2011) provide a comprehensive description of VOCALS experiments and Zheng et al. (2011) provide a description of ~~for the~~ TO aircraft data during the VOCALS. ~~Thirteen out of eighteen VOCALS TO flights were analyzed to consider typical Sc decks exclusively, by excluding~~ TO ~~d~~data ~~obtained~~ from flights with decoupled boundary layers, abnormally higher cloud bases, and moist layers above cloud tops were excluded, reducing the total number of flights analyzed to thirteen from the original total of eighteen (Table 1).

From July to August 2011, the Eastern Pacific Emitted Aerosol Cloud Experiment (E-PEACE) took place off the coast of Monterey, California to better understand the response of marine stratocumulus to aerosol perturbations (Russell et al., 2013). E-PEACE ~~combined~~ included sampling controlled releases of i) smoke from the deck of the research vessel *Point Sur*, and ii) salt aerosol from the TO research aircraft ~~(*Twin Otter* (TO), and~~, along with sampling ~~i~~iii) exhaust from container ships transiting across the study area (see Fig. 2 from Russell et al., 2013). During nine out of thirty E-PEACE flights, salt powder (d~~D~~iameter of 1-10 µm) was directly introduced into the cloud decks to examine the effects of g~~G~~iant cloud condensation nuclei (GCCN) on the initiation of warm precipitation (Jung et al., 2015). After excluding the seeding

cases and the non-typical Sc decks, 13 flights remained from which we analyzed data (Table 1). Detailed information about E-PEACE and TO data can be found elsewhere (Russell et al., 2013; Wonaschütz et al., 2013).

2.3 Marine cumulus cloud field campaigns: BACEX and KWACEX

Shallow marine cumulus clouds are by far the most frequently observed cloud type over the Earth's oceans, yet remain poorly understood, and have not been investigated as extensively as ~~the other major oceanic warm cloud, Sc~~oceanic stratocumulus. The marine environments in the Caribbean Sea and the Atlantic Ocean provide an excellent area to sample shallow marine cumulus clouds with a high propensity to precipitate. In addition, African dust is transported from westward off of Africa ~~to Miami~~ periodically over the North-Atlantic, affecting clouds in its path including around Barbados and Key West, and thus providing an excellent opportunity to observe aerosol-cloud-precipitation interactions. To better understand such interactions in these trade cumuli regimes, the Barbados Aerosol Cloud Experiment (BACEX) was carried out off the Caribbean island of Barbados during mid March and mid April 2010 (Jung et al., 2013), and the Key West Aerosol Cloud Experiment (KWACEX) during May 2012 near Key West (Fig. 1). For the BACEX, we analyzed 12 flights (Table 1). Readers are referred to Jung et al. (2016) for detailed information about the cloud and aerosol properties during the BACEX. The marine atmosphere during KWACEX was dry overall. ~~S and s~~ix out of 21 flights ~~involved~~ sampled~~ing in~~ shallow marine cumulus clouds, of~~among~~ which four had sufficient data for analysis (Table 1).

2.4 S_o calculation details

The distribution of N_d and R, with the corresponding H, is shown in Fig. 2 for each field campaign as scatter diagrams of N_d and R. All data shown in Fig. 2 were obtained during the cloud-base level-leg flights. ~~Figure 2 essentially shows that as N_d increases, R decreases.~~ The ~~marine environments of~~ Southeast Pacific (SEP) Sc decks (VOCALS, Fig. 2a) were overall drier and more polluted than those in the Northeast Pacific (NEP) Sc decks (E-PEACE, Fig. 2c); R=0.03 mm day^{-1} (median) and N_d=232 cm^{-3} in VOCALS, but R=1.04 mm day^{-1} and N_d=133 cm^{-3} in E-PEACE. ~~In a few cases, high N_d is observed~~ Dduring E-PEACE, high N_d was~~is~~ observed~~ in a few cases,~~ (e.g., N_d > 400 cm^{-3} in Fig. 2c), and they were~~are~~ likely associated with the emitted aerosols from the ship exhaust and smoke (Russell et al., 2013; Wang et al., 2014; Sorooshian et al., 2015). The marine environments of the Caribbean Seas ~~(Fig. 2b and Fig. 2d)~~ showed wide variations of R (e.g., order of 10^{-2} to 10^{2} mm day^{-1}; Fig. 2b and Fig. 2d). In Fig. 2,The Barbados ~~shows~~ campaign sampled the most pristine environment of the four campaigns ~~s~~ (N_d < 350 cm^{-3}, N_d = 61 cm^{-3} on average), reflecting the isolated location of the island in the North Atlantic even though the experiment period included the most intense dust events during the year of 2010 (Jung et al., 2013). ~~On the other hand,~~The marine environments near Key West was more ~~show~~ polluted than Barbados throughout the KWACEX campaign~~conditions~~ (Fig. 2d, N_d = 206 cm^{-3} on average).

Formatted: Indent: First line: 0.5"

S_o wa~~i~~s about 0.62 for E-PEACE (linear regression correlation coefficient r=0.34), if ~~it is~~ calculated ~~by~~ using all the individual 1 Hz data points shown in Fig. 2 where H ranges from ~100 m to 500 m. However, S_o wa~~i~~s about 0.42 (r=0.21) if one rainy day (shown as double circles in Fig. 10~~6~~ later) was~~is~~ excluded from the analysis, suggesting the ~~possible~~ artifact~~s~~ of wet scavenging ~~effects~~ (see Sect. 4), a different predominant ~~ or~~ cloud microphysical process (auto-conversion versus accretion) or the influence of macrophysical properties other than H. These E-PEACE S_o values agree~~s~~ with values estimated in previous campaigns in the same ~~study~~ northeast Pacific region for H ~200-600 m~~:~~; S_o ~0.46-0.48 using H and S_o ~0.60-0.63 using LWP (Lu et al., 2009). S_o during VOCALS is about 1.07 (r=0.46) for H ~ 150-700 m. Overall, S_o values in this study are within the range of S_o from the previous field studies of precipitating stratocumulus clouds (S_o ~0.8 to 1.75 for a fixed LWP in the studies of Pawlowska and Brenguier, 2003; Comstock et al., 2004; vanZanten and Stevens, 2005). Values of S_o for BACEX and KWACEX are about 0.89 (r=0.38) and 0.77 (r=0.39), respectively. ~~The values of S_o for marine cumulus clouds from the field studies have not been reported yet in previous studies.~~

Although ~~The~~ single power law fits ~~by using all the data points~~ for a given field campaign give the general sense of S_o values, they do ~~but do~~ not show the qualitative behavior of S_o with H, which reveals which thickness is most susceptible to aerosol perturbations. ~~In this study, to examine the qualitative behavior of S_o with respect to H~~To further examine this, ~~*for each campaign,*~~ S_o is calculated by assigning R and N_d into the given intervals of cloud thickness for each campaign. The width of each H interval is taken to be 30 m for Sc and 50 m for Cu. The H intervals are arbitrary, but chosen to contain a similar number of data points within each interval and provide a robust S_o regardless of the interval choice~~The H interval here is arbitrary, but we choose the interval containing similar number of data points (or at least the same order of the data point) at each interval and gives the robust S_o regardless of the choice of the H~~. Within each H interval, we performed a linear regression to find a best fit for the natural log of the precipitation rate against natural log of N_d, and the S_o is the slope of the fit (see Fig. 3, Fig. 6, for example). Cloud data are included in the analysis if the given precipitation rate is greater than a threshold of 0.001 mm day^{-1}. The lowe~~r~~ R threshold is intended to include both non-precipitating and precipitating clouds. The impacts of the R threshold and H intervals on the S_o estimates are discussed in Appendix B and C, respectively. ~~cloud data (1 s resolution of N_d, R, and H) were assigned to specific H intervals first. Then, the linear regression line was obtained for a given H interval, on the log (N_d) and log (R) diagram.~~ An example of S_o is shown in Fig. 3 from ~~for the~~ E-PEACE using e~~.~~ ~~E~~very ~~single~~ 1-second cloud data point (i.e., N_d and R) for H~~-~~ between 160 m and 190 m is shown in Fig. 3~~(a)~~. The slope (i.e., linear fit) in Fig. 3~~a~~ corresponds to an~~the~~ S_o value of 0.24. The value of S_o (0.24) is then plotted in the corresponding H on the H- S_o diagram (e.g., Fig. 4 at the H of 174 m, which corresponds to the average H of the interval). The same procedure is repeated for all H intervals to obtain the complete pattern of S_o with H. We tested and applied a few criteria in the S_o calculations, such as minimum R thresholds, and the total number of cloud data points and spans of N_d for a given H interval. ~~We noted that S_o tended to be unphysically high in the case of small N_d variations (i.e., short spans of N_d) (not shown).~~ Based on these sensitivity tests, we calculated ~~it was decided that~~ S_o ~~would be calculated~~ exclusively if N_d

varieds a sufficient amount (e.g., dlnog(N_d) spans at least 2.2) and the number of data points exceeds six for a given H interval since little variation of N_d does not provide the proper perturbation of aerosols. For example, in Fig. 3a, dlogln(N_d) spans about 3.5 and the number of data points exceeds 444. Slightly different and broader criteria were applied for Cu mainly due to the larger number of data points sampled in Sc. However, the qualitative behavior of S_o was robust as long as the variation of N_d waiis sufficiently large, regardless of the other criteria, although the details were different (e.g., Fig. B1). s. 1-2 in the Appendix). Most of the slopes are statistically significant at the 99 % confidence level (e.g., filled symbols in Fig. 4). The number of data points used to calculate S_o and the linear correlations and the P-values indicating the statistically significant level of confidence for the fitted lines are summarized in Table A2 for given H intervals. The number of data points used to calculate the value of S_o, and the (statistically significant) level of confidence for the fitted line, for a given H interval, is summarized in Table A2. Additionally, S_o is calculated by considering e-folding time and by randomly resampling the flights (Sect. 3.2), and the results are robust. This will be discussed later.

Additionally, S_o is calculated by resampling the cloud data every nth interval to examine how sample size affects S_o values. For example, in Fig. 3(b), S_o is calculated from the subsets of data that are sampled every 4th interval (every 4 seconds, equivalently). That being said, cloud data every ~200-240 m apart from one to the next were used to calculate S_o (the aircraft speed during E-PEACE was about 50-60 m s^{-1}, and thus, every 4th interval corresponds to ~200-240 m distance in general). The ranges of S_o are shown as vertical bars in Fig. 4 where S_o was calculated from the subsets of data with a sample size ranging from 1/n to 1/10 of the initial sample size (i.e., from n=1 to n=10). S_o values that are calculated with a sample size of n=4 and n=7 are shown in Fig. 3(b-e) as an example. In Fig. 3(b-e), S_o tends to be overestimated as the sample size decreases (i.e., the spatial and temporal resolution decreases).

S_o during VOCALS is calculated in slightly different ways from other experiments since the cloud radar failed. [PZ: maybe say this when first mentioning the instruments also]during VOCALS. First, H is estimated from the vertical structure of LWC for each day (daily mean H). Once H is determined for each flight, it is assigned to a certain H bin. For example, H of 9 Nov. (164±18 m) and 10 Nov. (194±21 m) are similar and thus assigned to the same H bin (i.e., group 1 in Table 1). VOCALS H is classified into only four distinct groups without overlapping with H from the next group.with a similar daily H Once N_d and R are assigned to the corresponding H, S_o then is estimated by using all the data points that are assigned to the same H group.

LWP is commonly used as the macrophysical factor when quantifying Eq. (1). However, in this study, we use H as a macrophysical factor since we aim to compare S_o for both Sc and Cu. H corresponds well to LWP for adiabatic clouds, for which LWP ~ H^2. The adiabatic assumption, which may be valid in Sc, is not valid in Cu (Rauber et al., 2007; Jung et al., 2016) to calculate LWP. Further, even if we calculate LWP by integrating LWC with height (e.g., in Sc), we would obtain one LWP valueprofile that could be used for the entire cloud layer on a given day, as opposed to many H estimated from the

cloud radar sampling at 3 Hz~~which is inferior to H that was estimated from the cloud radar with higher temporal resolution (3 Hz versus daily)~~. Moreover, the TO did not carry an instrument that measures LWP directly such as a G-band Vapor Radiometer (e.g., Zuidema et al., 2012). Consequently, the direct comparison with previous results of S_o with LWP (e.g., quantitative) is not possible. ~~,~~We also note that LWC decreases as drizzle rates increase (e.g., see Fig. 8d of Jung et al., 2015). Consequently, clouds that are precipitating (higher R) may have a LWP that is lower than the adiabatic value, and a cloud with a small R may have a LWP close to the adiabatic value. It should be also noted that the ranges of H (and possibly LWP) differ substantially between Cu and Sc. For example, H of Cu in this study can be as high as 1700 m, whereas H of Sc is generally less than 500 m (e.g., Fig. 4). Additionally, H for clouds that begin to precipitate may differ in Sc and Cu. Further, ~~Besides,~~ the LWP for clouds that precipitate would be sub-adiabatic and would have a smaller value of LWP than the LWP for non-precipitating clouds. Consequently, S_o that is calculated from cloud fields with diverse cloud types (e.g., Mann et al., 2014; Terai et al., 2015) may be complicated since LWP is shifted to smaller values for (heavily) precipitating clouds, and the H at precipitation initiation may differ between cloud types~~and the H that begins the precipitation may differ from cloud types as discussed above~~. In general, the results are used with caution when comparing with ~~to~~ other studies in quantifying S_o since the dominating cloud process and the choices applied in how to calculate parameters involved with Eq. (1) can differ widely (e.g., Duong et al., 2011).

3 Results

3.1 S_o in Sc and Cu

In this section, we show S_o calculated in ~~with~~ three different ways. First, S_o is calculated with 1-second data (Fig. 4) for BACEX, KWACEX, E-PEACE and VOCALS. Second, S_o is calculated with reduced data points that are averaged over the e-folding time of N_d. We show the results for BACEX, E-PEACE and VOCALS (Figs. 5 and 6). Lastly, S_o is calculated with randomly resampled E-PEACE flights (Figs. 8 and 9). We will show the results in turns.

S_o as a function of H is shown in Fig. 4a for Cu. S_o is calculated from Eq. (1) with ~~N_d~~ and R that are sampled ~~sampled~~ during the cloud-base level-leg flights at 1-second resolution. Cloud level-leg flights usually last 7-15 minutes on average, with an aircraft speed of 50-60 m s^{-1}. In Fig. 4a, S_o during BACEX fluctuates around zero for ~~is about 0 for the~~ clouds shallower than 5400-600 m, above which ~~it slightly increases to 0.2-0.3 for 500 < H < 700 m. For H > ~700 m,~~ S_o begins to increase rapidly with a peak of ~1.6 near H~1400 m. After that, S_o starts to decrease as H increases. The S_o ~~trend~~ during KWACEX follows S_o ~~that~~ from BACEX, especially in the thicker cloud regime where the majority of KWACEX data were sampled. ~~Only four flights were available for KWACEX data analysis and no data were available between 800 m and 1500 m that satisfied the data analysis criteria. Therefore, S_o may peak somewhere for an H between 600 m and 1700 m [by referring to its overall trend. PZ I don't understand this phrase]~~

The qualitative behavior of S_o for Sc is shown in Fig. 4b. S_o during E-PEACE shows H-dependent S_o patterns that are similar to those from BACEX. In the small H regime (H < 240 m), S_o is almost constant at ~0.2. For H > ~240 m, S_o increases gradually with increasing H and peaks at S_o ~ 1.0 near ~~around~~ H ~ ~~values between~~ 350~~- m and~~ 400 m. After that, S_o decreases with increasing H. Figure 4b further shows that the overall pattern of S_o is similar regardless of how the cloud bases were determined, although the H at which S_o peaks changes slightly (cb-mean, cb-local, cb-lcl).

During VOCALS, S_o increases with increasing H, from S_o ~0.1 near 170 m to S_o ~0.5 near 300 m. A~~Then, a~~ minimum S_o value is shown near H ~ 640 m. The negative values of S_o in the largest H regime possibly result from ~~either~~, ~~or both,~~ uncertainties in the S_o estimation ~~in that category~~ ~~or and or/and~~ in~~from~~ unaccounted-for ~~the~~ macrophysical properties~~-~~, such as, cloud lifetime. The failure of the cloud radar during VOCALS was responsible for the fewer (four) *H* groups (Table 1) ~~(e.g., Seifert and Stevens, 2010)that affect the precipitation other than LWP or H in that category~~. ~~The data used to calculate that point stemmed from one day (1 Nov., Table 1), and further, only one sounding was made during the day. Consequently, it is possible that the negative value of S_o was due to the uncertainty in H, if the H varied substantially during the cloud-base level-leg flight on the day while S_o was calculated with a daily mean H. However, it is also possible that the negative value of S_o in the thicker clouds (i.e., high LWP) was due to the other factors that control the precipitation such as turbulence (Baker, 1993; Ayala et al., 2008), stronger updrafts due to the latent heat release from the precipitation (Rosenfeld, 2008), or increased GCCN in a high N_d environment (e.g., Jung et al., 2015; Terai et al., 2015). The negative value of S_o in the thicker cloud regime is also found in the CAM5 GCM simulation with an excessive accretion rates (e.g., Fig. 7 in Gettelman et al., 2013).~~

~~The failure of the cloud radar during VOCALS was responsible for the small resolvable ranges of H that led to only four H groups (Table 1).~~ Additionally, no data were~~as~~ available for H ~ ~~between~~ 350~~- m and~~ 600 m (Fig. 3), and thus, it is possible that S_o peaks anywhere between H values of 300 m and 600 m. The results of VOCALS clearly show the disadvantage of no cloud radar (i.e., high resolution of LWP or H) for the S_o estimates.

3.2 S_o calculated with an e-folding time and randomly resampled flights.

The dependence of 1-second data (N_d, R) on each other is tested two ways. First, we calculated S_o by considering the e-folding time scale (Leith, 1973), and, secondly, we calculated S_o by randomly resampling the flights. The e-folding time of N_d during E-PEACE was found to vary from four minutes to ten minutes, while the e-folding time of R varied from a few seconds to one to two minutes. The e-folding time of N_d within the VOCALS-TO flights varied from two to six minutes, and for the cloud-base precipitation was less than (or approximately) 1 minute (for a horizontal distance of less than 3 km, consistent with Terai et al., 2012). In the case of BACEX (Cu), the overall e-folding times were much shorter, varying from one-two minutes for N_d and less than one minute for R. The e-folding times of N_d and R are summarized in Table 1 for VOCALS, E-PEACE and BACEX. KWACEX was not included since there were only four flights.

Formatted: Indent: First line: 0"

We calculated S_o with data averaged over the upper bounds of the e-folding time (i.e., e-folding time of N_d) for E-PEACE, BACEX and VOCALS flights, and the qualitative behaviour of S_o reported with 1-second data is unchanged: S_o increases with H then peaks before it decreases again (Fig. 5 for BACEX and E-PEACE and Fig. 6 for VOCALS). However, it should be noted that the H that S_o peaks at is shifted toward the lower H consistent with the results of Duong et al. (2011). The shift of H to the lower H is substantial in Sc where the overall H is smaller than H of Cu. Additionally, the effect of the H-interval on the S_o estimates is discussed in Appendix C. In general, the results are robust regardless of the H interval. However, if the H interval is chosen across a cloud thickness range in which S_o changes substantially, the pattern of S_o can be changed, indicating that the finer H interval provide a more accurate S_o variation.

Second, we estimated S_o by randomly resampling the flights of E-PEACE to see whether the sequential 1-second samples are statistically independent. S_o calculated with random flights, at first glance, showed two distinctive types of behavior (not shown, but similar to Fig. 8a shown later). One is a similar pattern to that of the current S_o shown in Fig. 4 while the other is an almost constant S_o near zero. The cloud data sampled during E-PEACE formed two groups (denoted as A and B in Figure 7). The S_o pattern calculated with cloud data of group A is similar to S_o shown in Fig. 4: S_o is constant at lower H, followed by increase then decrease (Fig. 8a). In contrast, S_o values calculated from group B were relatively constant near zero S_o with the descending branch only (blue in Fig. 8c). Further analysis revealed that the two RFs (RF13 and RF03) that have relatively small N_d with high R explain the differences in the S_o patterns (Fig. 9). If S_o is calculated with cloud data that do not include data from clean with heavy precipitating environments (i.e., RF13 and RF03), S_o shows a similar pattern as that in Fig. 4.

~~Figure 4 further shows that, in general, S_o tends to be overestimated as the size of data samples (equivalently, temporal and/or spatial resolution of sampling) decreases contrast grey squares to the circles for both Sc and Cu, where S_o of grey squares are analogous (but not equivalent) to larger averaging lengths to circles. The results are similar to Terai et al. (2012), showing high values of S_o when larger averaging length scales are used (see 5 km versus 20 km in their Fig. 7). The higher S_o values, compared with lower values of S_o that are calculated by using all available data points, probably show the impacts of meteorology on S_o within the fixed H, because the cloud data points close to each other with similar H are more likely to experience the same meteorology.~~

3.3~~2~~ The effect of a~~A~~utoconversion and a~~A~~ccretion p~~P~~rocesses on S_o ~~in VOCALS-REx and E-PEACE~~

For cloud droplets to become raindrops (typical diameters of cloud droplets and drizzle drops are about 20 and 200 µm, respectively (Rogers and Yau, 1989)), they have to increase in size significantly by the collision-coalescence process (autoconversion and accretion)~~. Here autoconversion refers to the precipitation process caused by interactions between cloud droplets. That being said~~, Here, autoconversion primarily refers to f~~f~~aster-falling large cloud droplets that collect

Formatted: Font: Italic

Formatted: Font: Italic, Subscript

smaller cloud droplets in their paths as they fall through a cloud and grow larger; the accretion process refers to the precipitation process caused by precipitation embryos that collect cloud droplets. In the intermediate LWP regime where S_o increases with LWP or H (ascending branch of S_o) the auto-conversion process dominates. On the other hand, in the high LWP regime where S_o decreases with LWP or H (descending branch of S_o) the accretion process dominates (Feingold and Siebert, 2009; Feingold et al., 2013). The transition from the dominance of autoconversion to accretion is reported to occur when D_e exceeds ~ 28 µm, and has been used as a rain initiation threshold in Sc (e.g., Rosenfeld et al., 2012). Jung et al. (2015) also showed that the precipitation embryos appeared (and warm rain initiated) when the mean droplets diameters were slightly less than 30 µm from the salt seeding experiments during E-PEACE, in the NEP Sc decks (e.g., see Table 3, Fig. 6a, and Fig. 7 in their study). Figure 10(a) shows that cClouds during VOCALS consisted of numerous small droplets (D < 15 µm in Fig. 5a), which primarily are involved with the autoconversion process except for one flight (D ~37 µm, RF09, Nov. 1). The dominance of smaller droplets during VOCALS-TO flights agree with the dominance of ascending branch of S_o in Fig. 4(b). On the other hand, Figure 5a also shows that the size of droplets increases with increasing height, and thus, the overall cloud droplet sizes are slightly larger in the mid-cloud level (red) than those in the cloud base level (black). Compared with VOCALS Sc decks, Fig. 6 shows that E-PEACE Sc clouds are composed of larger-sized droplets as well as small droplets (Fig. 10b).

Feingold et al. (2013) showed that time available for collision-coalescence t_e influences the value of S_o. That being said, an increase in t_e shifts the balance of rain production from autoconversion to accretion with all else (e.g., LWP and/or H) being equal. Further, they showed that radar reflectivity Z is a good indicator of t_e: higher Z coincides with longer t_e. To examine how or whether t_e relates to the discrepancy of S_o responses in Sc between previous and current studies, Z with height is shown in Fig. 5b. Fig. 5c is the same as Fig. 5b, but H is used as y-ordinate. Figure 5c essentially shows that Z increases as cloud deepens, indicating a longer t_e in the thicker clouds. Accordingly, accretion process would dominate (or play major roles) in the thicker cloud regimes, and in turn, S_o estimated from the thicker clouds will show a descending branch of S_o predominantly, whereas S_o estimated from the thinner clouds will show an ascending branch of S_o mainly, which are consistent with the behavior of S_o in Fig. 4. In Fig. 5b-c, overall, Z calculated from the mid-cloud levels (red) are stronger than Z from cloud base levels (black) (expect for extremely thick or thin clouds), indicating a longer t_e for the clouds sampled at mid-cloud level compared with those sampled at cloud-base. The reversed reflectivity pattern shown in the extremely deep or shallow clouds (i.e., Z decreases with height) could be related to a different stage of cloud life time (e.g., growth or dissipating). But it is not discussed here. Since longer t_e shifts the balance of rain production from autoconversion to accretion, the accretion process would be dominated in the mid levels, and thus, a descending branch of S_o would be apparent in the clouds sampled at mid-level compared with clouds sampled at cloud-bases. In contrast, the ascending branch of S_o (equivalently, autoconversion process) would appear predominantly in the clouds sampled close to cloud bases. The

~~effect of the location of in-cloud sampling (mid-cloud versus cloud-base) on the qualitative behavior of S_o will be discussed in the following section by comparing current results with those of Terai et al. (2012).~~

4 Discussion

This study shows the consistent behavior of S_o as a function of a key macrophysical cloud property regardless of cloud type; i.e., S_o increases with increasing H (ascending branch) and peaks at intermediate H before S_o decreases with H (descending branch) in both Sc and Cu (Fig. 4). The results from marine cumulus clouds (BACEX and KWACEX) are consistent with previous modeling and observational studies of warm cumulus clouds (Sorooshian et al., 2009, 2010; Jiang et al., 2010; Duong et al., 2011; Feingold and Siebert, 2009; Feingold et al., 2013). However, S_o values estimated from marine stratocumulus clouds (E-PEACE and VOCALS) are inconsistent with previous in-situ observations of warm stratocumulus clouds (Terai et al., 2012; Mann et al., 2014~~; Hill et al., 2015~~), but are consistent with previous satellite observations of weakly precipitating Sc (Sorooshian et al., 2010), global climate model simulations (Gettelman et al., 2013; Hill et al., 2015), and box and parcel model studies (Feingold et al., 2013) of Sc.

Possible reasons for why the current results differ from those in previous studies of Sc are discussed here mainly by comparing results to those from the Terai et al. (2012) study. ~~Although we compare our results with those of Terai et al. (2012), the issues discussed here apply to any results that used the same methods or data analysis as discussed here.~~ The inconsistent behaviors of S_o between our study and theirs may be due to a number of factors. One of the most fundamental reasons could be in the differences in the cloud fields that were sampled. In the SEP Sc decks, drizzle intensity and frequency tend to increase westward from the coast (e.g., Bretherton et al., 2010) and their dataset included several Pockets of Open Cells (POCs) with strong precipitation (personal communication with C. Terai). It should be noted that the VOCALS C130 flights (Terai et al., 2012) sampled the cloud fields along 20 °S (mainly over the open Ocean), whereas the VOCALS TO flights sampled the Sc decks near the continents (Fig. 1). The westward increases in frequency and intensity of drizzle coincident with the westward decrease in aerosols and N_d, and also with larger LWP over the open ocean (e.g., ~~George and Wood, 2010~~Zuidema et al. 2012), suggesting that the discrepancy possibly is contributed to the different cloud microphysical process working on the cloud field (auto-conversion versus accretion processes). Indeed, Gettelman et al. (2013) showed that the accretion process dominated during VOCALS C-130 flights; the accretion to autoconversion ratio was above 1 for all LWP ranges during VOCALS observation (e.g., Fig. 5a in their studies). Therefore, the enhanced (major) accretion process ~~, which~~ appears as a descending branch of S_o predominantly. Hill et al. (2015) also showed that the monotonic decrease of S_o with LWP in case that the cloud data consist of exclusively larger particles (e.g., radius > 20 μm)

Second, the higher R threshold that Terai et al. (2012) used could contribute to the discrepancies. ~~First,~~ Terai et al. (2012) used R = 0.14 mm day^{-1} as a minimum R threshold to estimate S_o where 0.14 mm day^{-1} corresponds to -15 dBz from

the Z-R relationship that they used ($R=2.01Z^{0.77}$ from Comstock et al., 2004). ~~Note that not all of the data shown in Fig. 1 in Terai et al. (2012) are used for the S_o calculation in their study.~~ This R threshold is possibly too high to capture the autoconversion processes that occur in more lightly precipitating clouds ~~or clouds that are not precipitating yet but ready to precipitate~~ such as clouds sampled during VOCALS TO flights. As a result, the high value of minimum R threshold may primarily capture~~s~~ the accretion process ~~only (or predominantly)~~, which may contribute to the descending branch of S_o in their study. As an example, this R threshold rejects all the data in Fig. 2a (VOCALS TO flights) except for one day (RF09, Nov. 1) when the mean effective diameter is about 37 μm and the accretion process dominates for the day. Further, the impact of the R threshold on the S_o estimates is evident in Fig. B2. Figure B2 shows that S_o decreases as the larger minimum R threshold is used, in particular at larger H. Figure 9 also shows ~~that~~ how ~~the~~ clouds ~~data~~ of low N_d with high R (e.g., RF03 and RF13 of E-PEACE) alter the behavior of S_o. T~~However, it should be also noted that the R threshold had little effect on S_o estimates and its qualitative behavior for E-PEACE (Fig. A2) because the overall D_e during E-PEACE was larger than that during VOCALS (Fig. 5a versus Fig. 6). In turn, the higher R threshold (which is proportional to ~ D^4) did not alter the overall characteristics of the E-PEACE dataset. Nonetheless, it is clear that t~~he choice of minimum R threshold can change the ~~change the overall character of the~~ dataset that will be used for the estimates of~~to calculate~~ S_o. The ~~, which is evident in the VOCALS TO flight data.~~ S_o metric is designed to show the impact of aerosols on precipitation; as aerosol increases, smaller sizes of numerous droplets form, and those droplets suppress the collision-coalescence process, and in turn, precipitation. Therefore, to study the extent that aerosols suppress precipitation, it would be more appropriate~~reasonable~~ to ~~cover~~ encompass the full range of non-precipitating to precipitating clouds ~~(i.e., from lower R to higher R,)~~ that include both autoconversion and accretion processes. It is also noted that the framework of precipitation susceptibility is to measure the impact of aerosol perturbations on the precipitation suppression, and thus, the concept of S_o may not adequately apply to the clouds that are already heavily precipitating since the accretion process has little dependence on N_d. In addition to decreasing the LWP, the precipitation itself can scavenge aerosols leading to lower N_d.

~~Second, the discrepancy possibly is contributed by the predominant cloud microphysics. Indeed, Gettelman et al. (2013) showed that the accretion process dominated during VOCALS C-130 flights; the accretion to autoconversion ratio was above 1 for all LWP ranges during VOCALS observation (e.g., Fig. 5a in their studies). Therefore, the enhanced (major) accretion process, which appears as a descending branch of S_o predominantly.~~

~~the in-cloud data (R and N_d) used in Terai et al. (2012) were mainly obtained from the mid-cloud levels, whereas data used in the current study were obtained from the cloud base heights. While the VOCALS C-130 flights consist of one in-cloud level-leg (mid-cloud level in most cases), TO flights consist of 2-3 in-cloud level-leg flights that include cloud base, mid-cloud, and cloud top level legs. Cloud data sampled from mid-cloud levels reflect enhanced accretion processes if D_e increases with heights (as discussed in 3.2). In fact, Painemal and Zuidema (2011) showed that D_e increased with heights in~~

~~the SEP Sc decks during VOCALS, which is based on C-130 measurements. The increase in D_e with height (e.g., Fig. 5 of Painemal and Zuidema, 2011) is consistent with the D_e distribution shown from the TO flight (Fig. 5a). Therefore, the enhanced (major) accretion process, which appears as a descending branch of S_o predominantly, is expected in the mid-cloud levels compared with that from the cloud bases (Sect. 3.2). Indeed, Gettelman et al. (2013) showed that the accretion process dominated during VOCALS C-130 flights; the accretion-to-autoconversion ratio was above 1 for all LWP ranges during VOCALS observation (e.g., Fig. 5a in their studies).~~

Third, the overall high values shown in Terai et al. (2012) (S_o begins with around 3 near H~50 m and ends with S_o ~0.8 near H~500 m) may reflect the effects of wet scavenging (Fig. 7a; see also Duong et al., 2011), especially by considering that ~~the drizzle intensity and frequency in SEP Sc decks tended to increase westward from the coast (e.g., Bretherton et al., 2010), and~~ their dataset included several ~~Pockets of Open Cells (~~POCs~~)~~ with strong precipitation. ~~(personal communication). It should be noted that the VOCALS C130 flights (Terai et al., 2012) sampled the cloud fields along 20 °S whereas the VOCALS TO flights sampled the Sc decks along the Chille coast (Fig. 1). The westward increases in frequency and intensity of drizzle coincident with the westward decrease in aerosols and N_d and also with larger LWP over the open ocean (e.g., George and Wood, 2010).~~ We also noted that S_o calculated from the 13 E-PEACE flights was about 0.62. However, S_o calculated from 12 E-PEACE flights that excluded one rainy day was about 0.42, which is consistent with larger S_o in the presence of (heavy) precipitation possibly due to the wet scavenging (but it is also possible the lower So is due to the microphysical process). Consistently, S_o values calculated from 9 BACEX flights (Cu), which excluded three heavy precipitation cases, were also shifted to lower values than those estimated from the entire 13 flights (not shown).

Fourth, Terai et al. (2012) used column-maximum Z and then converted the Z to R by using a Z-R relationship for those time periods when the lidar could not determine the cloud-base height due to interference from heavy precipitation~~when cloud-base was not determined from the lidar due to the attenuation by the heavy precipitation~~. This procedure can overestimate precipitation for a given N_d. If the procedure (i.e., overestimates of R) occurs ~~happens~~ in a low N_d regime (left half of the dotted line in Fig. 7b), the steeper slope (i.e., higher S_o) would be obtained (Fig. 7b). If the procedure happens in a high N_d regime, the lower slope would be attained (Fig. 7c). Based on Fig. 1 of their study, the former scenario (Fig. 7b) would occur, resulting in higher S_o than expected.

Fifth, the Z-R relationship that Terai et al. (2012) used ($R=2.01Z^{0.77}$, followed Comstock et al. (2004)'s $Z=25R^{1.3}$) derived for stratocumulus off of the coast of Peru, using a shipboard scanning C-band radar. The Sc sampled during the ~~was derived from Sc that was combined near Peru with off the coast of Mexico (ship measurement). The Sc during~~ VOCALS C-130 flights may have a different microphysical process from which the original Z-R relationship was derived. The microphysical processes are responsible for the formation of DSD, and the variability of DSD determines the theoretical limit of precipitation accuracy by radar via Z-R relationship. That being said, changes in DSD imply different Z-R

relationships. The DSD variability (e.g., day to day, within a day, between physical processes and within a physical process) causes about 30-50 % of errors in *R* estimates with a single Z-R relationship (e.g., see Lee and Zawadzki, 2005 and references therein). Besides, the Comstock et al. (2004) Z-R relationship was derived from drop-sizes ranged from 2 µm to 800 µm in diameter (for drops larger than 800 µm, extrapolation was used). The Sc from VOCALS C-130 flights included several POCs, while the clouds that the Z-R relationship was derived were characterized by persistent Sc, sometimes continuous and other times broken with intermittent drizzle throughout. Therefore, using the Z-R relationship of Comstock et al. (2004) may result in some additional uncertainties in *R* estimates in Terai et al. (2012) as the error of Z-R relationship becomes larger in the bigger drop sizes (Z and R are proportional to ~D^6 and ~D^4, respectively). Further, applying a Z-R relationship to W-band (3 mm) radar returns is not valid if there are any droplets greater than 1 mm since non-Rayleigh scattering (Mie effects) can dominate the radar reflectivity. Note that the Terai et al. (2012) *R* retrievals were made with a W-band radar. However, it is also true that the in-situ sampling of rain used in this study may miss a lot of raindrops because of the small sample volume of the probe. The errors in *R* estimates with a single Z-R relationship or R measured from probes, however, may not critically affect the differences in S_o between studies as the S_o metric (Eq. 1) is less sensitive to data uncertainty by using the logarithmic form of the data.

Lastly~~Nevertheless, using a Z-R relationship is not an ideal, unless there are no alternatives and/or the microphysical processes are the same in the regions where the relationship is derived and where the relationship is applied. PZ I don't really agree with that. In situ sampling of rain may miss a lot because of the small sample volume of the probe, e.g., Wood 2005~~

~~Sixth~~, Terai estimated N_d from the sub-cloud aerosols using an empirical relationship, which ~~the usage of the assumption that Terai et al. (2012) made for the linear relationship between sub-cloud aerosol concentrations in the So matrix and cloud-base N_d~~ may also contribute to the differences. According to Jung (2012 in Fig. 4.5), the ~~linear relationship between~~ sub-cloud aerosols ~~are~~ well represent~~ed~~ the~~and~~ cloud-base N_d ~~is well established only~~ in the updraft regime~~, and the linearity gets stronger as a function of updraft velocity~~, although these results are shown for the marine shallow cumulus clouds. Similarly, using the aerosol proxy from the satellite data for the S_o calculation also needs caution. Jung et al. (2016) showed that Aerosol optical depth (AOD) is not always a good indicator of the sub-cloud layer aerosols especially when the fine particles from long-distance continental pollution plumes reside above the boundary layer (e.g., Fig 4-5 their study). Mann et al. (2014) ~~also assumed the linearity between~~used a sub-cloud ~~cloud-base N_d and~~ 10 m CCN (at 0.55 % super-saturation) for the S_o calculation and ~~and~~ showed a decreasing trend of S_o with LWP as Tera~~e~~i et al. (2012) but their overall S_o is smaller than those estimated from other field studies. In cases where sub-cloud aerosols are used for the S_o estimates, these estimates give a~~it gives~~ smaller S_o than those using N_d due to the decreasing fraction of aerosol activated with N_d increasing, all else being equal (e.g., Lu et al., 2009)

Formatted: Indent: First line: 0"

~~Lastly, to estimate S_o for a given H and LWP interval, Terai et al. (2012) used 30 % of the highest and the lowest N_d and R data on the log (N_d) and log(R) diagram instead of using all available data. This method possibly could affect/change the slope (i.e., S_o) more readily (but not necessarily) than the way using all the available data.~~

5 Conclusions

The suppression of precipitation due to the enhanced aerosol concentrations (N_a) is a general feature of warm clouds. In this study we examined precipitation susceptibility S_o in marine low clouds by using in situ data obtained from four field campaigns with similar datasets; two of them focused on marine stratocumulus (Sc), and two targeted shallow cumulus (Cu) clouds. We estimate S_o with 1-second data, with data averaged over an e-folding time scale, and data subsampled randomly from flights, with the key results preserved regardless of the method used. This study shows that the maximum values of S_o are ~1.0 for Sc and ~1.5 for Cu, which are less than the values of S_o of ~2.0 that climate models tend to use for the value of $-\beta$ in Eq. 2. This study is the first to show with airborne data that for both Sc and Cu, S_o increases with increasing cloud thickness H and peaks at an intermediate H, before decreasing. For example, R is most susceptible for clouds of medium-deep depth, such as H ~380 m for Sc in NEP where H varies between 100-450 m, and H~1200-1400 m for Cu in the Caribbean Sea where H ranges from 200-1600 m. On the other hand, R is less susceptible to N_d in both shallow non-precipitating and deep heavily precipitating cloud regimes for both Sc and Cu. The results are consistent with previous studies of warm cumulus clouds, but inconsistent with those of warm marine stratocumulus clouds in-situ observations.

We suggest several possible reasons for why these results differ from those in previous studies of Sc, f~~. F~~or example, by comparing with in-situ measurements of Terai et al. (2012). The sources of these uncertainties include the following: (i) geographical location of cloud decks that may be related to the predominant cloud microphysical process at work (e.g., accretion process), (ii) R threshold differences ~~(ii) the location of in-cloud sampling (mid-cloud versus cloud-base)~~, (iii) wet scavenging effects (causing high values of S_o), (iv) the use of maximum column Z to convert R under heavy rain conditions where cloud-base is not defined, ~~(~~v) the use of the Z-R relationship to estimate ~~for the~~ R ~~estimates~~, and (vi) the use of ~~linearity assumption between~~ sub-cloud aerosols ~~instead of~~to estimate ~~and~~ cloud-base N_d.

~~We also note that Z increases with height that is consistent with the H-dependent behavior of S_o that suggests the predominance of autoconversion process (predominance of ascending branch of S_o) in the small H regime, and the dominance of accretion process (predominance of descending branch) in the large H regime.~~ We also found~~note~~ that the details of N_d ~~and R thresholds~~ (e.g., Fig. B1~~(Appendix Fig. 1)~~ or how the cloud base is determined have little effect on both S_o values and the qualitative H-dependent behavior (Fig. 4). Further, h~~; however, the robust behavior of S_o was because the chosen thresholds did not change the overall character of the dataset. H~~ere we emphasize and caution that the choice of the R

threshold for the data analysis is important because the chosen threshold possibly can alter the character of the dataset used to calculate S_o by subsampling the data. For example, if a high value of the minimum R threshold is chosen in a dataset where the majority of data have low precipitation (e.g., VOCALS TO flights, Fig. 3a) and/or in the bimodal population of precipitation, the threshold would, by chance, eliminate/reduce the influence of the autoconversion process in favor of the accretion process. The VOCALS C-130 flight datasets are likely dominated by the accretion process occurring naturally (geographically remote ocean areas where ~~in the~~ POCs is often observed) ~~by the adapted flight strategy (mid-level cloud sampling),~~ and by the choice of high R thresholds.

The values of S_o in this study were calculated from in-situ measurements, and thus, no issues associated with the retrieval (e.g., satellite data), empirical relationships (e.g., Z-R relationship), or ~~and~~ assumptions (e.g., relations between ~~linearity between~~ sub-cloud aerosols and cloud-base N_d) are encountered for the calculation of S_o. A drawback, however, is the much smaller sampling volume of the in-situ microphysical probes compared to a radar volume, as this may generate an underestimate of the rainrate. Further, we calculated S_o separately for Cu and Sc to avoid any possible issues that may arise from combining ~~mixing~~ different cloud types ~~of clouds~~ (Sect. 2.4). The results, however, should be used with caution when comparing to other studies in quantifying S_o as the dominating cloud process and the choices applied to calculate the parameters in S_o estimates (Eq. 1) can differ widely.

The results of this work motivate ~~further~~ future studies examining the same relationships with a more direct measurement of cloud depth using a cloud radar and/or LWP using a microwave radiometer, in addition to the instruments/sensors that measure/retrieve R and N_d (N_a is also desirable). For the flight strategy, in-cloud level legs at multiple altitudes (cloud-base, mid-cloud and cloud-top) with one sub-cloud level-leg would be ideal to calculate S_o and compare with other studies where S_o is calculated with cloud-base or vertically integrated variables. Level-legs near the ocean surface and sounding(s) to examine the background thermodynamic structures on a given day are also recommended.

~~The precipitation susceptibility in this study, quantified by the changes in precipitation rate to the changes in cloud droplet concentrations in the cloud base, showed that R is most susceptible for clouds of medium-deep depth, such as H ~ 380 m for Sc of which H varies between 100-450 m, and H~1200-1400 m for Cu that H ranges from 200-1600 m. However, R is less susceptible to N_a in both shallow non-precipitating and deep heavily precipitating cloud regimes for both Sc and Cu. The inconsistent behaviors of S_o for the stratocumulus clouds between the current and previous studies are partly attributed to the predominant accretion process in the study area along with some assumptions and thresholds applied to the data analyses. in the previous studies. To capture the characteristic features of the suppression of precipitation rate as a function of aerosol loading, the lower R minimum threshold is desirable to use. Otherwise, the data will be skewed more to conditions where accretion dominates over autoconversion. Further studies on which range of H (or LWP) is most susceptible to precipitation rate would advance our understanding of aerosol impacts on precipitation.~~

~~**Appendix A: Sensitivity of R and N_d thresholds to S_o estimates**~~

~~**Figure A1. The sensitivity of S_o to the N_d threshold value. One standard deviation of mean thickness for a given H interval is shown as horizontal bars.**~~

~~**Figure A2. The sensitivity of S_o to the R threshold value. One standard deviation of mean thickness for the given H interval is shown as horizontal bars.**~~

Appendix A: Data

Table A1. Table of acronyms and symbols.

Acronym	Expression
BACEX	Barbados Aerosol Cloud Experiment
CAS	Cloud Aerosol Spectrometer
CIP	Cloud Imaging Probe
Cu	(Shallow marine) Cumulus (cloud)
DSD	Drop Size Distribution
E-PEACE	Eastern Pacific Emitted Aerosol Cloud Experiment
H	Cloud thickness
KWACEX	Key West Aerosol Cloud Experiment
LCL	Lifting Condensation Level
LWC	Liquid Water Content
LWP	Liquid water path
N_d	Cloud droplet number concentration
PCASP	Passive Cavity Aerosol Spectrometer Probe
POCs	Pockets of Open Cells
R	Rainfall (Precipitation) Rate
Sc	Stratocumulus (clouds)
S_o	Precipitation susceptibility
TO	Twin Otter
VOCALS-REx	VAMOS Ocean-Cloud-Atmosphere-Land Study-Regional Experiment
Z	Radar reflectivity

Formatted: Font: Times
Formatted: Font: Times, 10 pt
Formatted: Font: Times
Formatted: Font: Times, 10 pt
Formatted: Font: Times
Formatted: Font: Times, 10 pt
Formatted: Font: Times
Formatted: Font: Times, 10 pt
Formatted: Font: Times
Formatted: Font: Times, 10 pt
Formatted: Font: Times
Formatted: Font: Times, 10 pt
Formatted: Font: Times
Formatted: Font: Times, 10 pt
Formatted: Font: Times
Formatted: Font: Times, 10 pt
Formatted: Font: Times
Formatted: Font: Times, 10 pt
Formatted: Font: Times
Formatted: Font: Times, 10 pt
Formatted: Font: Times
Formatted: Font: Times, 10 pt
Formatted: Font: Times

Table A2. H interval and number of data points used in Fig. 4 for each field study.

E-PEACE, H (m)	H < 130	130-160	160-190	190-220	220-250	250-280	280-310	310-340	340-370	370-400	400-430	H>430
E-PEACE, # of data points (cb-mean)	537	499 (99%)	444 (99%)	508 (99%)	886 (99%)	781 (99%)	606 (99%)	610 (99%)	821 (99%)	373 (99%)	97 (99%)	10
E-PEACE (cb-local)	530	482 (99%)	582 (99%)	683 (99%)	726 (99%)	474 (99%)	497 (99%)	525 (99%)	602 (99%)	758 (99%)	236 (99%)	77 (99%)
E-PEACE (cb-lcl)	514 (< 65%)	379 (80%)	341 (90%)	255 (85%)	489 (99%)	823 (99%)	627 (99%)	621 (99%)	670 (99%)	389 (99%)	283 (< 65%)	781 (80%)
VOCALS H (m)	Group1 170±27	Group 2 225±46	Group 3 307±24	Group 4 641±201	–	–	–	–	–	–	–	–
VOCALS # of data points	1113 (80%)	1280 (99%)	833 (99%)	224 (95%)	–	–	–	–	–	–	–	–
BACEX H (m)	0-250	250-500	500-600	600-800	800-1000	1000-1250	1250-1500	H>1500	–	–	–	–
BACEX # of data points	23	86 (90%)	40 (90%)	87 (70%)	52 (99%)	38 (99%)	30 (99%)	27 (99%)	–	–	–	–
KWACEX H (m)	H<1500 m	1500-1800	H > 1800 m	–	–	–	–	–	–	–	–	–
KWACEX # of data points	56 (90%)	32 (99%)	42 (65%)	–	–	–	–	–	–	–	–	–

Numbers in parenthesis indicate statistical significance of the linear fits (two-tailed t-test).

Table A2. H interval and number of data points used in Fig. 4 for each field study.

E-PEACE, H (m)	H < 130	130-160	160-190	190-220	220-250	250-280	280-310	310-340	340-370	370-400	400-430	*H*>430
E-PEACE (cb-mean) (#, *r*, *P*)	537 *r*=0.03 *P*=0.548	499 *r*=0.13 ***P*=0.0025**	444 *r*=0.16 ***P*=0.0006**	508 *r*=0.16 ***P*=0.0004**	886 *r*=0.13 ***P*=0.0001**	781 *r*=0.27 ***P*<0.00001**	606 *r*=0.41 ***P*<0.00001**	610 *r*=0.50 ***P*<0.00001**	821 *r*=0.58 ***P*<0.00001**	373 *r*=0.74 ***P*<0.00001**	97 *r*=0.43 ***P*<0.0001**	10 *r*=0.05 *P*=0.89
E-PEACE (cb-local) (#, *r*, *P*)	530 *r*=0.07 *P*=0.09	482 *r*=0.14 ***P*=0.0029**	582 *r*=0.11 ***P*=0.0076**	683 *r*=0.12 ***P*=0.0015**	726 *r*=0.14 ***P*=0.0002**	474 *r*=0.20 ***P*<0.00001**	497 *r*=0.44 ***P*<0.00001**	525 *r*=0.48 ***P*<0.00001**	602 *r*=0.51 ***P*<0.00001**	758 *r*=0.62 ***P*<0.00001**	236 *r*=0.77 ***P*<0.00001**	77 *r*=0.56 ***P*<0.00001**
E-PEACE (cb-lcl) (#, *r*, *P*)	514 *r*=0.03 *P*=0.46	379 *r*=0.07 *P*=0.19	341 *r*=0.10 *P*=0.067	255 *r*=0.10 *P*=0.102	489 *r*=0.17 ***P*=0.0002**	823 *r*=0.20 ***P*<0.00001**	627 *r*=0.36 ***P*<0.00001**	621 *r*=0.45 ***P*<0.00001**	670 *r*=0.54 ***P*<0.00001**	389 *r*=0.46 ***P*<0.00001**	283 *r*=0.02 *P*=0.782	781 *r*=0.05 *P*=0.174
VOCALS H (m)	Group1 170±27	Group 2 225±46	Group 3 307±24	Group 4 641±201	-	-	-	-	-	-	-	-
VOCALS (#, *r*, *P*)	1113 *r*=0.04 *P*=0.161	1280 *r*=0.27 ***P*<0.00001**	833 *r*=0.45 ***P*<0.00001**	224 *r*=0.14 *P*=0.042	-	-	-	-	-	-	-	-
BACEX H (m)	0-250	250-500	500-600	600-800	800-1000	1000-1250	1250-1500	*H*>1500	-	-	-	-
BACEX (#, *r*, *P*)	23 *r*=0.03 *P*=0.88	89 *r*=0.03 *P*=0.76	46 *r*=0.29 *P*=0.05	87 *r*=0.12 *P*=0.25	52 *r*=0.60 ***P*<0.00001**	37 *r*=0.58 ***P*=0.0002**	30 *r*=0.59 ***P*=0.0006**	27 *r*=0.52 ***P*=0.005**	-	-	-	-
KWACE XH (m)	*H*<1500	1500-1800	*H* > 1800	-	-	-	-	-	-	-	-	-
KWACE X (#, *r*, *P*)	56 *r*=0.23 *P*=0.095	32 *r*=0.52 ***P*=0.002**	42 *r*=0.16 *P*=0.32	-	-	-	-	-	-	-	-	-

Numbers indicates that the total number of data points, followed by the linear regression correlation coefficient (*r*) and P-value (two-tailed t-test). Bold P-values indicate that correlations are statistically significant at the 99% confidence level.

Appendix B: Sensitivity of R and N_d thresholds to S_o estimates

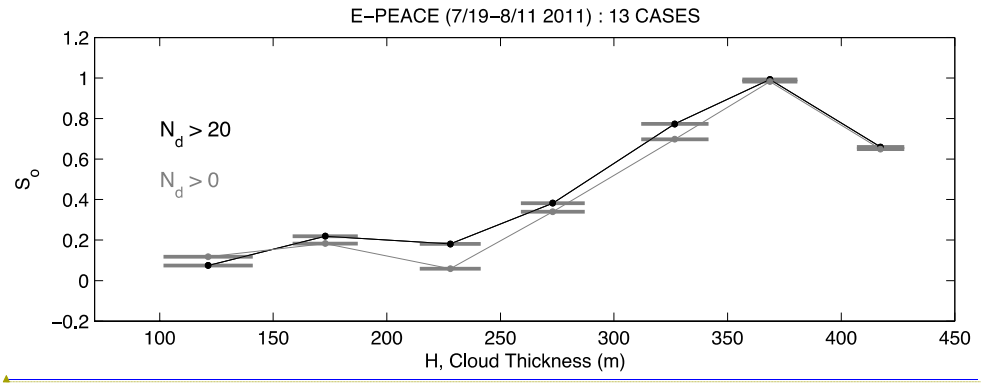

Figure B1. The sensitivity of S_o to N_d threshold values. One standard deviation of mean thickness for given H intervals are shown as horizontal bars.

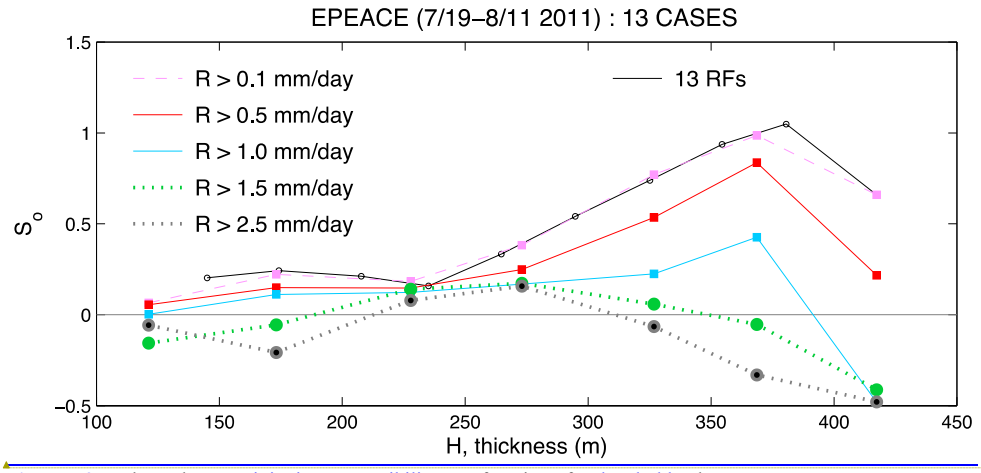

Figure B2. H-dependent precipitation susceptibility as a function of R threshold values.

Formatted: Font: Times

Formatted: Font: Times

Formatted: Font: Bold

Formatted: Font: Italic

Formatted: Font: Bold

Formatted: Font color: Auto

Appendix C. The effect of H intervals on So estimates.

S_o calculated with different H intervals can be seen by comparing Fig. 4 and Fig. A1 as an example. H intervals in Fig. 4(b) are about 30 m, while H intervals in Fig. A1 are about 50 m. The qualitative H-dependent behavior of S_o is robust regardless of the chosen H intervals in case 1-second data are used. However, the chosen H interval may have effect on the estimate of S_o that is calculated with a fewer data points, such as S_o that is calculated with data averaged over the e-folding time.

The effect of H-intervals on S_o estimates, which is estimated with data averaged over the e-folding time, is shown in Fig. B1. In summary, the results are robust regardless of H interval in general. However, if the H interval is chosen across the cloud thickness where the S_o changes substantially (such as in which the cloud properties change substantially), the pattern of S_o can be changed, indicating that the finer H interval would provide more accurate S_o. This is shown in Figs. 7 and 8. In Fig. 7, an H interval of 50 m hides the variation of S_o between H 150 m and 200 m. The ln (N_d) and –ln(R) diagrams for H widths of 40 am nd 50 m are shown in Fig. 7. However, in case that the S_o does not change substantially across the H intervals, the S_o does not change even if the larger H interval is used (e.g., Fig. 8d). For example, S_o calculated with subsets of data (e.g., 220 ≤H<250m, 250≤H<280m, 280≤H<310m) are about ~ 0.24 to 0.25. If the S_o is estimated with all the data that fall into the three intervals (e.g., H > 200 m), the value is about 0.28, which is similar to three individual S_o values. The results may indicate that the cloud properties such as cloud thickness where the cloud begins to precipitate could be of importance for accurate estimates of S_o by affecting the optimal H interval and/or ranges.

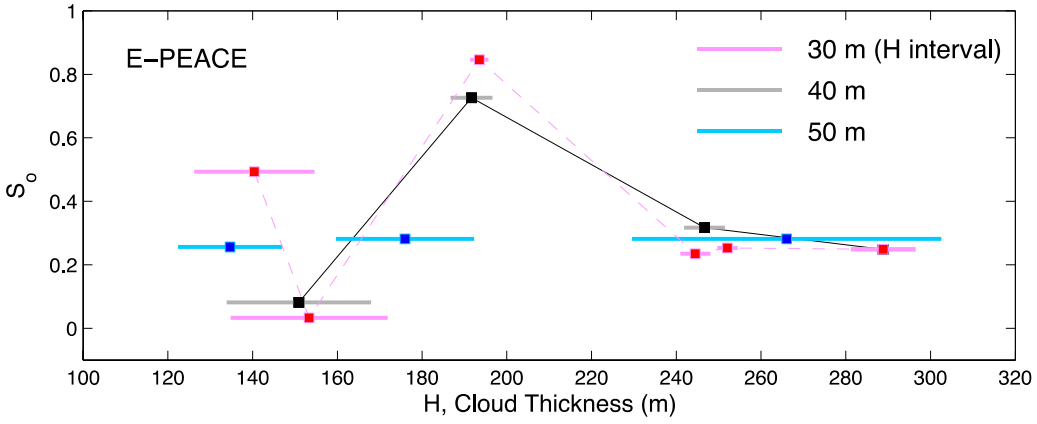

Figure C1. S_v is calculated with cloud data that are averaged over an e-folding time for E-PEACE. S_v calculated with three H intervals (Δ30 m, Δ40 m, and Δ50 m) are shown. Horizontal bar indicates ±1σ +/1sigma cloud thickness for a given H interval.

Formatted: Font: Times, Bold, Font color: Auto
Formatted: Font: Bold, Font color: Auto
Formatted: Font: Times, Bold, Font color: Auto
Formatted: Font: Times, Font color: Auto
Formatted: Font: Times, Italic, Font color: Auto
Formatted: Font: Times, Italic, Font color: Auto, Subscript
Formatted: Font: Times, Font color: Auto
Formatted: Font: Times, Italic, Font color: Auto
Formatted: Font: Times, Italic, Font color: Auto, Subscript
Formatted: Font: Times, Font color: Auto
Formatted: Font: Times, Font color: Auto
Formatted: Font: Times, Font color: Auto
Formatted: Font: Times, Font color: Auto
Formatted: Font: Times, Font color: Auto
Formatted: Font: Times, Font color: Auto
Formatted: Font: Times, Font color: Auto
Formatted: Font color: Auto
Formatted: Font color: Auto
Formatted: Font: Times, Font color: Auto

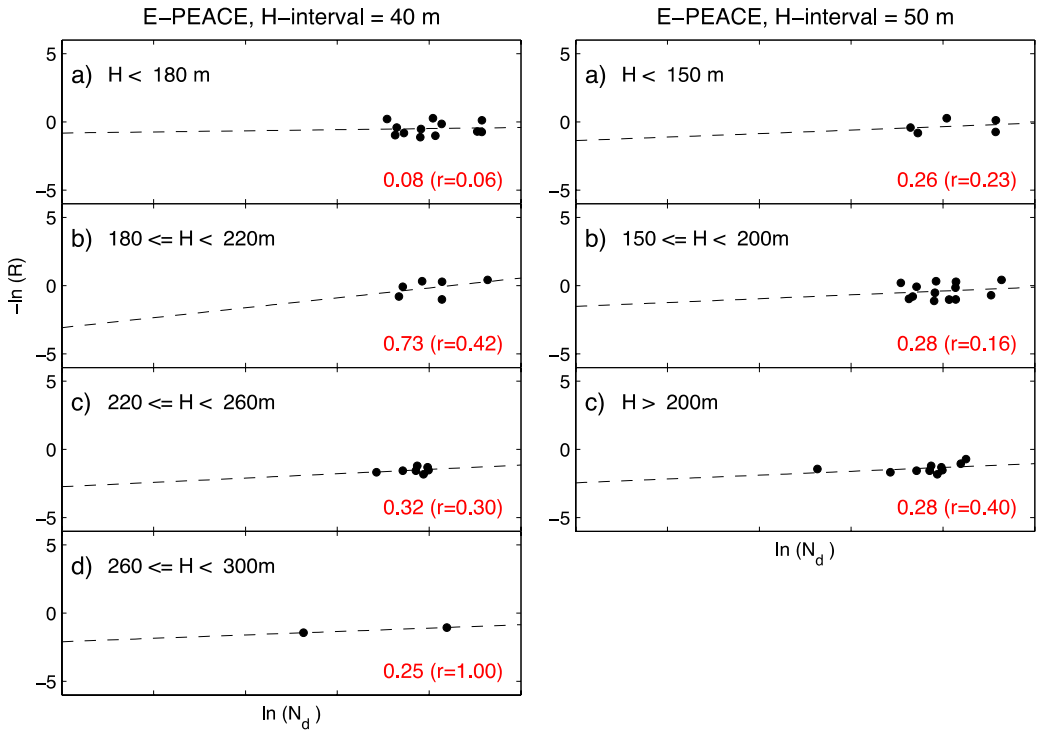

Formatted: Font: Times

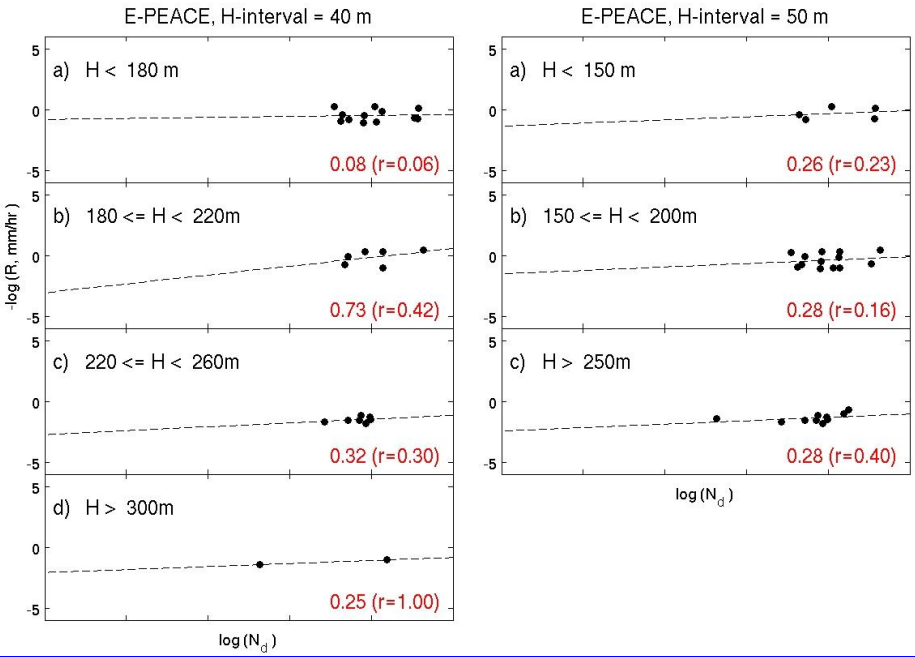

Figure C2. The ln (N_d) and –ln (R) diagrams with fixed H intervals: (left) ΔH=40 m, (right) ΔH=50 m.

Formatted: Font: Times, Font color: Auto
Formatted: Font: Times, Font color: Auto
Formatted: Font: Times, Bold, Font color: Auto
Formatted: Font: Bold, Font color: Auto
Formatted: Font: Times, Bold, Font color: Auto
Formatted: Font: Times, Font color: Auto
Formatted: Font color: Auto
Formatted: Font: Times, Font color: Auto
Formatted: Font: Times, Italic, Font color: Auto
Formatted: Font: Times, Italic, Font color: Auto, Subscript
Formatted: Font: Times, Font color: Auto
Formatted: Font color: Auto
Formatted: Font: Times, Font color: Auto
Formatted: Font: Times, Italic, Font color: Auto
Formatted: Font: Times, Font color: Auto
Formatted: Font: Times, Font color: Auto
Formatted: Font: Times, Font color: Auto
Formatted: Font: Times, Font color: Auto
Formatted: Font: Times, Font color: Auto
Formatted: Font: Times, Font color: Auto
Formatted: Font: Times, Font color: Auto

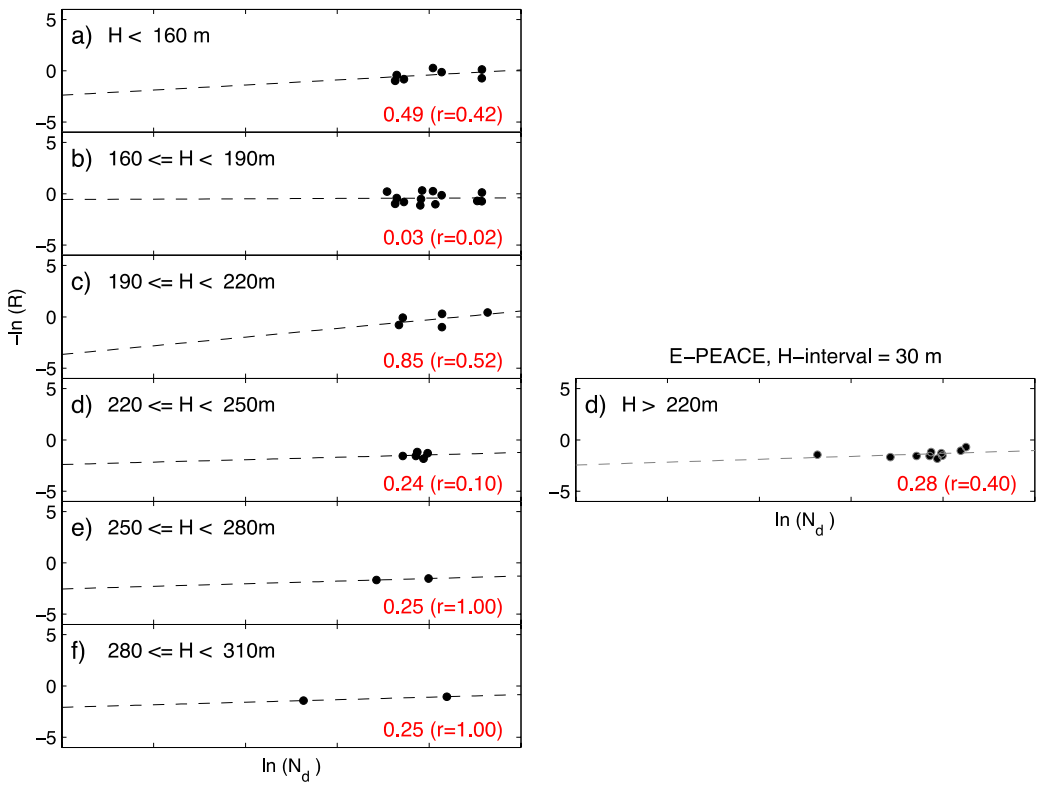

Formatted: Font: Times

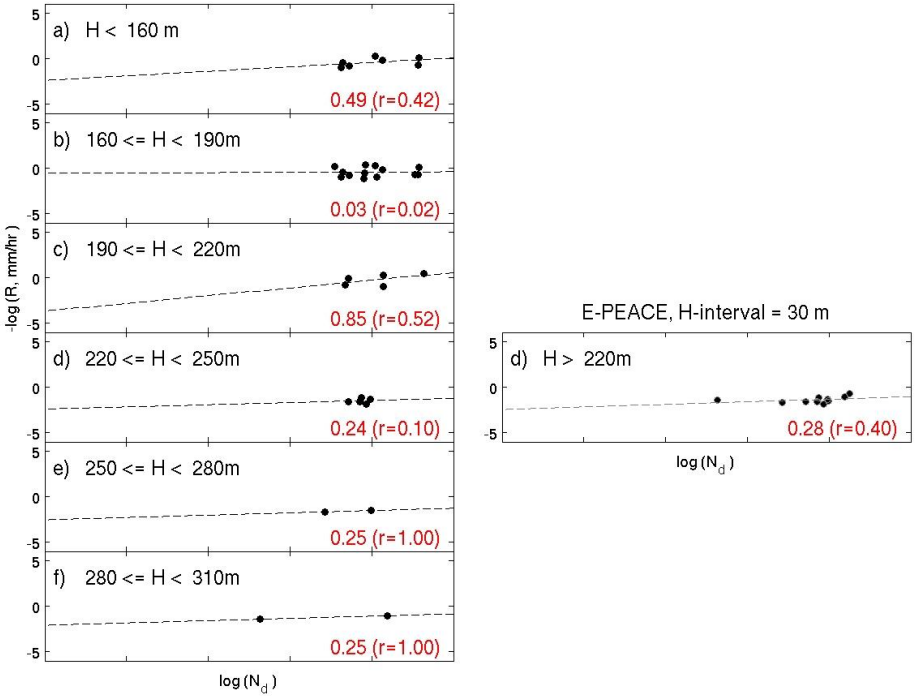

Figure C3. The ln (N_d) and –ln (R) diagrams with fixed H intervals (ΔH=30 m).

Formatted: Font: Times, Font color: Auto

Formatted: Font: Times

Formatted: Font: Bold, Font color: Auto

Formatted: Font: Times, Bold, Font color: Auto

Formatted: Font: Times, Font color: Auto

Formatted: Font color: Auto

Formatted: Font: Times, Font color: Auto

Formatted: Font: Times, Italic, Font color: Auto

Formatted: Font: Times, Font color: Auto

Formatted: Font color: Auto

Formatted: Font: Times, Font color: Auto

Formatted: Font: Times, Italic, Font color: Auto

Formatted: Font: Times, Font color: Auto

Formatted: Font: Times, Font color: Auto

Formatted: Font: Times, Font color: Auto

Formatted: Font: Times

Formatted: Font: Times, Font color: Auto

Formatted: Font: Times

Formatted: Font: Times, Font color: Auto

Formatted: Font: Times

Acknowledgements

The authors gratefully acknowledge the crews of the CIRPAS Twin Otter for their assistance during these field campaigns. EJ acknowledges Chris Terai for his helpful discussion of the estimate of precipitation susceptibility. This study was funded by ONR Grants N000140810465, N00014-10-1-0811, N00014-16-1-2567, and NSF Grant AGS-1008848. We thank both reviewers for thoughtful suggestions and constructive criticism that have helped to improve the manuscript.

References

~~Ayala, O., Rosa, B., Wang, L. P., and Grabowski, W. W.: Effects of turbulence on the geometric collision rate of sedimenting droplets: Part 1. Results from direct numerical simulation, New J. Phys., 10, 075015, doi:10.1088/1367-2630/10/7/075015, 2008.~~

~~Baker, M. B.: Variability in concentrations of cloud condensation nuclei in the marine cloud-topped boundary layer, Tellus, 45B, 458–472,1993.~~

Bretherton, C. S., Wood, R., George, R. C., Leon, D., Allen, G., and Zheng, X.: Southeast Pacific stratocumulus clouds, precipitation and boundary layer structure sampled along 20 S during VOCALS-REx, Atmos. Chem. Phys., 10, 10639–10654, doi:10.5194/acp-10-10639-2010, 2010.

Comstock, K. K., Wood, R., Yuter, S. E., and Bretherton, C. S.: Reflectivity and rain rate in and below drizzling stratocumulus, Quart. J. Roy. Meteor. Soc., 130, 2891–2918, 2004.

Duong, H. T., Sorooshian, A., and Feingold, G.: Investigating potential biases in observed and modeled metrics of aerosol-cloud-precipitation interactions, Atmos. Chem. Phys., 11, 4027-4037, doi:10.5194/acp-11-4027-2011, 2011.

Feingold, G. and Siebert, H.: In Clouds in the Perturbed Climate System: Their Relationship to Energy Balance, Atmospheric Dynamics, and Precipitation, edited by: Heintzenberg, J. and Charlson, R. J., Strüngmann Forum Reports, 2, Cambridge, MA: The MIT Press, 597, 2009.

Feingold, G., McComiskey, A., Rosenfeld, D., and Sorooshian, A.: On the relationship between cloud contact time and precipitation susceptibility to aerosol, J. Geophys. Res., 118, 10544–10554, 2013.

Gerber, H., Arends, B. G., and Ackerman, A. S.: A new microphysics sensor for aircraft use, Atmos. Res., 31, 235–252, 1994.

Gettelman, A., Morrison, H., Terai, C. R., and Wood, R.: Microphysical process rates and global aerosol–cloud interactions, Atmos. Chem. Phys., 13, 9855-9867, doi:10.5194/acp-13-9855-2013, 2013.

~~Gorge and Wood 2010 (from Terai)~~George, R. C. and Wood, R.: Subseasonal variability of low cloud radiative properties over the southeast Pacific Ocean, Atmos. Chem. Phys., 10, 4047–4063, doi:10.5194/acp-10-4047-2010, 2010.

Formatted: Font: Times
Formatted: Font: Times
Formatted: Font: Times, Font color: Auto
Formatted: Tab stops: 5.31", Left
Formatted: Font: Times
Formatted: Font: Times
Formatted: Font: Times, 10 pt
Formatted: Font: Times, 10 pt
Formatted: Justified, Indent: Left: 0", Hanging: 0.2", Automatically adjust right indent when grid is defined, Line spacing: 1.5 lines, Widow/Orphan control, Adjust space between Latin and Asian text, Adjust space between Asian text and numbers
Formatted: Font: Times, 10 pt
Formatted: Font: Times, 10 pt

Intergovernmental Panel on Climate Change (IPCC): The Physical Science Basis. Contribution of Working Group I to the Fifth Assessment Report of the Intergovernmental Panel on Climate Change. Stocker, T.F., Qin, D., Plattner, G.-K., Tignor, M., Allen, S.K., Boschung, J., Nauels, A., Xia, Y., Bex, V. and Midgley, P.M. (eds.), Cambridge University Press, Cambridge, United Kingdom and New York, NY, USA, 2013.

Jiang, H., Feingold, G., and Sorooshian, A.: Effect of aerosol on the susceptibility and efficiency of precipitation in trade cumulus clouds, J. Atmos. Sci., 67, 3525–3540, 2010.

Jones, A., Roberts, D. L., Woodage, M. J., and Johnson, C. E.: Indirect sulphate aerosol forcing in a climate model with an interactive sulphur cycle, J. Geophys. Res., 106, 20,293–20,310, doi:10.1029/2000JD000089, 2001.

Jung, E.: Aerosol-Cloud-Precipitation Interactions in the Trade Wind Boundary Layer, PhD dissertation, 184pp, http://scholarlyrepository.miami.edu/oa_dissertations/900, 2012.

Jung, E., Albrecht, B. A., Feingold, G., Jonsson, H. H., Chuang, P., and Donaher, S. L.: Aerosols, Clouds, and Precipitation in the North-Atlantic Trades Observed During the Barbados Aerosol Cloud Experiment. Part I: Distributions and Variability, submitted to Atmos. Chem. Phys., ACP, 2016.

Jung, E., Albrecht, B. A., Prospero, J. M., Jonsson, H. H., and Kreidenweis, S. M.: Vertical structure of aerosols, temperature and moisture associated with an intense African dust event observed over the Eastern Caribbean, J. Geophys. Res., 118, 4623–4643. doi: 10.1002/jgrd.50352, 2013.

Jung, E., Albrecht, B. A., Jonsson, H. H., Chen, Y.-C., Seinfeld, J. H., Sorooshian, A., Metcalf, A. R., Song, S., Fang, M., and Russell, L. M.: Precipitation effects of giant cloud condensation nuclei artificially introduced into stratocumulus clouds, Atmos. Chem. Phys., 15, 5645-5658, doi:10.5194/acp-15-5645-2015, 2015.

Khairoutdinov, M., and Y. Kogan, Y.: A new cloud physics parameterization in a large-eddy simulation model of marine stratocumulus, Mon. Weather Rev., 128, 229–243, 2000.

Lee, G., and I. Zawadzki, I.: Variability of drop size distributions: time-scale dependence of the variability and its effects on rain estimation, J. Appl. Meteor. , 44, 241–255, doi:10.1175/JAM2183.1, 2005.

Leith, C. E.: The Standard Error of Time-Average Estimates of Climatic Means, J. Appl. Meteorl., 12, 1066–1069, doi:10.1175/1520-0450(1973)012<1066:TSEOTA>2.0.CO;2,1973.

Lu, M. -L., Sorooshian, A., Jonsson, H. H., Feingold, G., Flagan, R. C., and Seinfeld, J. H.: Marine stratocumulus aerosol-cloud relationships in the MASE-II experiment: Precipitation susceptibility in eastern Pacific marine stratocumulus, J. Geophys. Res., 114, D24203, doi:10.1029/2009JD012774, 2009.

Mann, J. A. L, Chiu, J. C., Hogan, R. J., O'Connor, E. J., L'Ecuyer, T. S., Stein, T. H. M., and Jefferson, A.: Aerosol impacts on drizzle properties in warm clouds from ARM Mobile Facility maritime and continental deployments, J. Geophys. Res., 119, doi:10.1002/2013JD021339, 2014.

Nuijens, L., Serikow, I., Hirsch, L., Lonitz, K., and Stevens, B.: The distribution and variability of low-level cloud in the North- Atlantic trades, Q. J. Roy. Meteorol. Soc., 140, 2364-2374, 2014.

Formatted: Font: Times

Formatted: Font: Times

Formatted: Indent: Left: 0", Hanging: 0.2", Automatically adjust right indent when grid is defined, Line spacing: 1.5 lines, Widow/Orphan control, Adjust space between Latin and Asian text, Adjust space between Asian text and numbers

Formatted: Font: Times, 10 pt

Formatted: Indent: Left: 0", First line: 0"

Formatted: Indent: Left: 0", First line: 0"

Formatted: Font: Times

Formatted: Font: Times

Painemal, D., and Zuidema, P.: Assessment of MODIS cloud effective radius and optical thickness retrievals over the Southeast Pacific with VOCALS-REx in situ measurements, J. Geophys. Res., 116, D24206, doi:10.1029/2011JD016155, 2011.

Pawlowska, H. and Brenguier, J. L.: An observational study of drizzle formation in stratocumulus clouds for general circulation model (GCM) parameterizations, J. Geophys. Res., 108(D15), 8630, doi:10.1029/2002JD002679, 2003.

Rasch, P. J., and Kristjansson, J. E.: A comparison of the CCM3 model climate using diagnosed and predicted condensate parameterizations, J. Climate, 11, 1587–1614, 1998.

Rauber, R. M., Ochs III, H. T., Di Girolamo, L., Göke, S., Snod- grass, E., Stevens, B., Knight, C., Jensen, J. B., Lenschow, D. H., Rilling, R. A., Rogers, D. C., Stith, J. L., Albrecht, B. A., Zuidema, P., Blyth, A. M., Fairall, C. W., Brewer, W. A., Tucker, S., Lasher-Trapp, S. G., Mayol-Bracero, O. L., Vali, G., Geerts, B., Anderson, J. R., Baker, B. A., Lawson, R. P., Bandy, A. R., Thornton, D. C., Burnet, E., Brenguier, J-L., Gomes, L., Brown, P. R. A., Chuang, P., Cotton, W. R., Gerber, H., Heikes, B. G., Hudson, J. G., Kollias, P., Krueger, S. K., Nuijens, L., O'Sullivan, D. W., Siebesma, A. P., and Twohy, C. H.: Rain in shallow cu- mulus over the ocean, B. Am. Meteorol. Soc., 88, 1912–1928, 2007.

Rogers, R. R. and Yau, M. K.: A Short Course in Cloud Physics, Third Edition. International Series in Natural Philosophy, 290 pp, 1989.

~~Rosenfeld, D., Lohmann, U., Raga, G. B., O'Dowd, C. D., Kul- mala, M., Fuzzi, S., Reissell, A., and Andreae, M. O.: Flood or Drought: How Do Aerosols Affect Precipitation?, Science, 312, 1309–1313, 2008.~~

Rosenfeld, D., Wang, H., and P. J. Rasch, P. J.: The roles of cloud drop effective radius and LWP in determining rain properties in marine stratocumulus, *Geophys. Res. Lett.,39,* L13801, doi:10.1029/2012GL052028, 2012.

Rotstayn, L. D., and Y. Liu, Y.: A smaller global estimate of the second indirect aerosol effect, Geophys. Res. Lett., 32, L05708, doi:10.1029/2004GL021922, 2005.

Russell, Lynn M., and Coauthors: Eastern Pacific Emitted Aerosol Cloud Experiment, Bull. Amer. Meteor. Soc., 94, 709–729. doi: http://dx.doi.org/10.1175/BAMS-D-12-00015.1, 2013.

Sorooshian, A., Feingold, G., Lebsock, M. D., Jiang, H., and Stephens, G.: On the precipitation susceptibility of clouds to aerosol perturbations, Geophys. Res. Lett., 36, L13803, doi:10.1029/2009GL038993, 2009.

Sorooshian, A., Feingold, G., Lebsock, M. D., Jiang, H., and Stephens, G.: Deconstructing the precipitation susceptibility construct: improving methodology for aerosol-cloud-precipitation studies, J. Geophys. Res., 115, D17201, doi:10.1029/2009JD013426, 2010.

Sorooshian, A., Prabhakar, G., Jonsson, H., Woods, R., Flagan, R. C., and J. H. Seinfeld, J. H.: On the presence of giant particles downwind of ships in the marine boundary layer, Geophys. Res. Lett., 42, doi:10.1002/2015GL063179, 2015.

Stevens, B, and Feingold, G.: Untangling aerosol effects on clouds and precipitation in a buffered system, Nature, 461, 607-613, 2009.

Formatted: Font: Times

Formatted: Font: Times

Formatted: Default Paragraph Font, Font: Times New Roman, English (U.K.)

Takemura, T., Nozawa, T., Emori, S., Nakajima, T. Y., and Nakajima, T.: Simulation of climate response to aerosol direct and indirect effects with aerosol transport-radiation model, J. Geophys. Res., 110, D02202, doi:10.1029/2004JD005029, 2005.

Terai, C. R., Wood, R., Leon, D. C., and P. Zuidema, P.: Does precipitation susceptibility vary with increasing cloud thickness in marine stratocumulus?, Atmos. Chem. Phys., 12, 4567–4583, 2012.

Terai, C. R., Wood, R., and Kubar, T. L.: Satellite estimates of precipitation susceptibility in low-level marine stratiform clouds, J. Geophys. Res., 120, 8878-8889, 2015.

vanZanten, M. C., Stevens, B., Vali, G., and Lenschow, D. H.: Observations of drizzle in nocturnal marine stratocumulus, J. Atmos. Sci., 62, 88–106, 2005.

Wang, Z., Sorooshian, A., Prabhakar, G., Coggon, M. M., and Jonsson, H. H.: Impact of emissions from shipping, land, and the ocean on stratocumulus cloud water elemental composition during the 2011 E-PEACE Field Campaign, *Atmos. Environ., 89*, 570-580, doi.org/10.1016/j.atmosenv.2014.01.020, 2014.

Wonaschütz, A., Coggon, M., Sorooshian, A., Modini, R., Frossard, A. A., Ahlm, L., Mulmenstadt, J., Roberts, G. C., Russell, L. M., Dey, S., Brechtel, F. J., and Seinfeld, J. H.: Hygroscopic properties of smoke-generated organic aerosol particles emitted in the marine atmosphere, Atmos. Chem. Phys., 13, 9819-9835, 10.5194/acp-13-9819-2013, 2013.

Wood, R., Kubar, T. L., and Hartmann, D. L.: Understanding the Importantce of Microphysics and Macrophysics for Warm Rain in Marine Low Clouds. Part II: Heuristic Models of Rain Formation, J. Atmos. Sci., 66, 2973–2990, doi:10.1175/2009JAS3072.1, 2009.

Wood, R., Mechoso, C. R., Bretherton, C. S., Weller, R. A., Huebert, B., Straneo, F., Albrecht, B. A., Coe, H., Allen, G., Vaughan, G., Daum, P., Fairall, C., Chand, D., Gallardo Klenner, L., Garreaud, R., Grados, C., Covert, D. S., Bates, T. S., Krejci, R., Russell, L. M., de Szoeke, S., Brewer, A., Yuter, S. E., Springston, S. R., Chaigneau, A., Toniazzo, T., Minnis, P., Palikonda, R., Abel, S. J., Brown, W. O. J., Williams, S., Fochesatto, J., Brioude, J., and Bower, K. N.: The VAMOS Ocean-Cloud-Atmosphere-Land Study Regional Experiment (VOCALS-REx): goals, platforms, and field operations, Atmos. Chem. Phys., 11, 627-654, doi:10.5194/acp-11-627-2011, 2011.

Zheng, X., Albrecht, B., Jonsson, H. H., Khelif, D., Feingold, G., Minnis, P., Ayers, K., Chuang, P., Donaher, S., Rossiter, D., Ghate, V., Ruiz-Plancarte, J., and Sun-Mack, S.: Observations of the boundary layer, cloud, and aerosol variability in the southeast Pacific near-coastal marine stratocumulus during VOCALS-REx, Atmos. Chem. Phys., 11, 9943-9959, doi:10.5194/acp-11-9943-2011, 2011.

Zuidema, P., Leon, D., Pazmany, A., and Cadeddu, M.: Aircraft millimeter-wave passive sensing of cloud liquid water and water vapor during VOCALS-REx, Atmos. Chem. Phys., 12, 355-369, doi:10.5194/acp-12-355-2012, 2012.

Formatted: Font: Times

Table 1. Dates used for this analysis during each experiment.

No.	VOCALS (Sc)	E-PEACE (Sc)	BACEX (Cu)	KWACEX (Cu)
Period	Oct.-Nov., 2008	July-Aug., 2011	Mar.-Apr., 2010	May, 2012
Location	Southeast Pacific Sc decks	Northeast Pacific Sc decks (California coast)	Barbados (Caribbean Sea and North Atlantic)	Key West (Caribbean Sea)
RF1	10/16 (2), 232 [29,3]	7/19 [236, 2]	3/22 [39,25]	5/22 (1st flight)
RF2	10/18 (3), 292±22 [152,2]	7/21 [669,144]	3/23 [92,4]	5/22 (2nd flight)
RF3	10/19 (3) 323±16 [402,28]	7/22 [610, 39]	3/24 [69,1]	5/23
RF4	10/21 (1), 172 [376,2]	7/23 [369,20]	3/25 [68,8]	5/24
RF5	10/22 (2), 224 [364, N/A]	7/26 [258,131]	3/26 [28,1]	-
RF6	10/26 (2), 208 [395,11]	7/27 [702,7]	3/29 [103, N/A]	-
RF7	10/27 (1), 142±38 [336, 2]	7/29 [731,17]	3/30 [526, N/A]	-
RF8	10/30 (2), 213 [311,170]	8/2 [395,1]	3/31 [184, 2]	-
RF9	11/1 (4), 641 [146,8]	8/3 [629,1]	4/5 [138,4]	-
RF10	11/9 (1), 164±18 [392, 44]	8/4 [378,19]	4/7 [171,7]	-
RF11	11/10 (1), 194±21 [279, 1]	8/5 [364,93]	4/10 [133,43]	-
RF12	11/12 (2), 249 [409, 66]	8/10 [721,1]	4/11 [123,5]	-
RF13	11/13 (1), 183 [174, 35]	8/11 [10,4]	-	-

*RF indicates the Research Flight. However, note that RFs from E-PEACE and VOCALS are not the same as RF from Russell et al. (2013) and Zheng et al. (2011), respectively.

*The daily mean cloud thickness (mean±1σ) for VOCALS are shown with the H category (tThe group number is shown for VOCALS in the parenthesis). See the details in section 2.4.

*Numbers inside brackets indicate e-folding time (seconds) of N_d and R

~~*RF indicates the Research Flight. However, note that RFs from E-PEACE and VOCALS are not the same as RF from Russell et al. (2013) and Zheng et al. (2011), respectively.~~

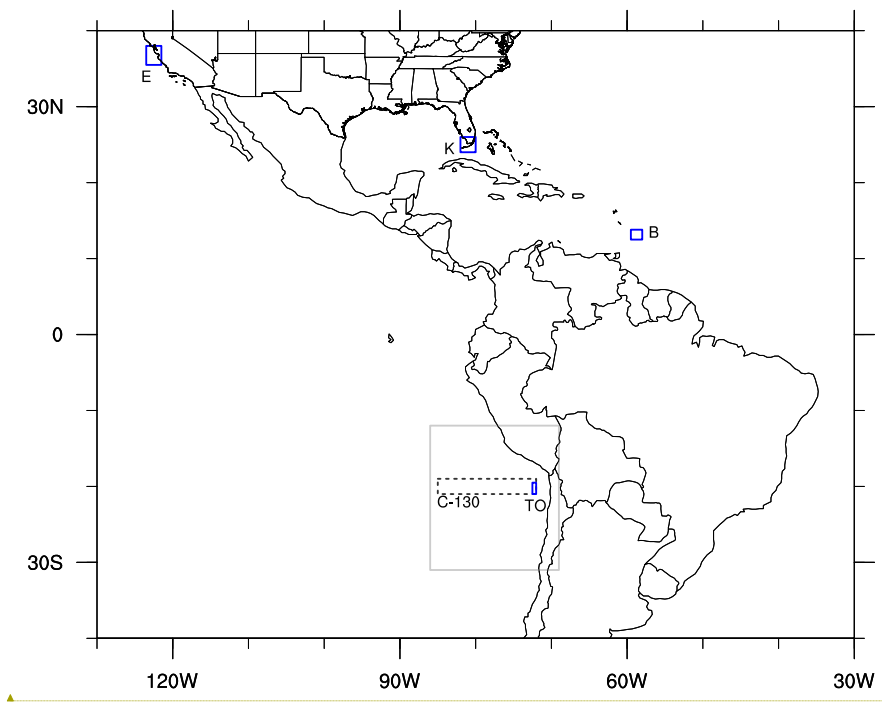

Figure 1: The geographical location of each field campaign (blue solid). E indicates E-PEACE, K indicates KWACEX, and B shows BACEX. The entire domain of VOCALS-REx is displayed as a solid grey box with domains of C-130 (dashed grey) and TO (solid blue) flights.

Formatted: Font: Times

Formatted: Font: Times

Formatted: Font: Times, 10 pt

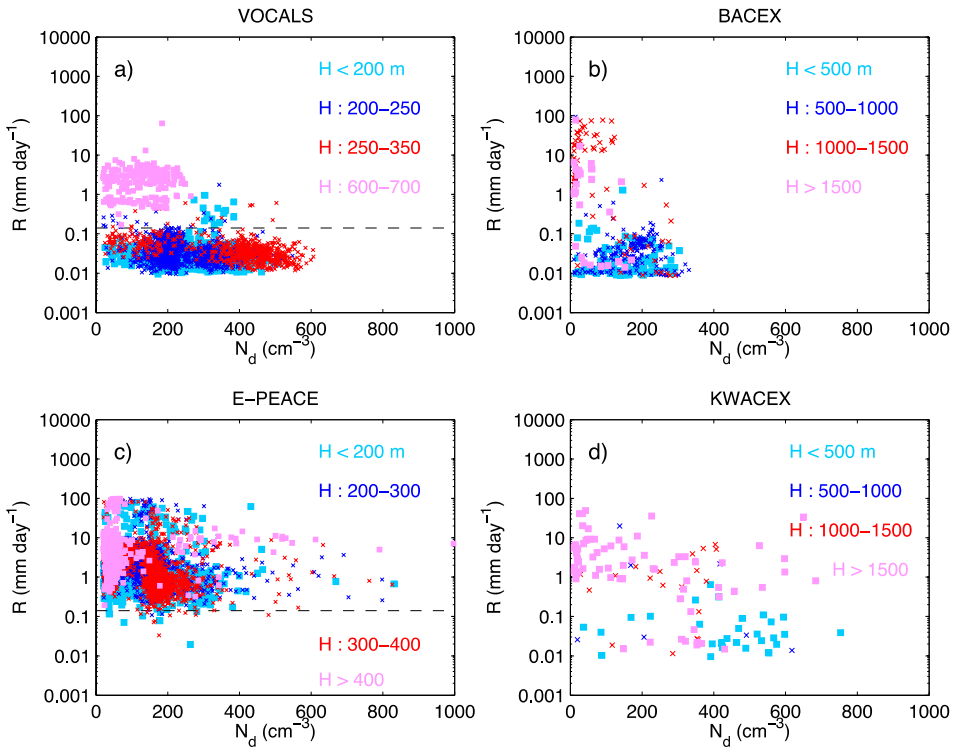

Formatted: Font: Times

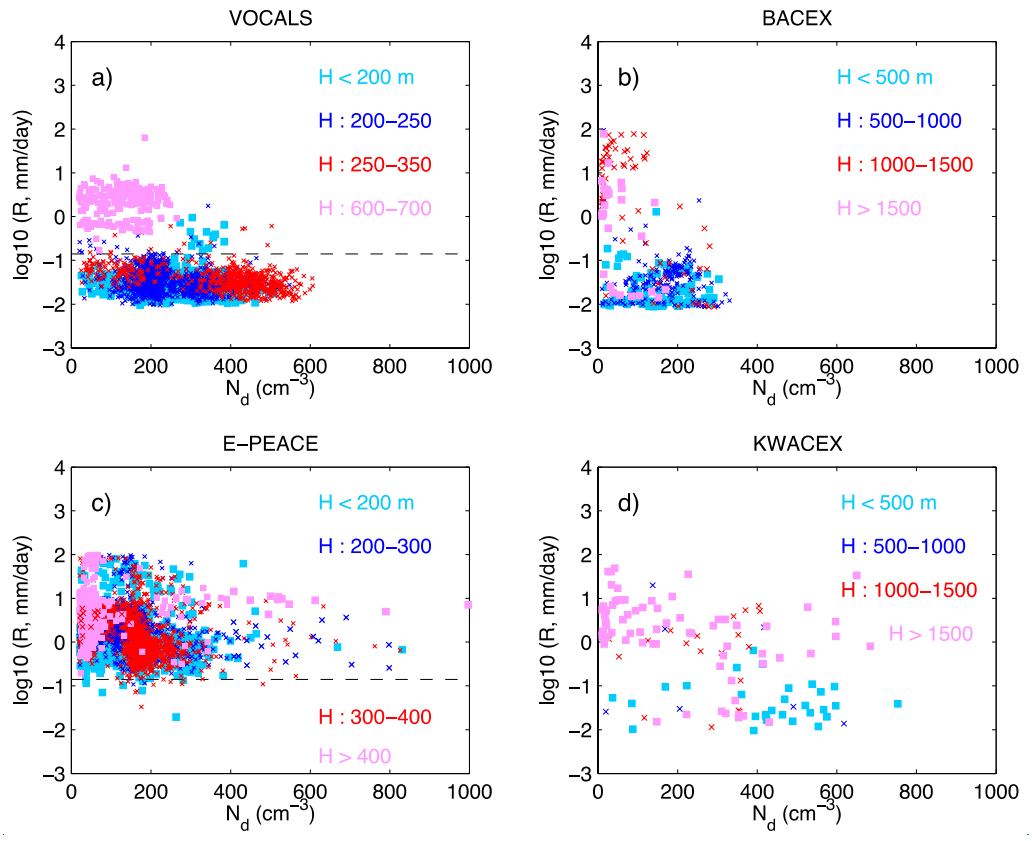
VOCALS
a)
H < 200 m
H : 200–250
H : 250–350
H : 600–700
log10 (R, mm/day)
N_d (cm^-3)
BACEX
b)
H < 500 m
H : 500–1000
H : 1000–1500
H > 1500
log10 (R, mm/day)
N_d (cm^-3)
E–PEACE
c)
H < 200 m
H : 200–300
H : 300–400
H > 400
log10 (R, mm/day)
N_d (cm^-3)
KWACEX
d)
H < 500 m
H : 500–1000
H : 1000–1500
H > 1500
log10 (R, mm/day)
N_d (cm^-3)

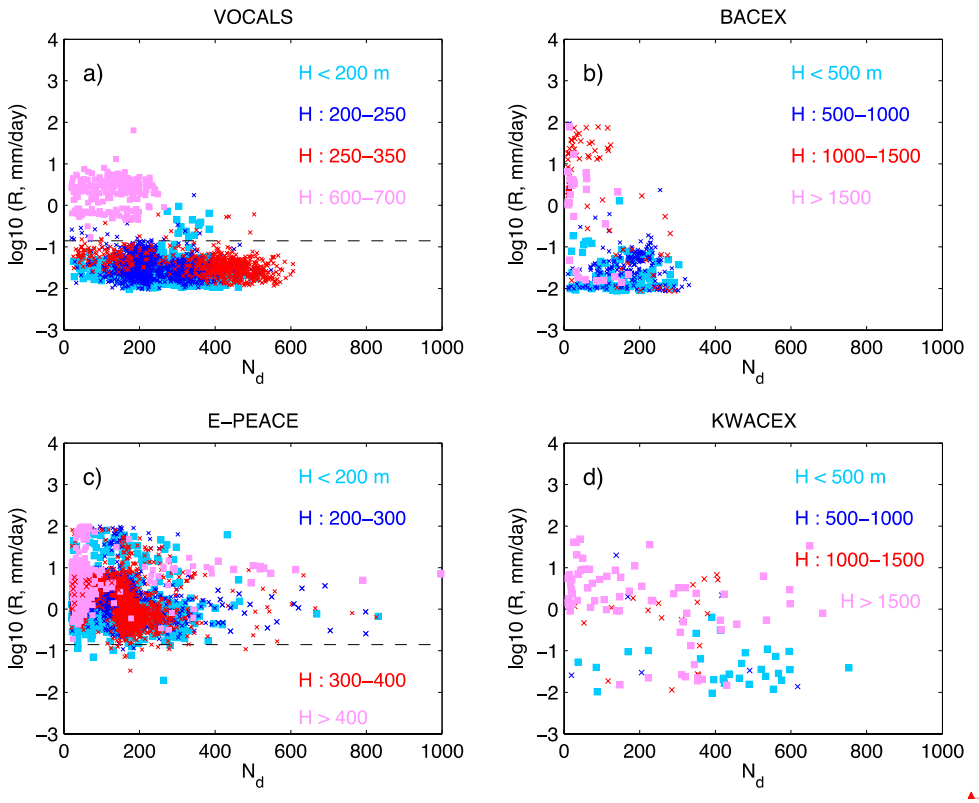

Figure 2: Scatter diagrams of cloud droplet number concentrations N_d and precipitation, R, for four field campaigns. Colors indicate cloud thickness H. ~~R increases upward in y ordinate and N_d increase toward the right direction in x abscissa~~. The dashed line indicates an R value of 0.14 mm day^{-1}.

Formatted: Font: Times

Formatted: Font: Times, 10 pt

Formatted: Font: Times, 10 pt, Italic

Formatted: Font: Times, 10 pt

Formatted: Font: Times, 10 pt

Formatted: Font: Times, 10 pt, Italic

Formatted: Font: Times, 10 pt

Formatted: Font: Times, 10 pt, Italic

Formatted: Font: Times, 10 pt

Formatted: Font: Times, 10 pt, Italic

Formatted: Font: Times, 10 pt

Formatted: Font: Times, 10 pt

Formatted: Font: (Default) Times, 10 pt

Formatted: Font: Times

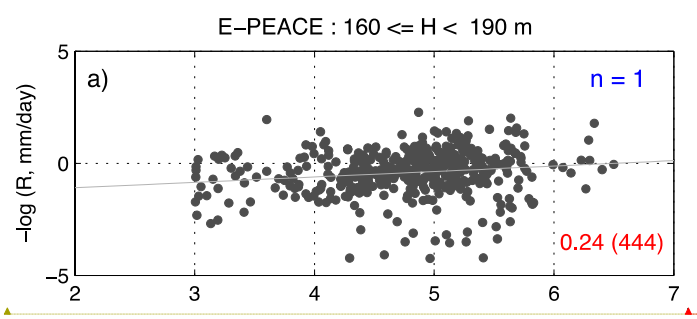

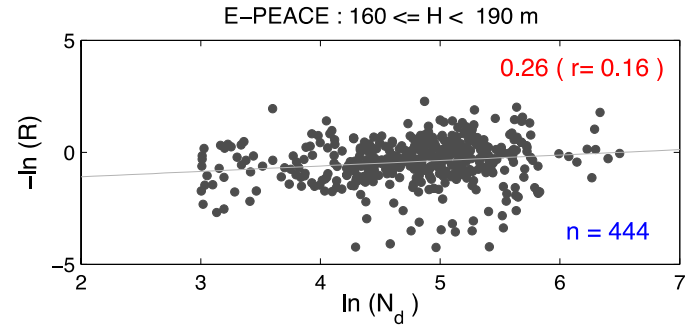

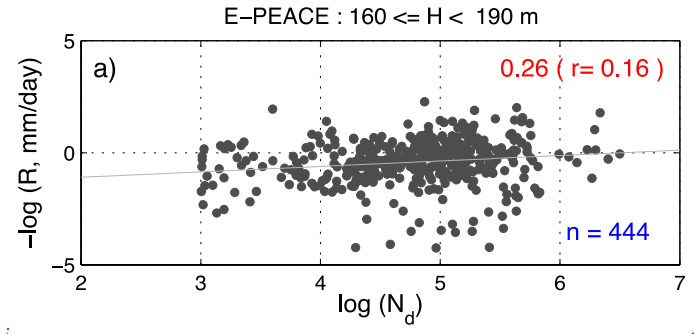

Figure 3: Examples of scatterplots used to calculate precipitation susceptibility S_o (i.e., the slope) for E-PEACE. Black dots ~~in each box~~ indicate data points for an H interval between 160 m and 190 m. Numbers on the bottom right (blue~~red~~) indicate the total number of data ~~, the S_o with a total number of data~~ used, S_o and linear coefficient (r) values are shown in the upper right corner. Precipitation, ~~*to calculate S_o inside the parentheses. Numbers on the upper right corner (blue) indicate the*~~

Formatted: Font: Times
Formatted: Font: Times
Formatted: Font: Times
Formatted: Font: Times
Formatted: Font: Times
Formatted: Font: Times
Formatted: Font: Times, 10 pt
Formatted: Font: Times, 10 pt
Formatted: Font: Times, 10 pt
Formatted: Font: Italic, Subscript
Formatted: Font: Times, 10 pt
Formatted: Font: Times, 10 pt, Italic
Formatted: Font: Times, 10 pt
Formatted: Font: Times, 10 pt, Italic

~~*interval of sampling size. For example, N=7 in Fig. 3(c) shows data at every 7 seconds (in sequence) were used.*~~ R_s increases downward in y ordinate, and N_d increases toward the right direction in x abscissa.

Formatted: Font: Times, 10 pt

Formatted: Font: Times, 10 pt, Italic

Formatted: Font: Times, 10 pt

Formatted: Font: Times

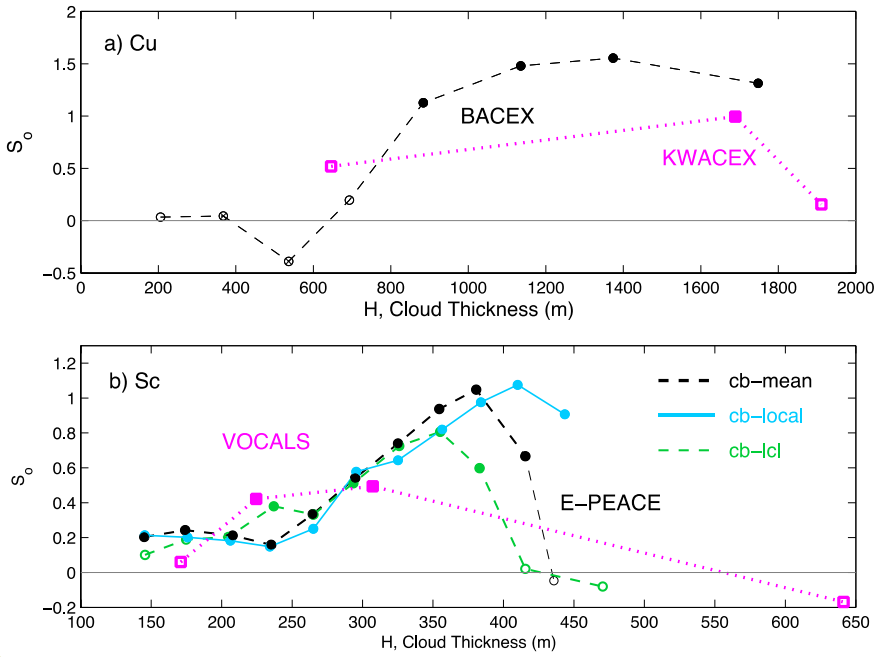

Formatted: Font: Times

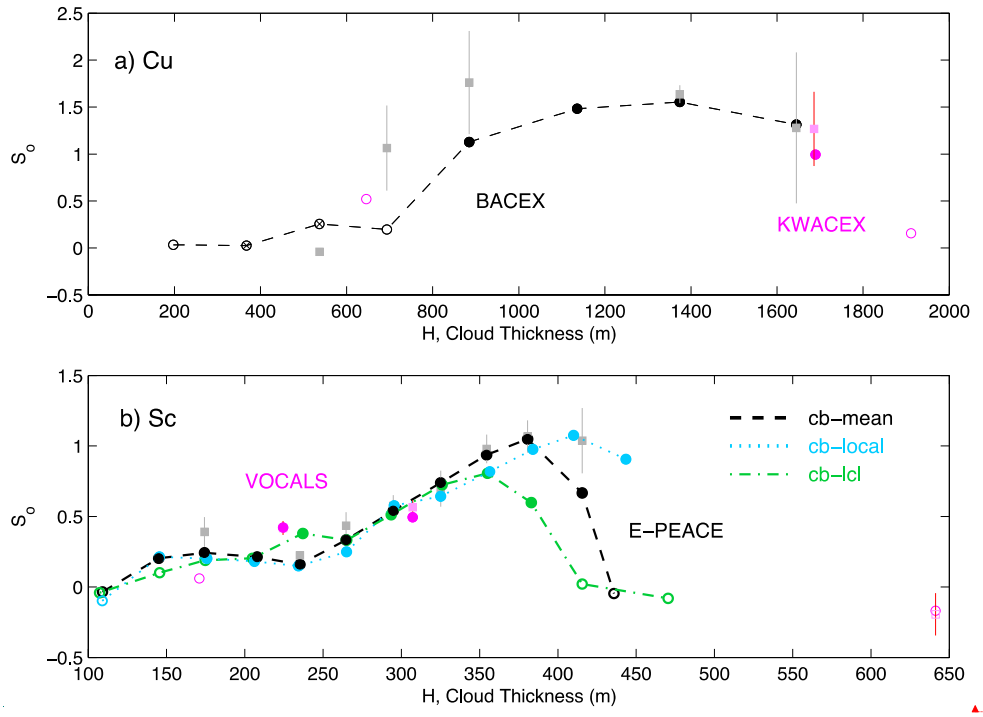

Figure 4: Precipitation susceptibility, S_o, estimated with aircraft measurements for (a) Cu (12 flights of BACEX and four flights of KWACEX) and (b) Sc (13 flights of E-PEACE and VOCALS-REx). ~~S_o of BACEX and E-PEACE are shown as connected lines since the data covers cloud thickness without gaps.~~ E-PEACE S_o is estimated from (i) the cloud base height, which is identified using LCL (cb-lcl) and ii) from the vertical structures of LWCs (lowest height that the vertical gradient of LWC is the greatest) as ~~that ii)~~ the aircraft enters to the cloud deck to conduct the cloud-base level leg flight (cb-local), and (iii) from the averaged cloud-base heights from the nearby soundings and cb-local (cb-mean). ~~S_o that is calculated with the subsets of data points (n=2 to 10 seconds in sequence) is shown as grey (mean) with vertical bars (±1σ).~~ Filled circles ~~and squares~~ are statistically significant at 99 % confidence level. The number of data points used for S_o estimates and their statistical significance are shown in Table A2.

Formatted: Font: Times

Formatted: Font: Times, 10 pt

Formatted: Font: Times, 10 pt

Formatted: Font: Times, 10 pt

Formatted: Font: Times, 10 pt

Formatted: Font: Times

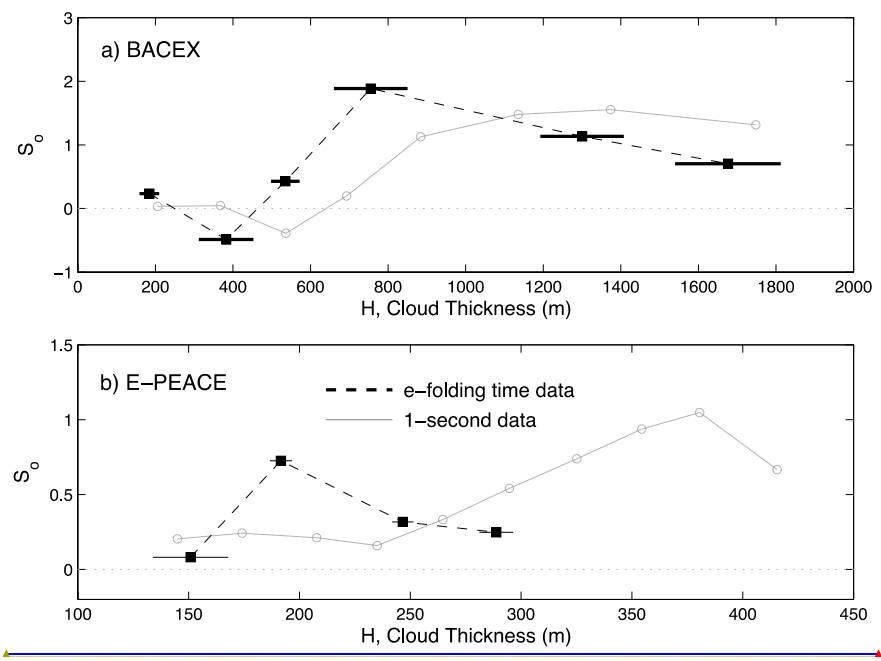

Figure 5. S_o estimated with aircraft measurements for (a) BACEX (Cu) and (b) E-PEACE (Sc). The 1-second data of individual flights are reduced by averaging over the e-folding time of N_d for each flight~~day~~ prior to the calculation.

Formatted: Font: Times
Formatted: Font: Times
Formatted: Font: Times, Bold
Formatted: Font: Times
Formatted: Font: Times
Formatted: Font: Times, Italic
Formatted: Font: Times
Formatted: Font: Times

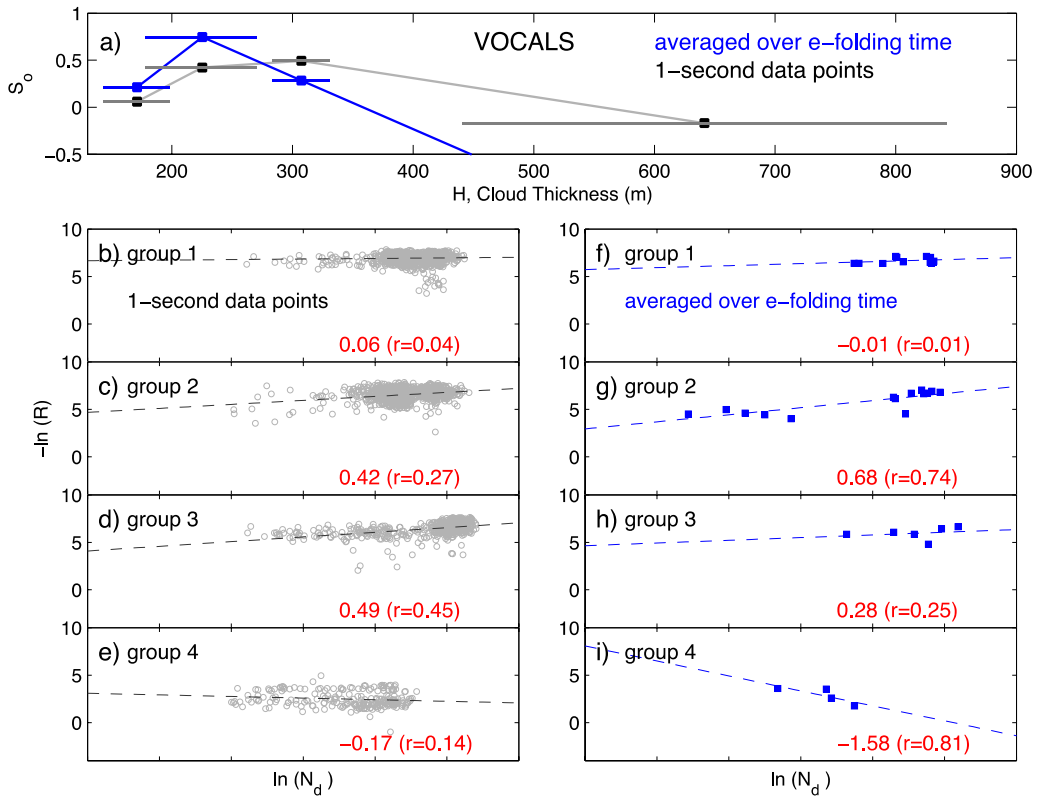

Formatted: Font: Times

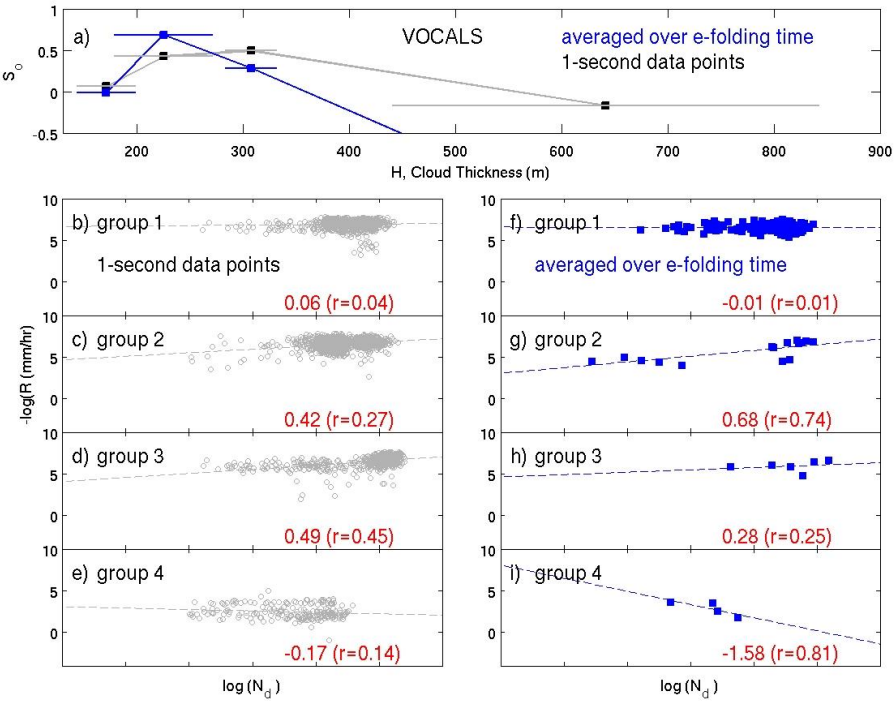

Figure 6. S_o for VOCALS TO flight is calculated with 1-second data (grey) and cloud data that are averaged over an e-folding time for each day (blue). The $\ln(N_d)$ and $-\ln(R)$ diagram is shown for each H interval. The horizontal bar in (a) indicates $\pm 1\sigma$. S_o is calculated for the cloud data in groups with similar H (shown in Table 1).

Formatted: Font: Times

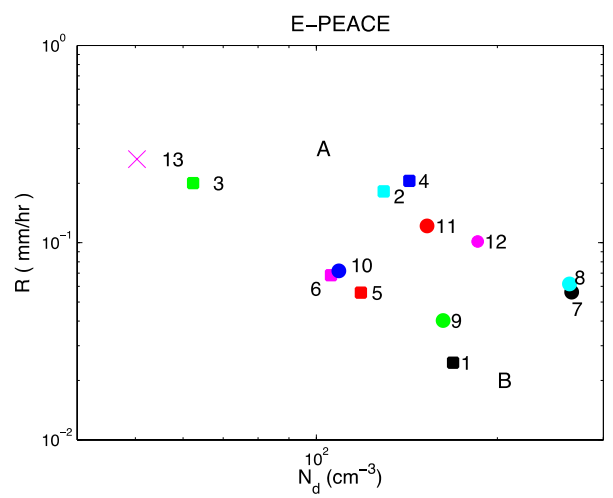

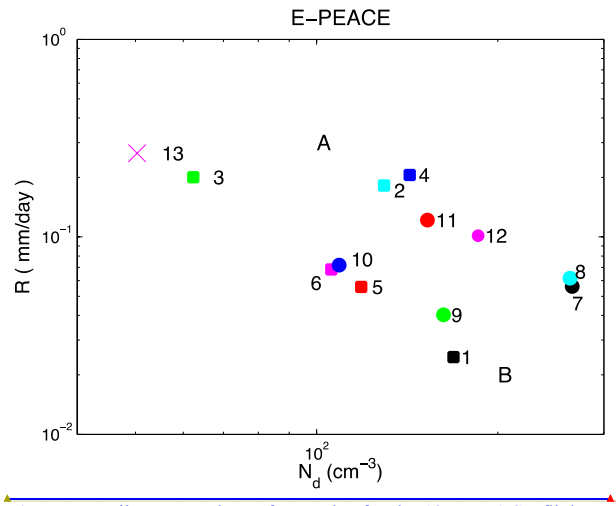

Figure 7. Daily mean values of N_d and R for the 13 E-PEACE flights. Numbers indicate the flight numbers shown in Table 1.

Formatted: Font: Times

Formatted: Font: Times, Font color: Auto

Formatted: Font: Times, Font color: Auto

Formatted: Font: Times, Bold, Font color: Auto

Formatted: Font: Times, Font color: Auto

Formatted: Font: Times, 10 pt, Font color: Auto

Formatted: Font: Times, 10 pt, Italic, Font color: Auto

Formatted: Font: Times, 10 pt, Font color: Auto

Formatted: Font: Times, 10 pt, Italic, Font color: Auto

Formatted: Font: Times, 10 pt, Font color: Auto

Formatted: Font: Times

Formatted: Font: Times, Font color: Auto

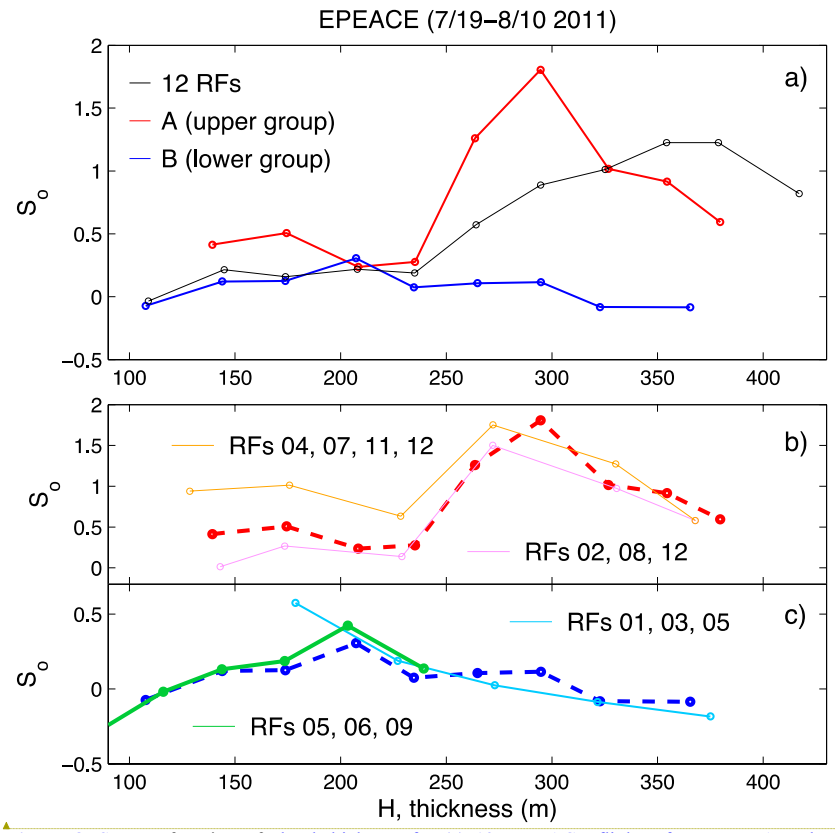

Figure 8. S_o as a function of cloud thickness for (a) 12 E-PEACE flights, for groups A and B shown in Fig. 7, (b) S_o calculated with randomly resampled RFs within groups (b) A and (b) B. RFs indicate Research Flights.

Formatted: Font color: Auto

Formatted: Font: Times, Bold, Font color: Auto

Formatted: Font: Times, Font color: Auto

Formatted: Font: Times, Font color: Auto

Formatted: Font color: Auto

Formatted: Font: Times, Font color: Auto

Formatted: Font: Times, Font color: Auto

Formatted: Font: Times, Font color: Auto

Formatted: Font: Times

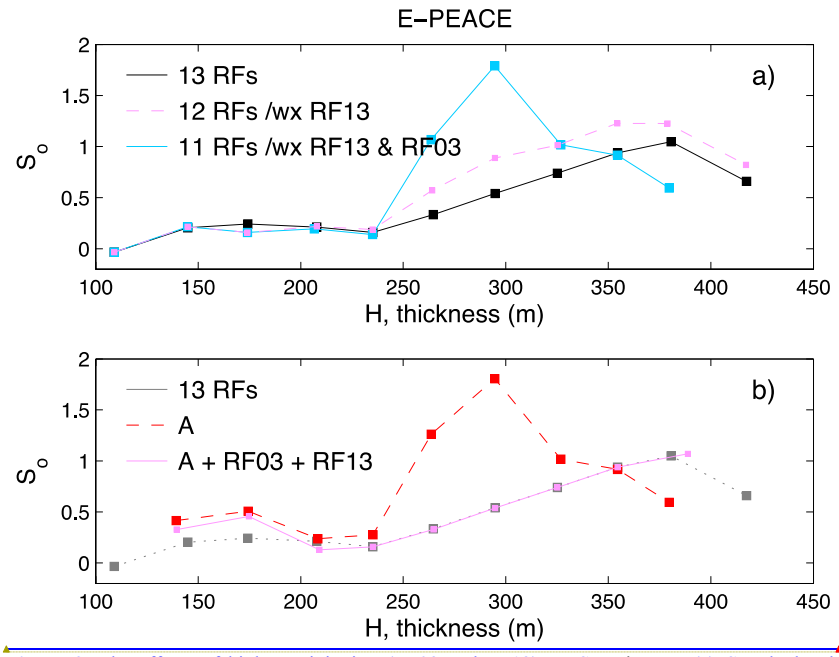

Figure 9. The effects of high precipitation (RF03 and RF13) on S_o estimates. (a) S_o calculated for 13 flights during E-PEACE in addition to when either, or both, RF03 and RF13 are excluded. RF03 and RF 13 are the flights of high precipitation rates. (b) S_o is calculated from group A with and without RF03 and RF13. R and N_t information for each flight is shown in Fig. 7.

Formatted: Font: Times

Formatted: Font: Times

Formatted: Font: Times, Bold, Font color: Auto

Formatted: Font: Times, Font color: Auto

Formatted: Font: Italic, Subscript

Formatted: Font: Times, Italic, Font color: Auto

Formatted: Font: Times, Italic, Font color: Auto, Subscript

Formatted: Font: Times, Font color: Auto

Formatted: Font: Times, Font color: Auto

Formatted: Font: Times, Font color: Auto

Formatted: Font: Times, Italic, Font color: Auto

Formatted: Font: Times, Font color: Auto

Formatted: Font: Times, Italic, Font color: Auto

Formatted: Font: Times, Font color: Auto

Formatted: Font: Times, Font color: Auto

Formatted: Font color: Auto

Formatted: Font: Times, Font color: Auto

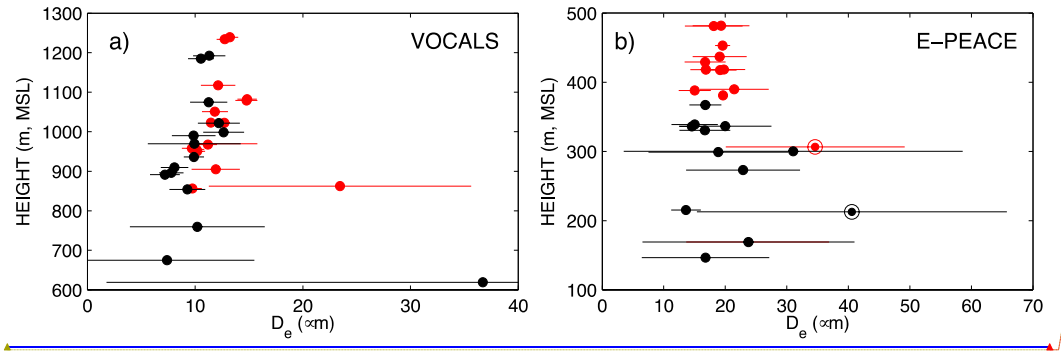

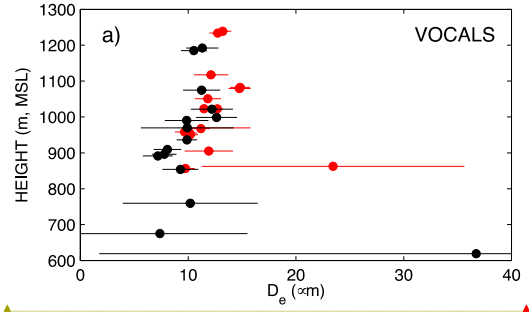

Figure 10~~5~~: Distribution of ~~(a)~~ effective diameters (mean ±1σ) for (a) VOCALS-TO flights and for (b) E-PEACE. Cloud droplets on 11 August are shown as double circles in Fig. 10~~5~~(b).

~~and (b) radar reflectivity of the Southeast Pacific Sc decks (VOCALS-Rex), sampled from mid-cloud (red) and cloud-base (black) levels. Radar reflectivity with cloud depth is shown in Fig. 5c. The pairs of clouds are connected with lines in Fig. 5b-c, and numbers in Fig. 5c indicate research flight (RF) numbers (see Table 2).~~

Formatted: Font: Times
Formatted: Font: Times
Formatted: Font: Times
Formatted: Font: Times
Formatted: Font: Times, 10 pt
Formatted: Font: Times, 10 pt
Formatted: Font: Times

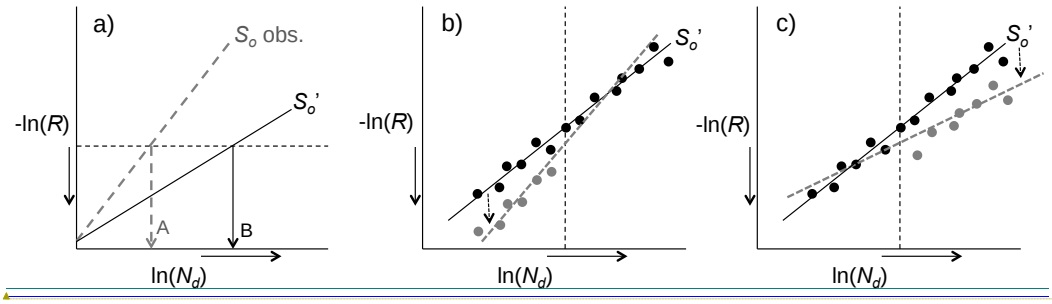

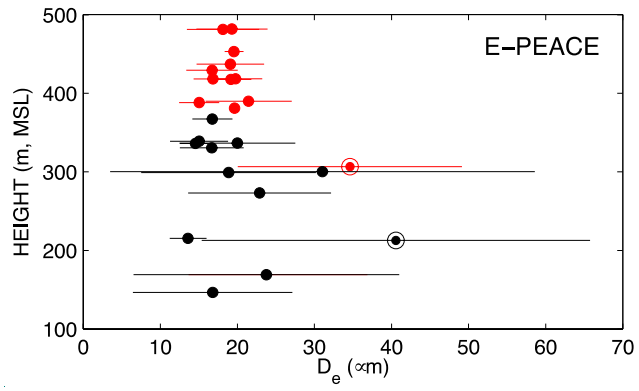

~~**Figure 6:** Effective diameters of Northeast Pacific Sc decks (E-PEACE) on the mid-cloud (red) and cloud-base (black) levels (mean ±1σ). Cloud droplets on 11 August are shown as double circles.~~

Formatted: Font: Times

Formatted: Font: Times

Formatted: Font: Times, 10 pt

Formatted: Space After: 0 pt, Line spacing: 1.5 lines

Formatted: Font: Times

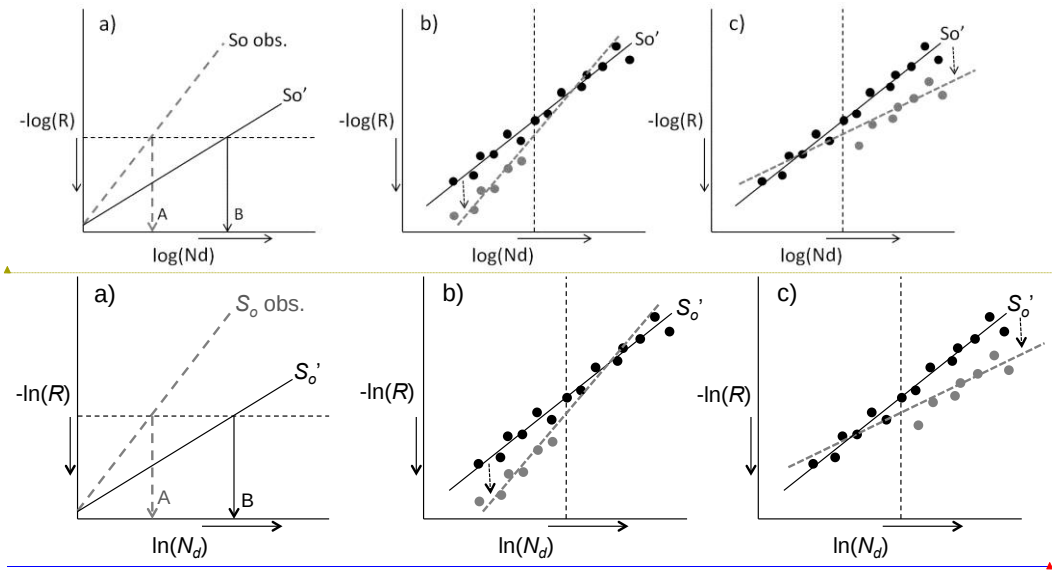

Figure 11~~7~~: A visual description of (a) the effect of wet scavenging and (b-c) the impact of an increase in rainfall rate for a given range of N_d on ~~the estimate of~~ S_o ~~-~~estimates. The solid line represents true (expected) S_o, whereas the dashed line indicates observed (or responded) S_o. The A and B in Fig. 11~~7~~(a) indicate N_d that are supposed to be for the expected (theoretical) S_o and responded (observed) S_o, respectively. The black filled circles in (b-c) indicate the initial (or actual) data and the grey filled circles indicate newly adjusted (responded) data accordingly to the scenario. R increases downward on~~in~~ y ordinate and N_d increase toward the right direction on~~in~~ x abscissa.

Formatted: Font: Times

Formatted: Font: Times

Formatted: Font: Times, 10 pt

Formatted: Font: Times, 10 pt

Formatted: Font: Times, 10 pt, Italic

Formatted: Font: Times, 10 pt

Formatted: Font: Times, 10 pt

Formatted: Font: Times, 10 pt

Formatted: Font: Times, 10 pt

Formatted: Font: Times, 10 pt, Italic

Formatted: Font: Times, 10 pt, Italic, Subscript

Formatted: Font: Times, 10 pt

Formatted: Font: Times, 10 pt, Italic

Formatted: Font: Times, 10 pt, Italic, Subscript

Formatted: Font: Times, 10 pt

Formatted: Font: Times, 10 pt, Italic

Formatted: Font: Times, 10 pt, Italic, Subscript

Formatted: Font: Times, 10 pt

Formatted: Font: Times, 10 pt, Italic

Formatted: Font: Times, 10 pt

Formatted: Font: Times, 10 pt

Formatted: Font: Times, 10 pt, Italic

Formatted: Font: Times, 10 pt

Formatted: Font: Times, 10 pt

Formatted: Font: Times